2009-04-17

Molecular Systematics of Spiny Pocket Mice (Subfamily Heteromyinae) Inferred from Mitochondrial and Nuclear Sequence Data

Melina Crystal Williamson
Brigham Young University - Provo

MOLECULAR SYSTEMATICS OF SPINY POCKET MICE (SUBFAMILY HETEROMYINAE) INFERRED FROM MITOCHONDRIAL AND NUCLEAR SEQUENCE DATA

by

Melina C. Williamson

A thesis submitted to the faculty of
Brigham Young University
in partial fulfillment of the requirements for the degree of

Master of Science

Department of Biology
Brigham Young University
August 2009

BRIGHAM YOUNG UNIVERSITY

GRADUATE COMMITTEE APPROVAL

of a thesis submitted by

Melina C. Williamson

This thesis has been read by each member of the following graduate committee and by majority vote has been found to be satisfactory.

Date	Duke S. Rogers, Chair
Date	Leigh A. Johnson
Date	Jack W. Sites, Jr.

BRIGHAM YOUNG UNIVERSITY

As chair of the candidate's graduate committee, I have read the thesis of Melina C. Williamson in its final form and have found that (1) its format, citations, and bibliographical style are consistent and acceptable and fulfill university and department style requirements; (2) its illustrative materials including figures, tables, and charts are in place; and (3) the final manuscript is satisfactory to the graduate committee and is ready for submission to the university library.

Date

Duke S. Rogers
Chair, Graduate Committee

Accepted for the Department

Russell B. Rader
Graduate Coordinator

Accepted for the College

Rodney J. Brown
Dean, College of Life Sciences

ABSTRACT

MOLECULAR SYSTEMATICS OF SPINY POCKET MICE (SUBFAMILY HETEROMYINAE) INFERRED FROM MITOCHONDRIAL AND NUCLEAR SEQUENCE DATA

Melina C. Williamson

Department of Biology

Master of Science

This study aims to determine species-level relationships within the genus *Heteromys*, as well as generic-level relationships among members of the subfamily Heteromyinae using a phylogenetic framework. Molecular sequence data were generated from two mitochondrial genes (cytochrome *b* and cytochrome oxidase I) and three nuclear gene segments (β-fibrinogen, engrailed protein II, and myosin heavy chain II), and analyzed under maximum parsimony, maximum likelihood, and Bayesian optimality criteria to infer relationships.

Chapter 1 focuses on the phylogenetic and taxonomic implications for *Heteromys* from the analyses of sequence data. Phylogenies also provided a framework for delimiting species boundaries within the wide-ranging *Heteromys desmarestianus* complex using the Wiens and Penkrot method. Several well-supported clades within this complex were recovered, including *H. goldmani*, *H. nubicolens*, and *H. oresterus*, as well as five groups identified as candidate species. *Heteromys oasicus* was not found to be

genetically diagnosable from *H. anomalus*, and was relegated to subspecific status. I present a revised taxonomy as follows: the monotypic subgenus *Xylomys* is maintained (*H. nelsoni*); the subgenus *Heteromys* is divided into three species groups – *anomalus* (*H. anomalus* [including *H. oasicus*], *H. australis*, and *H. teleus*), *desmarestianus* (*H. desmarestianus*, *H. goldmani*, *H. nubicolens*, *H. oresterus*, and the five candidate species), and *gaumeri* (*H. gaumeri*).

Chapter 2 describes phylogenetic inferences made from analyses of heteromyine taxa, genera *Heteromys* and *Liomys*. Many studies have recovered *Liomys* as paraphyletic relative to *Heteromys*, and the goal of this chapter was to address this taxonomic problem. The *Liomys pictus* species group (*L. irroratus*, *L. pictus*, and *L. spectabilis*) was recovered as sister to *Heteromys* rather than to the *L. salvini* group (*L. adspersus* and *L. salvini*). I recommend a revised taxonomy for the subfamily as follows: the genus *Heteromys* is retained as delineated in Chapter 1; the genus *Liomys* is reduced in scope to include only *L. irroratus*, *L. pictus*, and *L. spectabilis*; the subgeneric name *Schaeferia* is elevated to generic rank and includes *S. adspersus* and *S. salvini*. This classification better reflects the phyletic diversity within the subfamily Heteromyinae, and requires fewer name changes; thus providing nomenclatural stability.

ACKNOWLEDGMENTS

Sincere thanks to my advisor, Dr. Duke S. Rogers for his guidance and mentorship, and also to my committee: Drs. Leigh A. Johnson and Jack W. Sites, Jr. for their help on this project. I also thank the following investigators for providing tissue samples: Marisol Aguilera of the Universidad Central de Venezuela; Robert P. Anderson of the City College of New York; Elizabeth Arellano and Francisco González-Cózatl of the Universidad Autónoma del Estado de Morelos; Michael D. Carleton and Alfred E. Gardner of the National Museum of Natural History; Jim Dines of the Natural History Museum of Los Angeles County; Robert C. Dowler of Angelo State University; Mark D. Engstrom of the Royal Ontario Museum; Mark S. Hafner of Louisiana State University; Robert M. Timm of the University of Kansas Museum of Natural History; and Robert Voss of the American Museum of Natural History. I thank Ruth S. Rogers, whose translation of German text into English was an important factor in this project. I also greatly appreciate Sarah Frey, Rustin Reed, Ashley Pond, and Greg Crewdson for their assistance with lab work, as well as Greg Crewdson, Francisco González-Cózatl, Nicole Lewis-Rogers, Amanda Madsen, Ashley Pond, Rustin Reed and Quinn Shurtliff for their help collecting spiny pocket mice in Mexico. Thanks also to Nicole Lewis-Rogers and Matthew Bendall for their help with analyses and document formatting. I thank Mindy González for her work with the systematics of *Heteromys*, which has provided the springboard for my own project. I am very grateful to my family and parents, who have always encouraged me in my educational pursuits. Finally, I want to express deep gratitude to my husband, Ben, for all of his support and encouragement on my behalf.

TABLE OF CONTENTS

CHAPTER 1

SYSTEMATICS OF SPINY POCKET MICE (GENUS *HETEROMYS*)

Introduction

The rodent family Heteromyidae is exclusively Neotropical in distribution, and is endemic to the New World, with its origin in western North America (Wahlert 1993). The two extant members of the subfamily Heteromyinae (genera *Heteromys* and *Liomys*) are commonly known as spiny pocket mice and are found in southern Texas, throughout Mexico and Central America, and into northern South America (Colombia, Venezuela, and Ecuador—Schmidly *et al*. 1993; Williams *et al*. 1993). Heteromyines tend to demonstrate strong specificity to particular habitats, which collectively constitute an array of tropical environments including thorn scrub, pluvial rainforest, and montane cloud forests (Genoways 1973; Schmidly *et al*. 1993; Anderson 1999; 2003). The association, however, between particular taxa and their preferred habitat has yet to be investigated in a rigorous fashion. Moreover, the number of species-level taxa of heteromyines likely is underestimated (González 2005; Rogers and Vance 2005) and, given changes in land use practices throughout Latin America (e.g. Ochoa-Gaona 2000), there is a real risk to the long-term existence of some taxa.

Species of *Heteromys* (forest spiny pocket mice) can be distinguished from *Liomys* based on several morphological characteristics, including a V-shaped mesopterygoid fossa, more complex dentition, and relatively small optic foramina (Anderson 2003; Genoways 1973; Williams *et al*. 1993). Additionally, species of *Liomys* generally prefer drier habitats throughout their range than do *Heteromys* and as a result, instances of sympatry are rare (Genoways 1973; Rogers and Vance 2005). No

phylogenetic study had documented reciprocal monophyly between these two genera. Recently however, studies have demonstrated that the genus *Heteromys* is monophyletic relative to *Liomys*, which was recovered as paraphyletic relative to *Heteromys* (Anderson *et al*. 2006; Hafner *et al*. 2007; Rogers and Vance 2006).

Heteromys was originally described under the name *Mus anomalus* (= *H. anomalus*), from the island of Trinidad by Thompson in 1815 (Table 1). Following this initial description, several more species were assigned to the genus *Heteromys* in the decades that followed. By the mid-1800's, six species had been named, although of these only *H. anomalus* and *H. desmarestianus* (Gray 1868) are considered valid today. Allen and Chapman described *H. gaumeri* in 1897, and in 1901 Thomas described *H. australis*. In 1902 three new species, including *H. goldmani*, were added to the genus and the subgenus *Xylomys* was created, to which *H. nelsoni* was assigned (Merriam). In 1911, Goldman revised the subfamily Heteromyinae to include two genera, *Heteromys* and *Liomys*, and divided *Heteromys* into two subgenera, *Heteromys* and *Xylomys*. Two decades later, in 1932, Harris described the species *H. oresterus*. The taxonomy of *Heteromys* was summarized by Hall (1981) and Williams *et al*. (1993), but until recently this group had received little taxonomic treatment: *H. teleus* was described in 2002 from Ecuador, *H. oasicus*, from Venezuela, in 2003, *H. nubicolens*, from Costa Rica, in 2006, and *H. catopterius*, from Venezuela (Anderson and Jarrín-V 2002; Anderson 2003; Anderson and Timm 2006; Anderson and Gutiérrez in press, respectively).

Despite the recent alpha taxonomic work on this group, systematic problems remain. Rogers (1989) attempted to clarify relationships among *Heteromys* using karyotypes for five species of *Heteromys*. He reported differences in diploid number (2n)

and a substantial variation in the number of autosomal arms (FN) among the species examined. Most notably, the *H. desmarestianus* species complex was found to have a 2n=60 and a FN that ranged broadly from 66 to 90. Patton and Rogers (1993) suggested that FN variation within *H. desmarestianus* is most likely due to euchromatic structural transpositions, such as reciprocal translocations or pericentric inversions, which may induce changes sufficient to prohibit gene flow because of meiotic imbalance in heterozygotes. Rogers (1990) quantified allozyme variation among species of heteromyines and failed to resolve basal relationships, including those among the majority of *Heteromys* species. However, given what was known about the levels of genic and karyotypic variation within the wide ranging *H. desmarestianus*, previous workers predicted that this taxon likely represented a complex of several morphologically similar, but distinct species-level entities (Anderson 1999; Mascarello and Rogers 1988; Rogers 1986; 1989; 1990). This hypothesis has been supported by more recent investigations (Anderson *et al*. 2006; Anderson and Timm 2006), and based on first comprehensive analysis of sequence data, González (2005) recovered four clades formerly recognized as *H. desmarestianus* that she considered undescribed species, but cited the need for additional sampling.

Currently, 11 *Heteromys* species are recognized (Patton 2005), divided into three species groups (following Hall 1981): the *H. anomalus* group consisting of *H. anomalus*, *H. australis*, *H. oasicus*, and *H. teleus*; the *H. desmarestianus* group, consisting of *H. desmarestianus*, *H. goldmani*, *H. nubicolens*, and *H. oresterus*; and the monotypic *H. gaumeri* group. These 9 species are placed in the subgenus *Heteromys*, whereas *H. nelsoni* is arranged in the monotypic subgenus *Xylomys* (González 2005). *Heteromys*

catopterius recently was described by Anderson and Guitterez (in press), and is tentatively assigned to the *H. anomalus* group, bringing the total number of *Heteromys* species recognized to 11.

A number of species concepts and criteria have been developed over the past several decades (see for example Bradley and Baker 2001; Hey 2006; Wheeler 1999; Wiley and Mayden 2000), though few offer a framework with which species boundaries can be tested objectively. Fortunately, this area of systematics has seen renewed interest recently (see Sites and Marshall 2003; 2004; Wiens 2007), and while methods may not always agree, there has been progress toward objectively delimiting species boundaries. For example, the Wiens and Penkrot (WP—2002) method of species delimitation is a DNA tree-based approach in a hypothesis-testing framework. This approach is used in this study to make decisions at the species level, as it takes advantage of the more rapid coalescing time of mitochondrial DNA (mtDNA).

Thus, my objective is to provide a more clear resolution of relationships among *Heteromys* species and lineages, with focus on the *H. desmarestianus* group. I use increased taxon sampling as well as sequence data from five genetic markers (Cytochrome *b* [cyt *b*], Cytochrome oxidase I [CoI], Beta fibrinogen [*Fgb*-17], Engrailed II [*En2*], and Myosin heavy chain II [*Myh2*]) to estimate relationships among taxa and to test hypotheses of relationships developed by González (2005) and Rogers (1989). Additionally, I employ species delimitation methods to test whether monophyletic lineages are sufficiently unique to be considered species-level entities. Finally, I test biogeographical hypotheses to: 1) determine whether adaptation within *Heteromys* to new habitat types occurred once or more than once in different lineages; and 2) determine

whether colonization of South America by members of the genus *Heteromys* occurred once (e.g. monophyly of the *H. anomalus* group) or several times.

Materials and Methods

Taxon Sampling:

This study uses animals that were collected from natural populations and preserved as museum voucher specimens. Liver, spleen, kidney, heart, or lung tissue was removed from each individual and preserved in an ultralow freezer at -80°C or in 95% ethanol and maintained at -20°C. A sample representing *H. teleus* was a skin clip taken from a dried museum skin. Tissue samples of additional individuals were obtained via loans from cooperating museums and universities.

This study adds to the work of a previous investigator, González (2005). Her study included 123 specimens representing eight *Heteromys* and two *Liomys* species from 52 sampling localities, and she used sequence data from three genetic markers.

In the current study, sequence data for *Heteromys* specimens were obtained from 284 individuals representing 10 of 11 described species in the genus (*H. catopterius* is missing from this study), as well as several candidate species identified by González (2005). These specimens represent 88 collecting localities from Mexico, Belize, Guatemala, El Salvador, Nicaragua, Costa Rica, Panama, Venezuela, and Ecuador (Appendix). Figure 1 is a map of collecting localities showing the sampling sites included in this study.

Several taxa were used as outgroups for phylogenetic analyses. *Liomys irroratus*, *L. pictus*, and *L. spectabilis* were included as sister taxa to the genus *Heteromys*, as documented by Hafner *et al*. (2007), González (2005), and Rogers and Vance (2005). All *Liomys* (N=12) were collected in Mexico.

Molecular Data Collection:

Whole genomic DNA was extracted for each individual from the liver, kidney or spleen tissue (or skin for a single individual representing *H. teleus*) either preserved in 95% ethanol or frozen, using the Qiagen (Valencia, CA) DNeasy^{TM} Tissue Kit (Cat. No. 69504) and following the protocol for animal tissues (July 2006, pp 18-20). DNA was eluted with the manufacturer's AE buffer at a final volume of 200µl. Four microliters of DNA extraction product was electrophoresed on a 2.0% agarose gel stained with SYBR green to estimate the quality and amount of genomic DNA present.

PCR technique was used to amplify the entire cyt *b* gene using primers L14724 and H15915 (Irwin *et al*. 1991). Four internal primers were used for further amplification: CB3H (Palumbi 1996), MVZ16 (Smith and Patton 1993), H15149 (Irwin *et al*. 1991), and F1 (Whiting *et al*. 2003). Table 2 provides the PCR conditions used for all five genes or gene segments used in this study.

For a subset of individuals that represent the major clades based on cyt *b* sequence data analyses, additional genes or gene segments were sequenced following the hierarchical reduced sampling protocol of Morando *et al*. (2003). A second mtDNA gene, CoI, was amplified via PCR using primers CoI-5285F and CoI-6929R (Spradling *et al*. 2004). Five internal primers also were used for amplification and sequencing: MCo-173F, MCo-1345R, MCo-1480R (Hafner *et al*. 2007), CoI-R1, and CoI-F3 (this study). For both mtDNA genes, standard Taq polymerase (Promega –Madison, WI) was used with its accompanying salts and buffer.

Three nuclear introns also were amplified for the same subset of individuals using PCR technique. The seventh intron of the β-fibrinogen gene (*Fgb-17*) was amplified with

primers B17 (Wickliffe *et al*. 2003) and Fgb-571F (this study). Members of the genus *Heteromys* (and possibly more members of the heteromyid family) possess large, variably sized indels in *Fgb-17*, so specific primers were designed to amplify the portion of the intron that is homologous to other rodent *Fgb-17*. β-fibrinogen amplifications used Platinum Taq (Invitrogen – Carlsbad, CA) with pre-mixed buffer and salts. Engrailed protein 2 (*En2*) was amplified using 1:10 diluted DNA and the following primers, also diluted at a 1:10 ratio: EN2-F and EN2-R (Lyons *et al*. 1997). Similarly, myosin heavy chain 2 (*Myh2*) required 1:10 diluted DNA and primers: MYH2-F and MYH2-R (Lyons *et al*. 1997). For these last two PCRs, HotMaster Taq (Eppendorf – Westbury, NY), with its accompanying buffer and salts, worked best for amplification. Positive and negative controls were run with all amplifications.

Four microliters of double-stranded PCR product were assayed by electrophoresis on a 2% agarose gel. The remaining product (ca. 21µl) was purified using the Millipore (Billerica, MA) Multiscreen^{TM} PCR 96-Well Filtration System (Cat. No. MANU03050), and rehydrated with 25µl HPLC-H_20. All purified PCR products were then cycle sequenced using the Big Dye v3.1 Dye Terminator Cycle Sequencing Ready Reaction Kit (Applied Biosystems – Foster City, CA) with the same primers listed above for PCR amplification, all at a 1:10 dilution. Excess dye terminator was removed using a separation column made of a solution of Sephadex G50 in conjunction with Millipore (Billerica, MA) Multiscreen^{TM} Filter Plates for High Throughput Separations (Cat. No. MAHVN4510). Both strands of DNA fragments were sequenced in order to verify the accuracy of the sequenced nucleotides. Sequences were determined using the ABI 570

Genetic Analyzer (Applied Biosystems – Foster City, CA) located in the DNA Sequencing Center at Brigham Young University.

Sequence Alignment:

All sequences were compiled and edited using Sequencher v4.7 (Gene Codes Corporation, 2006). Base pairs exhibiting multiple peaks in the chromatographs of the nuclear markers were interpreted as heterozygous sites and coded as ambiguous characters. Manual alignment was possible with the Sequencher software for the cyt *b* and CoI genes, as well as the *En2* intron, as there were no insertion-deletions (indels) present. The *Myh2* intron contained only a single 1 base pair (bp) indel, and was also aligned manually. For the *Fgb-17* intron, alignment was less obvious due to variable-length indels. As a result, MAFFT (Katoh *et al*. 2005) and MUSCLE (Edgar 2004) programs were used to align these sequences. MAFFT multiple alignment software offers several general ways to align sequences, each differing in speed and accuracy. I employed the strategy that maximized accuracy rather than speed to obtain my *Fgb-17* alignment, and the iterative refinement method (L-INS-i) using the weighted sum-of-pairs (WSP) and consistency scores was selected by the automated program. This method (Katoh *et al*. 2005) undergoes four stages of alignment: (1) a distance matrix is made based on all pairwise alignments, (2) a guide tree is constructed, (3) progressive alignment, and (4) iterative refinement of the alignment using WSP scores (Gotoh 1995) and COFFEE-like scores (Notredame *et al*. 2000). MUSCLE is another multiple sequence alignment program, and it undergoes three stages of alignment: (1) an initial progressive alignment generated from a distance matrix, (2) refinement of the progressive alignment by generation of alternative trees and comparison of tree scores, and (3)

refinement of the alignment using a profile-profile alignment (Edgar 2004). MAFFT and MUSCLE produced very similar alignments, and I used the MAFFT alignment for all subsequent analyses.

In addition to multiple indels, *Fgb-17* also contained a poly-A region that varied in length among individuals. The varying lengths among taxa introduced gaps of different sizes, making statements of homology less clear. To clarify coding in this region, I removed a 10 bp portion from all *Fgb-17* sequences adjacent to the poly-A region so that the lowest common denominator of repeating adenines was still represented without the confusion of different sized gaps.

Phylogenetic Analyses:

Sequences were analyzed in Collapse v1.2 (available from http://darwin.uvigo.es) to identify redundant haplotypes in the cyt *b* data set. Redundant haplotypes were removed prior to data analysis. However, if redundant haplotypes represented different localities, at least one sequence was retained for each collecting location. In total, the cyt *b* data set was reduced from 284 to 156 individuals. Models of evolution were determined among 56 different models using ModelTest v3.7 (Posada and Crandall 1998) for cyt *b*, CoI, *Fbg-17*, *En2*, and *Myh2*. The Akaike information criterion (AIC) was used to obtain the best model and likelihood settings for each gene separately, as well as the combined data set comprised of five gene segments. Indels in the *Fgb-17* and *Myh2* markers were coded according to the simple indel coding (SIC) scheme outlined by Simmons and Ochoterena (2000) in the gap coding program SeqState (Müller 2005). Each SIC matrix was appended to its corresponding data matrix for *Fgb-17* and *Myh2* for use in Bayesian and parsimony analyses.

Maximum parsimony (MP) analyses were conducted in PAUP* v4.0 (Swofford 2002) as unweighted heuristic searches with 1000 random additions and TBR branch swapping. Separate analyses were conducted for each of the genetic markers individually, and also for a combined data set in which all five markers were concatenated into one data matrix. Two cyt *b* data sets were used for comparative analyses: the 156-taxon data set representing all unique haplotypes, and a 90-taxon data set that contained only specimens for which nuclear data also were available. All other single and multi-gene data sets were congruent, in that each represented the same 90 individuals. Nonparametric bootstrap values (Felsenstein 1985) also were obtained in PAUP* for each data set using 1000 pseudoreplicates and 100 random additions. Bootstrap values $\geq$70% were considered well supported (Hillis and Bull 1993). Partitioned Bremer supports (PBS) were generated for the most optimal five-gene MP tree in TreeRot v3 (Sorenson and Franzosa 2007). For the final parsimony search of 20 repetitions in the TreeRot protocol, the "maxtrees" setting was increased from its 100-tree default to 500 trees.

A maximum likelihood (ML) approach also was used to analyze the genetic markers for the independent and combined data sets. ML analyses were performed using the Garli v0.94 software (Zwickl 2006), and were set to autoterminate when resolution in log likelihood scores was <0.001 after 500 generations. The AIC model of evolution obtained from ModelTest v3.7 (Posada and Crandall 1998) was used in these analyses, and the parameters estimated in Garli. As the ML algorithm allows only one model of evolution, the most complex model, GTR+I+Γ, was employed for the combined analysis.

Bootstrap nodal support values were estimated in PhyML (Guindon and Gascuel 2003) using 1000 replicates.

Additionally, Bayesian inference (BI) was performed on individual genetic markers and on the combined data set using MrBayes v3.1 (Huelsenbeck and Ronquist 2001; Nylander *et al*. 2004). The appropriate AIC model of evolution was assigned for each analysis, as determined in ModelTest v3.7 (Posada and Crandall 1998). For the combined data set, a mixed-model Bayesian analysis was run using the appropriate model of evolution for each gene partition. Each data set was run twice for 20 million generations using Markov Chain Monte Carlo (MCMC) with four chains per run. Each run began with a random starting tree and trees were sampled every 2000 generations. Log-likelihood scores and standard errors from the log file were examined in Tracer v1.4 (Rambaut and Drummond 2007) to determine stationarity, and the first 20% of the trees were discarded as burn-in. Posterior probabilities were generated from the remaining trees in PAUP* v4.0 (Swofford 2002), using the 50% majority rule consensus tree function.

Hypothesis Testing:

Alternative phylogenetic hypotheses were tested under the maximum likelihood criterion. Tree searches were conducted with topology constraints designed to match each hypothesis. Differences in likelihood tree scores between all equally optimal trees from constrained searches were compared to overall optimal trees using the Shimodaira and Hasegawa test (S-H; Shimodaira and Hasegawa 1999) as implemented in PAUP* 4.0b10 (Swofford 2002). If topology constraints yielded likelihood tree scores

significantly worse than the optimal tree, with a $P \leq 0.05$, then this was considered strong evidence that the constraint did not represent a valid relationship.

Species Delimitation:

The WP (Wiens and Penkrot 2002) DNA tree-based approach was used to hypothesize species boundaries. This method takes advantage of the rapid coalescing time of mtDNA and it employs a dichotomous key approach to delimit species in a hypothesis-testing framework. Given a haplotype phylogeny for a selected set of populations currently classified as a species (the focal species), and one or more closely related species, the haplotype tree will show the focal species to be either exclusive (monophyletic) or nonexclusive by locality. A species is exclusive if no gene flow is detected between other lineages. If the selected haplotypes are recovered as strongly supported basal clades, which are exclusive by locality, then the terminal is considered distinct at the species level. Use of this method can identify species suggested by well-supported basal lineages that may have been previously overlooked when comparison of gross morphology was all that was taken into account. An important requirement of this method is the inclusion of two or more localities per "species," which is satisfied by my taxon sampling for all of the lineages represented in my study, except two.

Heteromys desmarestianus was selected as the focal species, as karyotypic (Rogers 1989), allozymic and morphological (Anderson *et al*. 2006), as well as DNA sequence data (González 2005) all suggested there were multiple species-level lineages in this complex. The WP method was used to delimit species at the deepest level of divergence in the combined data tree as well as the cyt *b* gene tree.

Results

Sequence Analysis:

The entire cyt *b* gene was sequenced for all 284 specimens represented in this study, including 10 outgroup taxa. Elimination of redundant haplotypes reduced the number of individuals to 156. Sequence data also was obtained for the entire CoI gene, and for *Fgb-17*, *En2*, and *Myh2* introns for 90 individuals (six of which were outgroup taxa) representing the majority of genetic diversity recovered from the analysis of the cyt *b* data set.

Alignment of the cyt *b* gene was trivial and yielded 1140 base pairs (bp), with 415 parsimony-informative characters and 33 variable non-informative characters across all taxa. The CoI alignment resulted in 1548 bp, with 534 parsimony-informative characters and 37 variable non-informative characters. For a number of *Heteromys* specimens (14 out of 90), the β-fibrinogen intron contained a large insertion adjacent to a poly-A region of hypervariable length. There were 19 indels [SeqState Simple Indel Coding (SIC) results] after the 10-character segment adjacent to the hypervariable poly-A region was removed. The aligned length of the *Fgb-17* intron was 878 bp, with 131 parsimony-informative characters and 51 variable non-informative characters. A data matrix with the 19 coded indels also was made for Bayesian analyses, and for this mixed-data matrix, there were 897 characters. The gene segment *En2* contained no indels, and was 146 bp in length with 12 parsimony-informative characters and 11 non-informative variable characters. The *Myh2* gene segment contained one indel (SeqState SIC results), and had an aligned length of 194 bp, with 20 parsimony-informative characters and 18 variable non-informative characters. A mixed-data matrix with the one coded indel for *Myh2* was

made for Bayesian analyses, and this resulted in 195 characters. The combined data set, with the concatenation of all five genetic markers (without the SIC matrices), generated a total alignment length of 3906 bp, with 1110 parsimony-informative characters and 148 variable non-informative characters.

Phylogenetic analysis of individual genes:

The cyt *b* data set generated a GTR+I+Γ model of evolution (ModelTest v3, AIC). The base frequencies were A=0.3357, C=0.3179, G=0.0526, and T=0.2938; transversion (tv) rates were (A-C)=0.3095, (A-G)=10.9957, (A-T)=0.6564, (C-G)=0.6514, (C-T)=6.5711, (G-T)=1.0000; the proportion of invariable sites (I) was 0.5009, and the gamma distribution shape parameter (Γ) was 0.8524. ML analysis of the 156-taxon cyt *b* data set yielded a single tree (lnL= -12597.68), with moderate-to-high bootstrap support for the majority of ingroup clades (Figure 2). MP analysis of the same data set also yielded a single best tree of 2530 steps (not shown; consistency index [CI]=0.272, retention index [RI]=0.864) with a topology very similar to that generated by the ML analysis. The ML and MP tree topologies also were congruent, in terms of the major internal nodes, to the trees (not shown) generated from the cyt *b* data set containing 90 specimens, each represented by the four additional genetic markers (see below). The BI cyt *b* tree (not shown) had a similar topology to the ML tree depicted in Figure 2, but with an unresolved polytomy among the clades B, C, D/E, and the remaining *desmarestianus* species group taxa (clade A, *H. oresterus*, *H. nubicolens*, *H. goldmani*, and *H. desmarestianus*). Gene tree topologies for the cyt *b* data set were congruent with those of González (2005), in that *H. anomalus*, *H. australis*, *H. gaumeri*, and *H. nelsoni* consistently were recovered as monophyletic clades with high support, and were basal to

those lineages belonging to the *H. desmarestianus* species group (*H. desmarestianus*, *H. goldmani*, *H. nubicolens*, and *H. oresterus*).

The model of evolution selected for the CoI gene also was GTR+I+Γ. (A=0.3346, C=0.2377, G=0.0978, and T=0.3298; tv rates [A-C]=0.6479, [A-G]=13.5460, [A-T]=1.1534, [C-G]=0.3841, [C-T]=10.7976, [G-T]=1.0000; I=0.6025; Γ=1.4551.) ML analysis of this gene produced a topology (lnL= -13624.48) similar to the cyt *b* gene tree, but with better resolution and higher nodal support values (Figure 3). MP analysis generated a single best tree of 2715 steps (CI=0.317, RI=0.793); this tree and the BI tree (both not shown) were identical to the ML topology.

The β-fibrinogen gene segment was analyzed using BI and ML optimality criteria under the GTR+Γ model of evolution. (A=0.2824, C=0.2320, G=0.2165, and T=0.2691; tv rates [A-C]=1.7847, [A-G]=4.8225, [A-T]=1.0700, [C-G]=2.0396, [C-T]=6.4067, [G-T]=1.0000; Γ=0.9373.) BI analysis was run for 10 million generations with and without a simple indel-coding (SIC) matrix, and the resulting trees yielded the same topology and similar pP values for both Bayesian analyses. Topologies were largely congruent for this gene segment among the ML, BI, and MP analyses. Figure 4 shows the ML topology (lnL= -2917.20) for *Fgb-17*, with bootstrap and pP support values mapped onto the nodes (pP values reported here are from the Bayesian analysis that included the SIC matrix). In each analysis, *H. nelsoni* was recovered as sister to the *anomalus* species group rather than basal. This relationship is supported by high bootstrap, but relatively low pP values. *Fgb-17* data generally support relationships among the deeper nodes in the tree, including *H. nelsoni* and the *anomalus* and *gaumeri* groups, but is less well resolved for all species

in the *desmarestianus* group (*H. desmarestianus*, *H. goldmani*, *H. nubicolens*, and *H. oresterus*).

The *En2* data set was analyzed under a K81uf+I+Γ model of evolution. (A=0.2636, C=0.3192, G=0.3026, and T=0.1145; tv rates [A-C]=1.0000, [A-G]=5.5079, [A-T]=2.2816, [C-G]=2.2816, [C-T]=5.5079, [G-T]=1.0000; I=0.9072; Γ=0.7251.) The ML topology produced (lnL= -405.52) is illustrated in Figure 5. Here, the *H. anomalus* species group (*H. anomalus*, *H. australis*, *H. oasicus*, and *H. teleus*) maintained its relatively basal position within the genus *Heteromys*. However, *Liomys* is arranged as polyphyletic, with three of the six *Liomys* taxa nested within the *Heteromys* clade. Overall, the *En2* gene segment yielded little phylogenetic resolution, as both the ML and BI searching methods resulted in trees containing several large polytomies. MP analysis was not conducted for *En2* because the intron contained relatively few parsimony-informative characters, resulting in excessive computation time.

The *Myh2* sequence data was analyzed using ML and BI criteria under a TrN+Γ model of evolution. (A=0.2706, C=0.2697, G=0.3117, and T=0.1479; tv rates [A-C]=1.0000, [A-G]=3.6270, [A-T]=1.0000, [C-G]=1.0000, [C-T]=10.0306, [G-T]=1.0000; Γ=0.4071.) The *Myh2* gene segment also yielded relatively little phylogenetic signal as evidenced in the results of the ML and BI analyses. However, ML analysis of this gene segment produced a tree (lnL= -566.97) that did recover several basal clades (Figure 6). *Liomys irroratus* was recovered as the most basal species, whereas *L. pictus* and *L. spectabilis* were arranged as a sister group to the genus *Heteromys*. Within *Heteromys*, however, there was no resolution among terminals.

Phylogenetic analysis of the combined data set:

The combined data set contained 90 specimens with a total aligned sequence length of 3906 bp. For ML analysis, the most complex model of evolution, GTR+I+Γ, was chosen (A=0.3041, C=0.2669, G=0.1433, and T=0.2857; tv rates [A-C]=1.5331, [A-G]=11.8479, [A-T]=2.6823, [C-G]=1.4379, [C-T]=21.7754, [G-T]=1.0000; I=0.5155; Γ=0.7611), whereas BI analysis involved a mixed-model analysis in which each gene partition was assigned its own model of evolution, as determined by ModelTest (cyt *b* and CoI = GTR+I+Γ; *Fgb-17* = GTR+Γ; *En2* = K81uf+I+Γ; *Myh2* = TrN+Γ). Figure 7 depicts the ML tree (lnL= -30181.07) with bootstrap and pP values mapped onto the nodes. Under both likelihood and Bayesian criteria, the same topology was recovered with relatively high nodal support values. MP analysis produced 26 equally parsimonious trees (5443 steps, not shown; CI=0.330, RI=0.789), which were congruent with the ML and BI topologies. In addition to ML bootstrap values and pP supports, Partitioned Bremer Support (PBS) values also were mapped onto the nodes (Figure 7—cyt *b*/CoI/*Fgb-17*/*En2*/*Myh2*).

Trees from ML, BI, and MP analyses each recovered a trichotomy among three clades representing outgroup and ingroup taxa as follows: (1) *L. irroratus*, (2) *L. pictus* and *L. spectabilis,* and (3) all *Heteromys* species. Within *Heteromys, H. nelsoni* was recovered as the most basal species. In turn, three clades within *Heteromys*, each with strong nodal support, were recovered. One clade consisted of the South American taxa (*H. anomalus, H. australis, H. oasicus* and *H. teleus*), a second was represented by *H. gaumeri*, and the third was comprised of the *H. desmarestianus* complex (*H. desmarestianus, H. goldmani, H. nubicolens,* and *H. oresterus*—Figure 7).

Heteromys teleus was recovered as the sister taxon to *H. australis* with high nodal support. Within *H. australis* there was a subdivision between the Ecuadorian and Panamanian specimens of this species. The clade containing *H. teleus* and *H. australis* was sister to *H. anomalus*, and *H. oasicus* did not show genetic differentiation from *H. anomalus*. Specimens of *H. gaumeri* were recovered as a monophyletic clade, sister to the *desmarestianus* complex.

Specimens representing desmarestianus clades D and E consistently were arranged as sister taxa with high nodal support. The node connecting clade C to other *Heteromys* taxa had relatively lower bootstrap support, but high pP support (pP=0.99); PBS indicated that only the CoI gene gave support to this node. Clade B also had high nodal support, and *H. nubicolens* and *H. oresterus* were always recovered as sister taxa relative to clade A.

Heteromys goldmani was placed sister to *H. desmarestianus* sensu stricto. Within *H. desmarestianus* three distinct groupings were recovered, which generally follow the geographic locations of the collecting localities. These groupings were as follows: 1-Costa Rica and Nicaragua, 2-Mainland Mexico, and 3-the Yucatan Peninsula region.

Hypothesis testing:

A-priori hypotheses were tested using topology constraints and the Shimodara-Hasegawa statistical test. Table 3 summarizes the results of the fifteen hypotheses tested. A topological constraint that yielded a likelihood tree score significantly worse than the optimal tree, with a $P \leq 0.05$, was interpreted to depict an invalid relationship. All constraint tests resulted in a significantly less likely tree with the exceptions of tests 8, 10, 12, and 13 (see Table 3).

Species delimitation:

The WP dichotomous key methodology was applied to the five-gene tree topology (Figure 7). Based on this phylogentic estimate, *H. desmarestianus* is non-exclusive (paraphyletic) relative to one or more distinct, exclusive species (*H. goldmani*, *H. nubicolens*, and *H. oresterus*). This suggests that the *desmarestianus* complex houses multiple species, and five candidate species (designated as clades A through E in Figure 7) are recognized.

An important requirement of this method is the inclusion of two or more localities per candidate species. Because of this, the WP method could not be applied to clade E for the combined data tree because there was only one terminal that represented this clade. However, the 156-terminal cyt *b* tree (Figure 2) included three clade E specimens (samples 73, 78, and 79; see Appendix), and when the WP method was applied to this gene tree topology, clade E animals were found to be exclusive by locality, suggesting that these mice represent a distinct haplotype clade.

Discussion

Relationships among species of Heteromys

Heteromys nelsoni consistently was recovered as the most basal clade relative to the remaining *Heteromys* taxa (Figures 2, 3, 4, and 7). This species occurs in cloud forest habitats, as do *H. nubicolens* and *H. oresterus*. All three species share the morphological feature of less spiny pelage, presumably an adaptation to the colder conditions of cloud forests. In topology constraint tests forcing the monophyly of cloud forest species (Table 3, test 1), the resulting trees were significantly less likely. Therefore, the hypothesis that evolution for adaptation to cloud forest habitats occurred once is rejected. Instead, I hypothesize that an ecological shift to cloud forest habitats from low- or mid-elevation forest habitats occurred independently in the common ancestor of the *H. nubicolens*/*H. oresterus* clade. Anderson *et al*. (2006) recovered *H. nelsoni* as sister to *H. oresterus*. In contrast, Rogers' phenetic analysis of allozyme, karyotypic, and morphological characters (1986; 1989; 1990) found that *H. nelsoni* either clustered with *H. desmarestianus*, *H. goldmani* and *H. oresterus* (exclusive of the *H. anomalus* group), or formed its own basal lineage. Based on the results of this study and those of González (2005), I support maintaining *H. nelsoni* in the monotypic subgenus *Xylomys.*

The *H. anomalus* group (*H. anomalus, H. australis, H. oasicus*, and *H. teleus*) represents a second, basal clade, with strong nodal support from cyt *b* and *Fgb-17* sequences (ML bootstrap>95% and pP>0.95 for both). CoI and *En2* also recovered this monophyletic group as basal, but with lower support values. This arrangement of the *anomalus* group is supported by combined cladistic analysis of morphological and allozyme data by Anderson *et al*. (2006), but is discordant with allozyme results of

Rogers (1990), which revealed no affinity between *H. anomalus* and *H. australis* (his study did not include *H. catopterius*, *H. oasicus*, or *H. teleus*). González (2005) included only *H. anomalus* and *H. australis* in her analyses, but also recovered these two taxa as a basal, monophyletic group. *Heteromys australis* is restricted in its distribution, known only from low- to middle-elevation localities in eastern Panama, western Colombia and northern Ecuador (Anderson 2003); at higher elevations in eastern Panama it is replaced by *H. anomalus* (Rogers 1986), which also occurs in Colombia, Venezuela, and Ecuador (Anderson 2003). Forcing non-monophyly of the *anomalus* group resulted in significantly less-likely trees (Table 3, test 2). Therefore, the most parsimonious explanation for colonization of South America by progenitors of the *anomalus* group suggests that it occurred once.

For the entity described by Anderson (2003) as *H. oasicus*, neither mitochondrial nor nuclear sequence data provide evidence of reciprocal monophyly between it and *H. anomalus*. As a result, *H. oasicus* is not distinct genealogically. However, *H. oasicus* is morphologically and ecologically diagnosable from adjacent populations of *H. anomalus*, and apparently *H. oasicus* is geographically isolated, as it occurs only on the Península de Paraguaná in Venezuela (sample 84, Figure 1). Given the lack of genetic differentiation exhibited by *H. oasicus*, it is likely that morphological and ecological divergence in *H. oasicus*, as described by Anderson (2003), occurred relatively recently. I therefore recommend that *H. oasicus* be relegated to subspecific status within *H. anomalus*.

Heteromys catopterius, a new species described from Venezuela by Anderson and Gutiérrez (in press), occurs in sympatry with *H. anomalus*. Pending sequence data to address the phylogenetic affinities of this taxon, I hypothesize that one of the two

phyletic groups within what is now considered *H. anomalus*, as documented by González (2005) and results presented herein, corresponds to this newly described species (note the structure of the *H. anomalus* clade in Figure 7).

Heteromys gaumeri was recovered as the sister clade to the *H. desmarestianus* species group in most analyses with strong nodal support (ML bootstrap=98, pP=1.0). Additionally, *H. gaumeri* showed no close relationship with the *H. desmarestianus* complex in allozyme or morphological analyses (Anderson *et al*. 2006; Rogers 1986; 1990), and has a unique karyotype (2n=56; FN=76). Based on phylogenetic analysis of sequence data, González (2005) concluded that this species was distinct from, and sister to the *H. desmarestianus* complex. Results of this study also are supportive of the recommendation by Engstrom *et al*. (1987) that *H. gaumeri* belongs in a species group of its own.

Species-level phylogenetics in the* H. desmarestianus *complex

As presently recognized, *H. desmarestianus* is not an exclusive species. Given that animals now recognized as *H. desmarestianus* are paraphyletic relative to *H. goldmani*, *H. nubicolens* and *H. oresterus* (see Figure 7), the first approach should be to determine whether these three lineages merit species-level status. If not, then the *H. desmarestianus* complex could be viewed as a wide-ranging species with high levels of genetic, karyotypic, morphological, and ecological diversity. The range of *H. desmarestianus* is very broad, spanning nearly 2,000 km from southern Mexico to northern South America (Rogers 1986; Williams *et al*. 1993), and previous studies have consistently suggested subdivisions in this species (Anderson *et al*. 2006; Rogers 1986; 1989; 1990). I will address the species-level status of *H. goldmani* first.

Rogers (1986) found that *H. goldmani* averaged larger than *H. desmarestianus* in many cranial features, and Rogers and Schmidly (1982) noted that *H. goldmani* had a smaller, more rounded baculum, and generally had darker pelage without the pronounced sprinkling of ochraceous hairs typical of *H. desmarestianus*. While these features fall within the range of morphological variation of *H. desmarestianus* from southern Mexico, other evidence would suggest that *H. goldmani* is distinct at the species-level. For instance, Rogers (1990) found that although *H. goldmani* did not differ significantly from nearby populations of *H. desmarestianus* based on morphology, *H. goldmani* did have fixed allozyme differences relative to *H. desmarestianus* at two loci. Additionally, *H. goldmani* possesses a karyotype distinct from *H. desmarestianus* (Rogers 1989—Table 4). In this study, there was one instance of sympatry for *H. desmarestianus* and *H. goldmani* in Chiapas, Mexico (locality 36—see Appendix). However, *H. goldmani*, from Chiapas, consistently was recovered as a well-supported clade, distinct from nearby *H. desmarestianus* in Chiapas and Oaxaca, Mexico. These results are consistent with those of González (2005). Constraint tests that forced non-monophyly of *H. goldmani* relative to adjacent populations of *H. desmarestianus* resulted in significantly less likely trees (Table 3, test 5). Therefore, I regard *H. goldmani* as a species-level taxon, and recommend that it remain in the *H. desmarestianus* species group within the subgenus *Heteromys*.

My analyses consistently recovered *H. oresterus* (San José and Cartago provinces, Costa Rica) as the sister group to individuals of *H. nubicolens* from the nearby provinces of Guanacaste and Puntarenas, Costa Rica (Figure 7; see Appendix for localities), with strong nodal support in all gene trees. These results are consistent with those of González

(2005). *Heteromys oresterus* (2n=60, FN=78) also differed from *H. nubicolens* (2n=60, FN=86) karyotypically, and forcing non-monophyly of samples regarded as either *H. oresterus* or *H. nubicolens* resulted in significantly less likely trees (Table 3, tests 3 and 4). Based on this evidence, I retain *H. nubicolens* and *H. oresterus* as valid species, and recommend their retention in the *H. desmarestianus* complex within the subgenus *Heteromys*.

The *H. desmarestianus* species complex contains at least five clades (Figure 7) that likely represent candidate species. González (2005) first proposed candidate species A, B, C, and D, and this study adds candidate clade E. This study supports recognition of these clades as candidate species-level taxa, inasmuch as each of these lineages was determined by the WP method to be exclusive by locality, and thereby representative of distinct haplotypes and unique evolutionary lineages.

Clade A consistently was recovered as sister to the *H. oresterus*/*H. nubicolens* clade (see Figure 7). Both *H. oresterus* and *H. nubicolens* inhabit cloud forests, whereas samples representing clade A were collected in low- or mid-elevation forest habitats. Forcing non-monophyly of clade A resulted in a significantly less likely tree topology (Table 3, test 9). According to Rogers (1990), specimens representing clade A differ from examples of *H. nubicolens* by three fixed allozyme differences. Clade A specimens and *H. nubicolens* apparently possess the same standard karyotype but differ from *H. oresterus* (see Table 4). These data, coupled with González's genetic divergence results (2005), confirm that candidate species A should be considered for formal description and assignment of species-level status.

Specimens representing clade B were collected from low elevation localities in Veracruz and Oaxaca, Mexico, and clade C individuals were found in low elevation sites in the humid forests of the Chiriqui province in Panama as well as the Puntarenas province in Costa Rica. While there was some incongruence between cyt *b* and CoI gene trees regarding the relative placement of these two clades, each is a distinct phyletic entity. Topological constraint tests forcing monophyly of either clades B or C with *H. desmarestianus* proper were significantly less likely. However, constraint tests that forced the paraphyly of clades B and C (Table 3, tests 10-13) yielded several non-significant P values. Clearly, constraint test results do not support retaining clades B or C as *H. desmarestianus*. Rogers (1990) examined Costa Rican mice representing clade C, and found that compared to other *Heteromys* from Costa Rica, these specimens possessed at least two fixed allozyme differences. Likewise, specimens from low elevations in Veracruz and Oaxaca also differed from nearby samples of *Heteromys* by three fixed allozyme differences (Rogers 1990). In addition, mice representing both clades B and C possess karyotypes that differ in the number of bi-armed chromosomes (FN value) compared to other samples of *Heteromys* from Mexico and Costa Rica (Rogers 1989). Given these allozyme results in combination with the phylogenies recovered by González (2005) and in this study, I recognize clades B and C as candidate species B and C, respectively.

Clades D and E consistently are recovered as sister taxa and this clade always was well supported in the mitochondrial (both cyt *b* and CoI) and combined data analyses. However, the placement of this node shifted based on different analyses and optimality criterion used. Mice representing clade D were collected from two localities in the

Darién province in Panama, and clade E specimens came from three localities in the Panamanian province of Bocas del Toro. Topological constraint tests forcing monophyly of either clades D or E with *H. desmarestianus* proper were significantly less likely. Likewise, constraint tests forcing non-monophyly of this group generated significantly worse tree scores (Table 3, tests 14 and 15). Additionally, allozyme data are available for clade D, and it has fixed allelic differences relative to *H. desmarestianus* proper at 13 allozyme loci. These data, coupled with González's (2005) genetic divergence results for clade D, suggest that clades D and E should each be considered as candidate species pending formal species description.

Within *H. desmarestianus* sensu stricto, three distinct clades (Figure 7) consistently were recovered with high nodal support values. These groups were consistent with geography as follows: group 1, Costa Rica and Nicaragua; group 2, southern Mexico (Chiapas and Oaxaca); and group 3, the Yucatan Peninsula region (Mexican states of Quintana Roo and Campeche together with samples from Belize, Guatemala and El Salvador). Karyotypic variation exists among these three groups (FN values varying among 67, 68, 72, and 86—Rogers 1989; see Table 4), as well as some diversity in habitat preference. For example, mice with FN = 67 and 68 occur in upper humid tropical forests at elevations greater than 1000 m, whereas animals that possess FN = 72 or 86 are found in lowland tropical forests. Based on these differences, I predict that more species-level lineages ultimately will be recognized.

Recommendations for *Heteromys* taxonomy are summarized in Table 4. The two subgenera *Xylomys* and *Heteromys* are retained, with the former remaining monotypic (*H. nelsoni*). The subgenus *Heteromys* is divided into three species groups: the *H.*

anomalus group (*H. anomalus* [including *H. oasicus*], *H. australis*, and *H. teleus*); the *H. desmarestianus* group (*H. desmarestianus*, *H. goldmani*, *H. nubicolens*, *H. oresterus*, and candidate species A, B, C, D, and E); and the *H. gaumeri* group (*H. gaumeri*). I follow Anderson and Guitérrez (manuscript in press) in assigning *H. caropterius* to the *anomalus* group, pending phylogeny reconstruction using sequence data.

Given that many names are available either in synonymy or as subspecies of *H. desmarestianus*, it would be unwise to suggest formal name changes at this time. However, sequence data from topotypes would shed light on the appropriateness of names in synonymy for these candidate species.

Literature Cited

Allen, J. A., and F. M. Chapman. 1897. On mammals from Yucatan with descriptions of new species. Bulletin of the American Museum of Natural History 9:1-12.

Anderson, R. P. 1999. Evaluating predictive models of species' distributions: criteria for selecting optimal models. Ecological Modeling 162:211-232.

Anderson, R. P. 2003. Taxonomy, distribution, and natural history of the genus *Heteromys* (Rodentia: Heteromyidae) in western Venezuela, with the description of a dwarf species from the Peninsula de Paraguana. American Museum Novitates 3396:1-43.

Anderson, R. P., and V. P. Jarrín. 2002. A new species of spiny pocket mouse (Heteromyidae: *Heteromys*) endemic to Western Ecuador. American Museum Novitates 3382:1-26.

Anderson, R. P., and R. M. Timm. 2006. A new montane species of spiny pocket mouse (Rodentia: Heteromyidae: *Heteromys*) from Nothwestern Costa Rica. American Museum Novitates 3509:1-38.

Anderson, R. P., M. Weksler, and D. S. Rogers. 2006. Phylogenetic analyses of spiny pocket mice (Heteromyidae: Heteromyinae) based on allozymic and morphological data. Journal of Mammalogy 87:1218-1233.

Bradley, R. D., and R. J. Baker. 2001. A test of the genetic species concept: Cytochrome-b sequences and mammals. Journal of Mammalogy 82:960-973.

Edgar, R. C. 2004. MUSCLE: multiple sequence alignment with high accuracy and high throughput. Nucleic Acids Research 32:1792-1797.

Engstrom, M. D., H. H. Genoways, and P. K. Tucker. 1987. Morphological variation, karyology, and systematic relationships of *Heteromys gaumeri* (Rodentia: Heteromyidae). Pages 289-303 *in* Studies in Neotropical mammalogy: essays in honor of Philip Hershkovitz. Fieldiana: Zoology, new series (B. D. Patterson, and R. M. Timm, eds.).

Felsenstein, J. 1985. Confidence-limits on phylogenies: an approach using the bootstrap. Evolution 39:783-791.

Genoways, H. H. 1973. Systematics and evolutionary relationships of spiny pocket mice, genus *Liomys*. Special Publications of the Museum, Texas Tech University 5:1-368.

Goldman, E. A. 1911. Revision of the spiny pocket mice (genera *Heteromys* and *Liomys*). North American Fauna 34:1-70.

González, M. 2005. Phylogenetic relationships of forest spiny pocket mice (Genus *Heteromys*) inferred from mitochondrial and nuclear markers with implications for species boundaries. M.S. thesis. Brigham Young University, Provo, Utah.

Gotoh, O. 1995. A weighting system and algorithm for aligning many phylogenetically related sequences. Computer Applications in the Biosciences 11:543-551.

Gray, J. E. 1868. Synopsis of the species of Saccomyinae, or pouched mice in the collection of the British Museum. Proceedings of the Zoological Society of London 1868:199-206.

Guindon, S., and O. Gascuel. 2003. PhyML: A simple, fast, and accurate algorithm to estimate large phylogenies by maximum likelihood. Systematic Biology 52:696-704.

Hafner, J. C., and M. S. Hafner. 1983. Evolutionary relationships of heteromyid rodents. Great Basin Naturalist 7:3-29.

Hafner, J. C., J. E. Light, D. J. Hafner, M. S. Hafner, E. Reddington, D. S. Rogers, and B. R. Riddle. 2007. Basal clades and molecular systematics of Heteromyid rodents. Journal of Mammalogy 88:1129-1145.

Harris, W. P., Jr. 1932. Four new mammals from Costa Rica. Occasional Papers of the Museum of Zoology, University of Michigan 248:1-6.

Hey, J. 2006. On the failure of modern species concepts. TRENDS in Ecology and Evolution 21:447-450.

Hillis, D. M., and J. J. Bull. 1993. An empirical test of bootstrapping as a method for assessing confidence in phylogenetic analysis. Systematic Biology 42:182-192.

Homan, J. A., and H. H. Genoways. 1978. An analysis of hair structure and its phylogenetic implications among heteromyid rodents. Journal of Mammalogy 59:740-760.

Huelsenbeck, J. P., and F. Ronquist. 2001. MRBAYES: Bayesian inference of phylogenetic trees. Bioinformatics 17:754-755.

Irwin, D. M., T. D. Kocher, and A. C. Wilson. 1991. Evolution of the cytochrome *b* gene in mammals. Journal of Molecular Evolution 32:128-134.

Katoh, K., K. Kuma, H. Toh, and T. Miyata. 2005. MAFFT version 5: improvement in accuracy of multiply sequence alignment. Nucleic Acids Research 33:511-518.

Lyons, L. A., T. F. Laughlin, N. G. Copeland, N. A. Jenkins, J. E. Womack, and S. J. O'Brien. 1997. Comparative anchor tagged sequences (CATS) for integrative mapping of mammalian genomes. Nature Genetics 15.

Mascarello, J. T., and D. S. Rogers. 1988. Banded chromosomes of *Liomys salvini*, *Heteromys oresterus*, and *H. desmarestianus*. Journal of Mammalogy 69:126-130.

Merriam, C. H. 1902. Twenty new pocket mice (*Heteromys* and *Liomys*) from Mexico. Proceedings of the Biological Society of Washington 15:41:50.

Morando, M., L., J. Avila, and J. W. Sites, Jr. 2003. Sampling strategies for delimiting species: Genes, individuals, and populations in the *Liolaemus elongatus-kriegi* complex (Squamata: Liolaemidae) in Andean-Patagonian South America. Systematic Biology 52:159-185.

Müller, K. 2005. SeqState: Primer design and sequence statistics for phylogenetic DNA datasets. Applied Bioinformatics 4:65-69.

Notredame, C., D. G. Higgins, and J. Heringa. 2000. T-Coffee: a novel method for fast and accurate multiple sequence alignment. Journal of Molecular Biology 302:205-217.

Nylander, J. A. A., F. Ronquist, J. P. Huelsenbeck, and J. L. Nieves-Aldrey. 2004. Bayesian phylogenetic analysis of combined data. Systematic Biology 53:47-67.

Ochoa-Gaona, S., and M. Gonzalez-Espinosa. 2000. Land use and deforestation in the highlands of Chiapas, Mexico. Applied Geography 20:17-42.

Palumbi, S. R. 1996. Nucleic acids I: The polymerase chain reaction. Pages 205-247 *in* Molecular systematics, 2nd ed. (D. M. Hillis, C. Moritz, and B. K. Mable, eds.). Sinauer, Sunderland, Massachusetts.

Patton, J. L. 2005. Family Heteromyidae. Pages 477-485 *in* Mammal Species of the World: a taxonomic and geographic reference, 2nd ed. (D. E. Wilson, and D. M. Reeder, eds.). Washington, DC: Smithsonian Institution Press.

Patton, J. L., and D. S. Rogers. 1993. Cytogenetics. Pages 236-258 *in* Biology of the Heteromyidae. Special Publications, American Society of Mammalogists (H. H. Genoways and J. H. Brown, eds.).

Posada D., and K. A. Crandall. 1998. Modeltest: testing the model of DNA substitution. Bioinformatics 14:817-818.

Rambaut, A., and A. J. Drummond. 2007. Tracer v1.4: MCMC trace analysis tool. University of Edinburgh and University of Auckland. (http://tree.bio.ed.ac.uk/software/tracer/)

Reid, F. A. 1998. A Field Guide to the Mammals of Central America and Southeast Mexico. Oxford University Press.

Rogers, D. S. 1986. Evolutionary relationships within the family Heteromyinae (genera *Heteromys* and *Liomys*). Ph.D. dissertation, 256 pgs. University of California, Berkeley.

Rogers, D. S. 1989. Evolutionary implications of chromosomal variation among spiny pocket mice, genus *Heteromys* (Order Rodentia). The Southwestern Naturalist 34:85-100.

Rogers, D. S. 1990. Genic evolution, historical biogeography, and systematic relationships among spiny pocket mice (subfamily Heteromyinae). Journal of Mammalogy 71:668-685.

Rogers, D. S., and V. L. Vance. 2005. Phylgenetics of spiny pocket mice (genus *Liomys*): analysis of cytochrome *b* based on multiple heuristic approaches. Journal of Mammalogy 86:1085-1094.

Rogers, D. S., and D. J. Schmidly. 1982. Systematics of spiny pocket mice (Genus *Heteromys*) of the *desmarestianus* species group from Mexico and Northern Central America. Journal of Mammalogy 63:375-386.

Schmidly, D. J., K. T. Wilkens, and J. N. Derr. 1993. Biogeography. Pages 319-356 *in* Biology of the Heteromyidae. Special Publications, American Society of Mammalogists (H. H. Genoways, and J. H. Brown, eds.).

Shimodaira, H., and M. Hasegawa. 1999. Multiple comparisons of log-likelihoods with applications to phylogenetic inference. Molecular Biology and Evolution 16:1114-1116.

Simmons, M. P., and H. Ochoterena. 2000. Gaps as characters in sequence-based phylogenetic analyses. Systematic Biology 49:369-381.

Sites, J. W., Jr., and J. C. Marshall. 2003. Delimiting species: a renaissance issue in systematic biology. TRENDS in Ecology and Evolution 18:462-470.

Sites, J. W., Jr., and J. C. Marshall. 2004. Operational criteria for delimiting species. Annual Review of Ecology and Evolutionary Systematics 35:199-227.

Smith, M. F., and J. L. Patton. 1993. The diversification of South American muroid rodents: evidence from mitochondrial DNA sequence data for the akodontine tribe. Biological Journal of the Linnaean Society 50:149-177.

Sorensen, M. D., and E. A. Franzosa. 2007. TreeRot, version 3. Boston University, Boston, MA.

Spradling T. A., S. V. Brant, M. S. Hafner, and C. J. Dickerson. 2004. DNA data support a rapid radiation of pocket gopher genera (Rodentia: Geomyidae). Journal of Mammalian Evolution 11:105-125.

Swofford, D. L. 2002. PAUP*: Phylogenetic analysis using parsimony (*and other methods). Version 4.0b10. Sinauer Associates, Sunderland, Massachusetts, USA.

Thomas, O. 1901. New South American *Sciuri, Heteromys, Cavia,* and *Caluromys*. Annals and Magazine of Natural History 7:192-196.

Thompson, J. W. 1815. Description of a new species of the genus *Mus*, belonging to the section of pouched rats. Transactions of the Linnaean Society, London 11:161-163.

Wahlert, J. H. 1993. The fossil record. Pages 1-37 *in* Biology of the Heteromyidae. Special Publication, American Society of Mammalogists (H. H. Genoways, and J. H. Brown, eds.).

Wheeler, Q. D. 1999. Why the phylogenetic species concept? Elementary. Journal of Nematology 31:134-141.

Whiting, A. S., A. M. Bauer, and J. W. Sites, Jr. 2003. Phylogenetic relationships and limb loss in sub-Saharan African scincine lizards (Squamata: Scincidae). Molecular Phylogenetics and Evolution 29:583-598.

Wickliffe, J. K., F. G. Hoffmann, D. S. Carroll, Y. V. Dunina-Barkovshaya, R. D. Bradley, and R. J. Baker. 2003. Intron 7 (*FGB*): a nuclear DNA phylogenetic marker for mammals. Occasional Papers, Museum Texas Tech University 219:1-6.

Wiens, J. J. 2007. Species delimitation: new approaches for discovering diversity. Systematic Biology 56:875-878.

Wiens, J. J., and T. A. Penkrot. 2002. Delimiting species using DNA and morphological variation and discordant species limits in spiny lizards (Sceloporus). Systematic Biology 51:69-91.

Wiley, E. O., and R. Mayden. 2000. The evolutionary species concept *in* Species Concepts and Phylogenetic Theory: A Debate (Q.D. Wheeler and R. Meier, eds.). Columbia University Press.

Williams, D. F., H. H. Genoways, and J. K. Braun. 1993. Taxonomy. Pages 38-196 *in* Biology of the Heteromyidae. Special Publications, American Society of Mammalogists (H. H. Genoways, and J. H. Brown, eds.).

Wood, A. E. 1935. Evolution and relationships of the heteromyid rodents with new forms from the Tertiary of western North America. Annals of Carnegie Museum 24:73-262.

Yang, Z. 1997. PAML: a program package for phylogenetics analysis by maximum likelihood. Computer Applications in the Biosciences 13:555-556.

Zwickl, D. J. 2006. Genetic algorithm approaches for the phylogenetic analysis of large biological sequence datasets under the maximum likelihood criterion. Ph.D. dissertation, The University of Texas at Austin. www.bio.utexas.edu/faculty/antisense/garli/Garli.html

Table 1: Chronology of species descriptions in the genus *Heteromys*. The following species are currently recognized as valid (Patton 2005; Anderson and Timm 2006; Anderson and Gutiérrez [in press]).

Year	Author	Species	Common Name	Distribution
1815	Thompson	*Mus anomalus* (= *H. anomalus*)	Caribbean spiny pocket mouse	Colombia, Venezuela, Trinidad, Tobago
1868	Gray	*H. desmarestianus*	Desmarest's spiny pocket mouse	Southern Mexico to Colombia
1897	Allen & Chapman	*H. gaumeri*	Gaumer's spiny pocket mouse	Mexico, Guatemala, Belize
1901	Thomas	*H. australis*	Southern spiny pocket mouse	Panama, Colombia, Ecuador, Venezuela
1902	Merriam	*H. goldmani*	Goldman's spiny pocket mouse	Mexico, Guatemala
		H. nelsoni (subgenus *Xylomys*)	Nelson's spiny pocket mouse	Mexico, Guatemala
1932	Harris	*H. oresterus*	Mountain spiny pocket mouse	Costa Rica
2002	Anderson & Jarrín-V	*H. teleus*	Ecuadorian spiny pocket mouse	Ecuador
2003	Anderson	*H. oasicus*	Paraguaná spiny pocket mouse	Northern Venezuela
2006	Anderson & Timm	*H. nubicolens*	Dark-tailed spiny pocket mouse	Costa Rica
in press	Anderson & Gutiérrez	*H. catopterius*	Overlook spiny pocket mouse	Northern Venezuela

Table 2: PCR conditions used for cytochrome *b* (cyt *b*), Cytochrome oxidase I (CoI), Intron 7 of β-fibrinogen (*Fgb-17*), Engrailed II protein (*En2*), and Myosin heavy chain II (*Myh2*). Final volume = 25µl. MM = Master Mix. See text for primer sources.

Gene	PCR conditions	Primer	Primer sequence
cyt *b*	94°/3min | 39 cycles: 94°/1min; 50°/1min, 72°/1min | 72°/3min 24µl MM + 1µl DNA	L14724 H15915 CB3H MVZ16 H15149 F1	5'-CGA AGC TTG ATA TGA AAA ACC ATC GTT G-3' 5'-AAC TGC AGT CAT CTC GGG TTT ACA AGA C-3' 5'-GGC AAA TAG GAA RTA TCA TTC-3' 5'-TAG GAA RTA TCA YTC TGG TTT RAT-3' 5'-AAA CTG CAG CCC CTC AGA ATG ATA TTT GTC CTC A-3' 5'-TGA GGA CAR ATA TCH TTY TGR GG-3'
CoI	94°/2min | 4 cycles: 94°/1min; 47°/1min, 72°/1min | 34 cycles: 94°/1min; 54°/1min, 72°/1min | 72°/10min 24µl MM + 1µl DNA	CoI-5285F CoI-6929R MCo-173F MCo-1345R MCo-1480R CoI-R1 CoI-F3	5'-CCY CTG TNY TTA GAT TTA CAG TCT A-3' 5'-ACA ARG TTA TGT AAT DDT TTT ACT A-3' 5'-TAT TAG GNG AYG AYC ARA T-3' 5'-TGT TGW GGG AAR AAD GTT A-3' 5'-GCT TCT CAR ATT ATR WAR ATT AT-3' 5'-ATG TAR ACT TCA GGG TGA C-3' 5'-GAT CWT TMT TAA TTA CTG CTG-3'
Fgb-17	85° Hot Start | 94°/10min | 32 cycles: 94°/1min; 65°/1min, 72°/1min 19.36µl MM + 3µl DNA + 2.64µl dNTP Mix	B17 Fgb-571F	5'-ACC CCA GTA GTA TCT GCC GTT TGG AT-3' 5'-CGT AGC CTT GTG CTT GCA ATA G-3'
En2	94°/10min | 32 cycles: 94°/1min; 57°/1min, 72°/1min 12.5µl MM + 12.5µl DNA (1:10)	EN2-F EN2-R	5'-CCC GAA AAC CAA AGA AGA AG-3' 5'-GTT CTG GAA CCA AAT CTT GAT C-3'
Myh2	85° Hot Start | 94°/10min | 32 cycles: 94°/1min; 62°/1min, 72°/1min 9.85µl MM + 12.5µl DNA (1:10) + 2.64µl dNTP Mix	MYH2-F MYH2-R	5'-GAA CAC CAG CCT CAT CAA CC-3' 5'-TGG TGT CCT GCT CCT TCT TC-3'

Table 3: Shimodaira-Hasegawa test results for topological constraints representing *a priori* hypotheses. Optimal Maximum Likelihood tree score for the combined data set was lnL= -35175.59. P-values less than 0.05 were considered significant (bolded).

Hypothesis	Log Score Difference	P-value
1. Force monophyly of cloud forest species (*H. nelsoni*, *H. oresterus*, and *H. nubicolens*)	287.23	**<0.0001**
2. Force non-monophyly of SA taxa (*H. anomalus* group)	66.84	**<0.0001**
3. Force non-monophyly of *H. nubicolens*	201.02	**<0.0001**
4. Force non-monophyly of *H. oresterus*	192.12	**<0.0001**
5. Force non-monophyly of *H. goldmani*	74.93	**<0.0001**
6. Force non-monophyly of *H. teleus*	51.90	**<0.0001**
7. Force monophyly of *H. anomalus* relative to *H. oasicus*	128.40	**<0.0001**
8. Force monophyly of the two clades recovered for *H. anomalus* relative to *H. oasicus*	5.06	0.3028
9. Force non-monophyly of clade A.	72.23	**0.0002**
10. Force non-monophyly of clade B relative to clade C	24.14	0.0656
11. Force non-monophyly of clade B relative to *nubicolens*/*oresterus*/clade A	57.20	**0.0018**
12. Force non-monophyly of clade C relative to clade D/E	8.79	0.2408
13. Force non-monophyly of clade C relative to clade D only	32.43	0.0772
14. Force non-monophyly of clade D relative to clade E	282.64	**<0.0001**
15. Force non-monophyly of clade D/E relative to clade C	56.12	**0.0036**

Table 4: Taxonomic recommendations for *Heteromys*, together with karyotypic data (2n = diploid number; FN = fundamental number) as reported in Rogers (1989), Patton and Rogers (1993), Anderson and Timm (2006) and Anderson *et al*. (2006).

Genus *Heteromys*	Standard karyotype
Subgenus *Heteromys*	
H. anomalus group	
H. anomalus	
H. a. anomalus	2n=60, FN=68
H. a. oasicus	Unknown
H. australis	Unknown
*H. catoperius**	Unknown
H. teleus	Unknown
H. desmarestianus group	
H. desmarestianus	2n=60, FN=67, 68, 72, 86
H. goldmani	2n=60, FN=78
H. nubicolens	2n=60, FN=86
H. oresterus	2n=60, FN=78
Candidate species A	2n=60, FN=86
Candidate species B	2n=60, FN=82, 86
Candidate species C	2n=60, FN=90
Candidate species D	Unknown
Candidate species E	Unknown
H. gaumeri group	
H. gaumeri	2n=56, FN=76
Subgenus *Xylomys*	
H. nelsoni	2n=42, FN=72

*No sequence data for *H. catopterius* were available for this study; assignment of this species is tentative.

Figure 1: Map of Mexico and Central America with an insert of northern South America. Dots indicate collecting localities of *Heteromys*. Triangles are collecting locations of *Liomys*. Collecting sites of *H. teleus* (locality no. 60), a single *H. australis* from Ecuador (locality no. 85), and outgroup taxa are not shown. Numbers correspond to localities as listed in the Appendix.

Figure 2: Phylogram (lnL= -12597.68) generated from ML analysis of the cyt *b* data set with 156 samples (redundant haplotypes omitted from this analysis) representing 10 *Heteromys* species, and selected *Liomys* taxa designated as outgroups. ML bootstrap support values (based on 1000 iterations) and BI pP values (based on 50% majority rule for the consensus tree) have been mapped onto the major nodes with relatively strong support. Bootstrap values $\geq$70 are above branches; pP values $\geq$0.95 are represented by a dot.

Figure 3: Phylogram (lnL= -13624.48) generated from ML analysis of the CoI data set with 90 taxa representing 10 *Heteromys* species, and selected *Liomys* taxa as the outgroups; nodal support values and symbols are as in Fig. 2.

Figure 4: Phylogram (lnL= -2917.20) generated from ML analysis of the 7th intron of the β-fibrinogen (*Fgb-17*) data set with 90 samples representing 10 *Heteromys* species, and selected *Liomys* taxa designated as outgroups. Clades labeled A-E correspond to the five *H. desmarestianus* clades, as denoted in Figs. 2 and 3; nodal support values and symbols are as in Fig. 2.

Figure 5: Phylogram (lnL= -405.52) generated from ML analysis of the *En2* data set with 90 taxa representing 10 *Heteromys* species, and selected *Liomys* taxa designated as outgroups. Clades labeled A-E correspond to the five *H. desmarestianus* clades, as denoted in Figs. 2 and 3; nodal support values and symbols are as in Fig. 2.

Figure 6: Phylogram (lnL= -566.97) generated from ML analysis of the *Myh2* data set with 90 taxa representing 10 *Heteromys* species, and selected *Liomys* taxa designated as outgroups. Clades labeled A-E correspond to the five *H. desmarestianus* clades, as denoted in Figs. 2 and 3; nodal support values and symbols are as in Fig. 2.

Figure 7: Phylogram (lnL= -30181.07) generated from ML analysis of the combined (5-gene) data set with 90 taxa representing 10 *Heteromys* species, and selected *Liomys* taxa designated as outgroups; nodal support values and symbols are as in Fig. 2. Additionally, PBS values are below the branches to show partitioned support for each node (cyt *b*/CoI/*Fgb-17*/*En2*/*Myh2*). Within *H. desmarestianus*, there are three monophyletic clades that correspond to geography: 1=Costa Rica and Nicaragua, 2=Mainland Mexico, and 3=Yucatan Peninsula region.

Figure 1

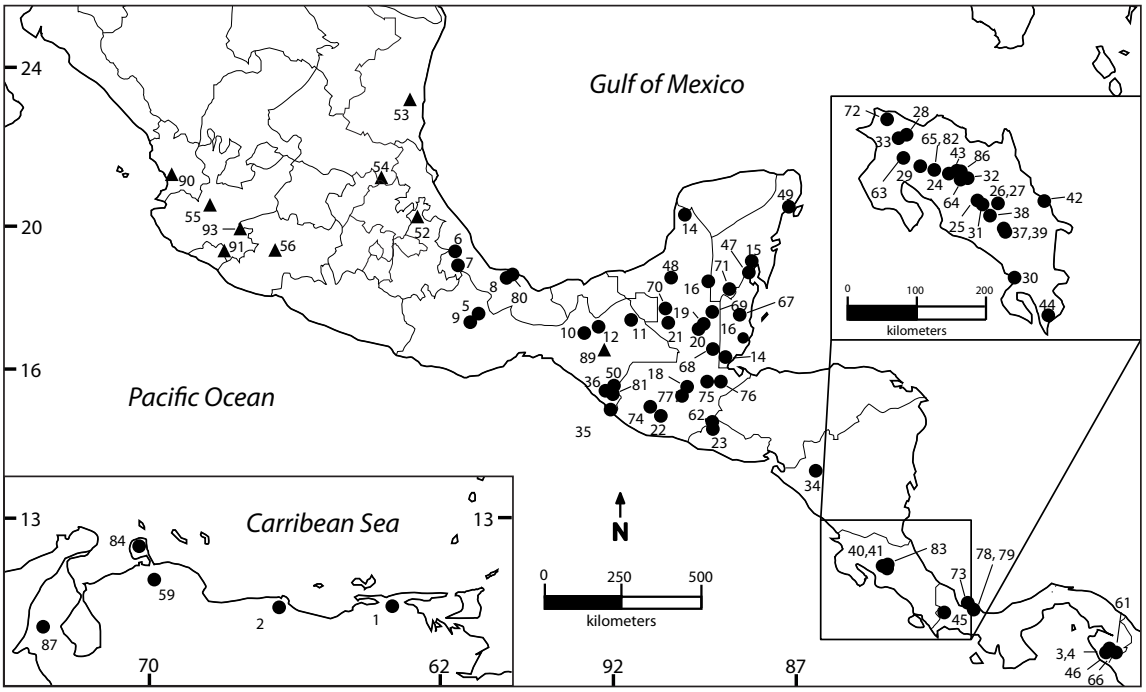
Gulf of Mexico
Pacific Ocean
Carribean Sea
N
0 250 500
kilometers
0 100 200
kilometers
24
20
16
13
70
62
92
87

Figure 2

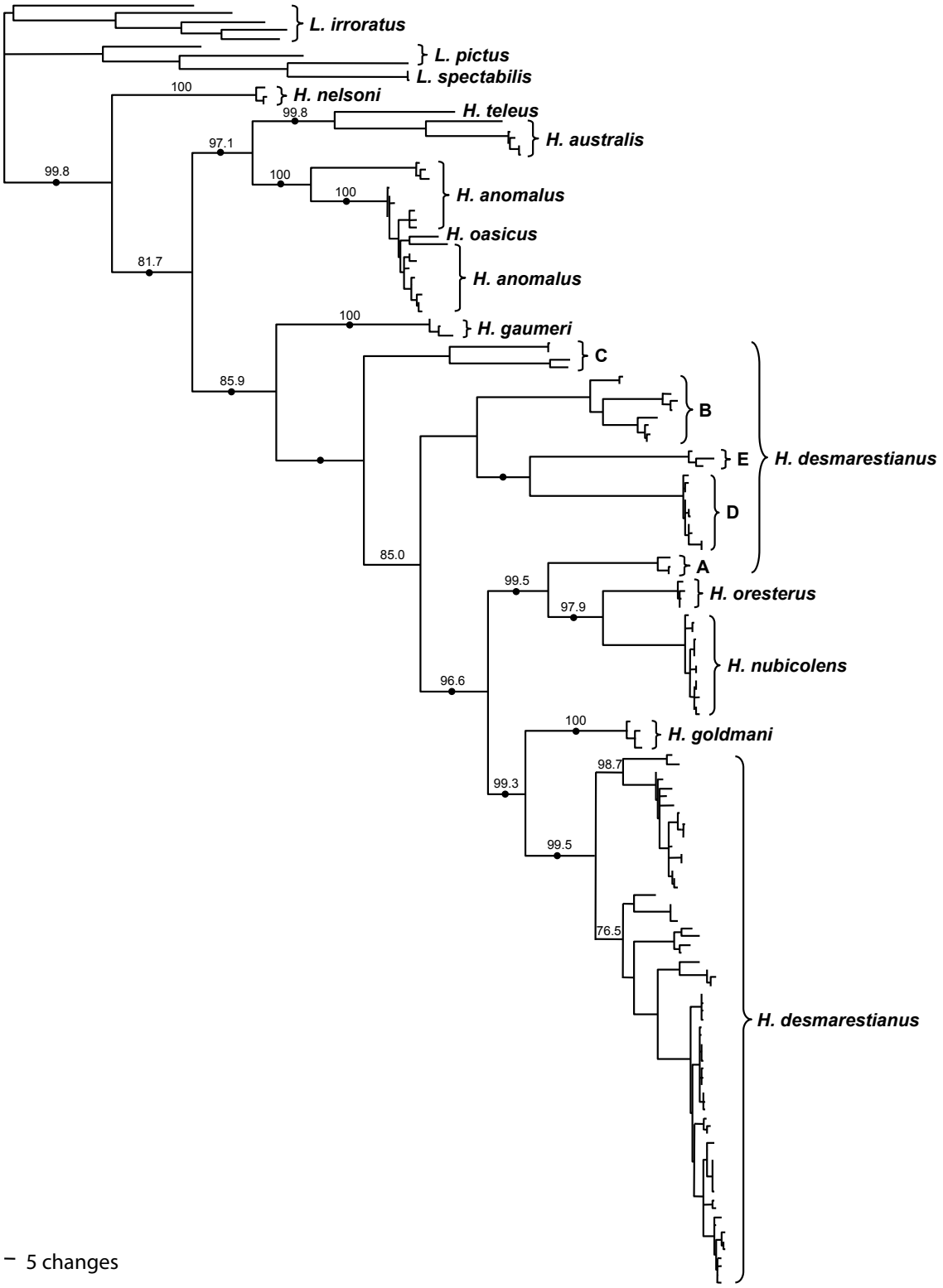
L. irroratus
L. pictus
L. spectabilis
H. nelsoni
H. teleus
H. australis
H. anomalus
H. oasicus
H. anomalus
H. gaumeri
C
B
E
D
A
H. desmarestianus
H. oresterus
H. nubicolens
H. goldmani
H. desmarestianus
100
99.8
97.1
99.8
100
100
81.7
100
85.9
85.0
99.5
97.9
96.6
100
98.7
99.3
99.5
76.5
5 changes

Figure 3

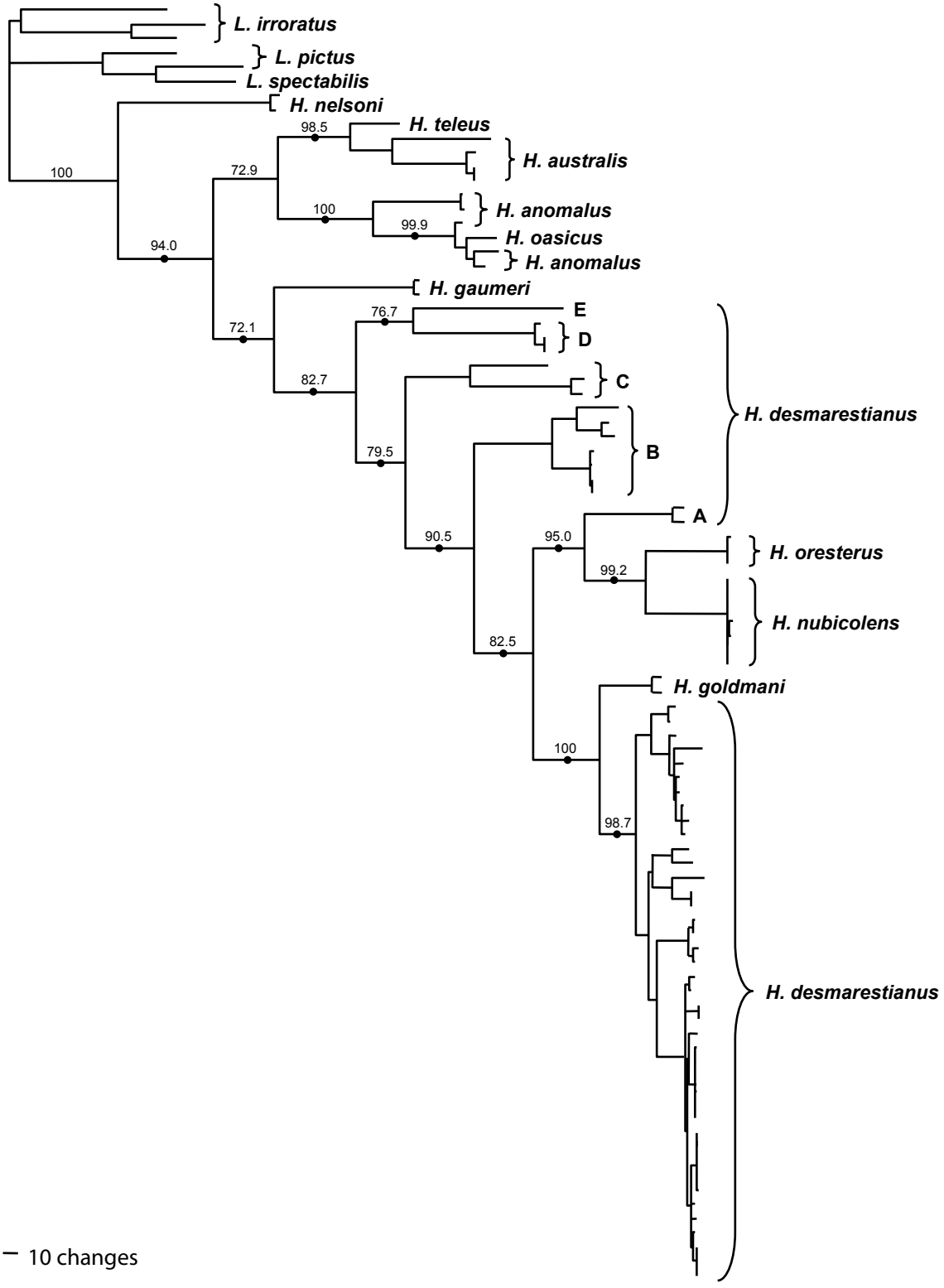
L. irroratus
L. pictus
L. spectabilis
H. nelsoni
H. teleus
H. australis
H. anomalus
H. oasicus
H. anomalus
H. gaumeri
E
D
C
B
A
H. desmarestianus
H. oresterus
H. nubicolens
H. goldmani
H. desmarestianus
98.5
100
72.9
100
99.9
94.0
72.1
76.7
82.7
79.5
90.5
95.0
99.2
82.5
100
98.7
10 changes

Figure 4

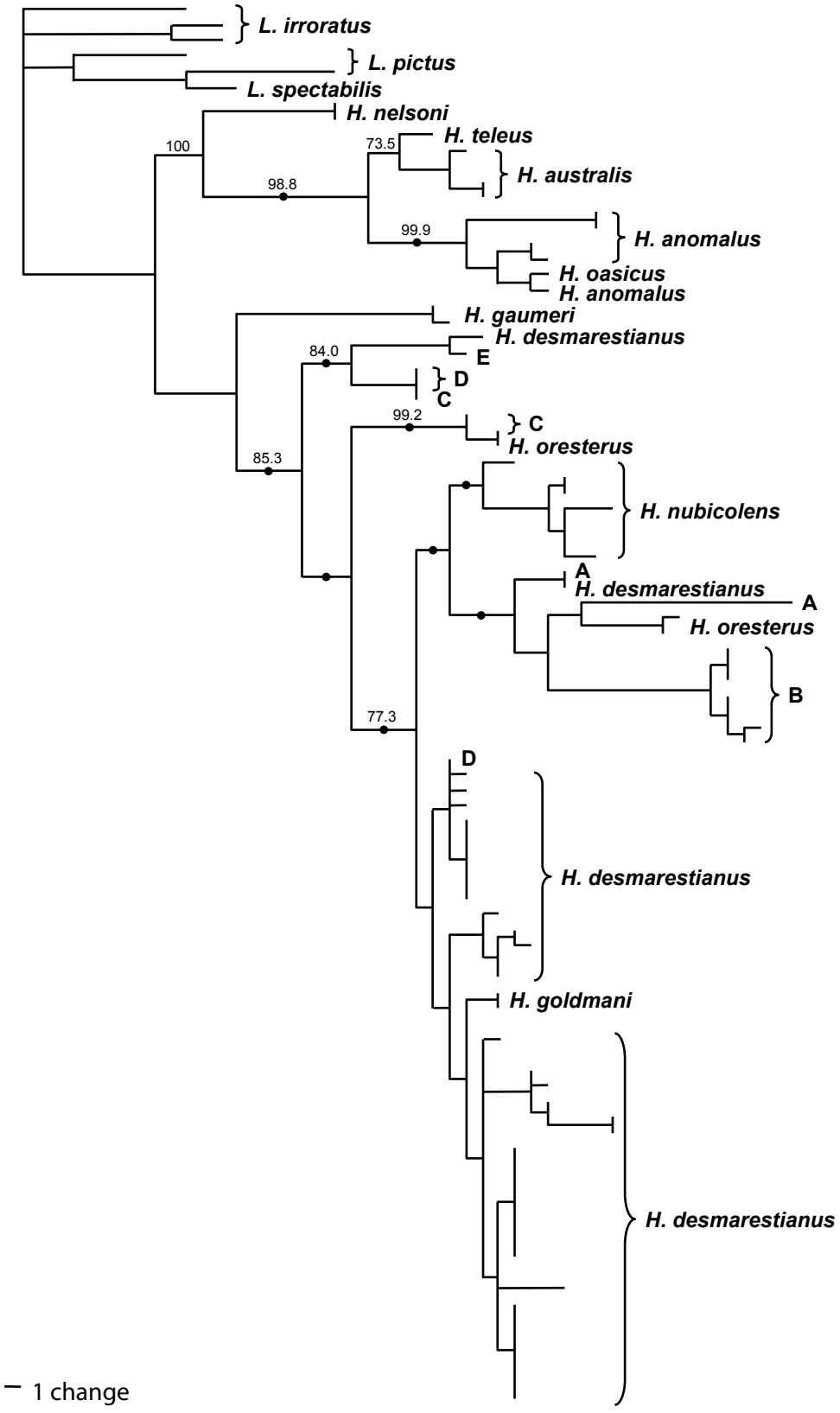
L. irroratus
L. pictus
L. spectabilis
H. nelsoni
H. teleus
H. australis
H. anomalus
H. oasicus
H. anomalus
H. gaumeri
H. desmarestianus
E
D
C
C
H. oresterus
H. nubicolens
A
H. desmarestianus
A
H. oresterus
B
D
H. desmarestianus
H. goldmani
H. desmarestianus
100
73.5
98.8
99.9
84.0
99.2
85.3
77.3
1 change

Figure 5

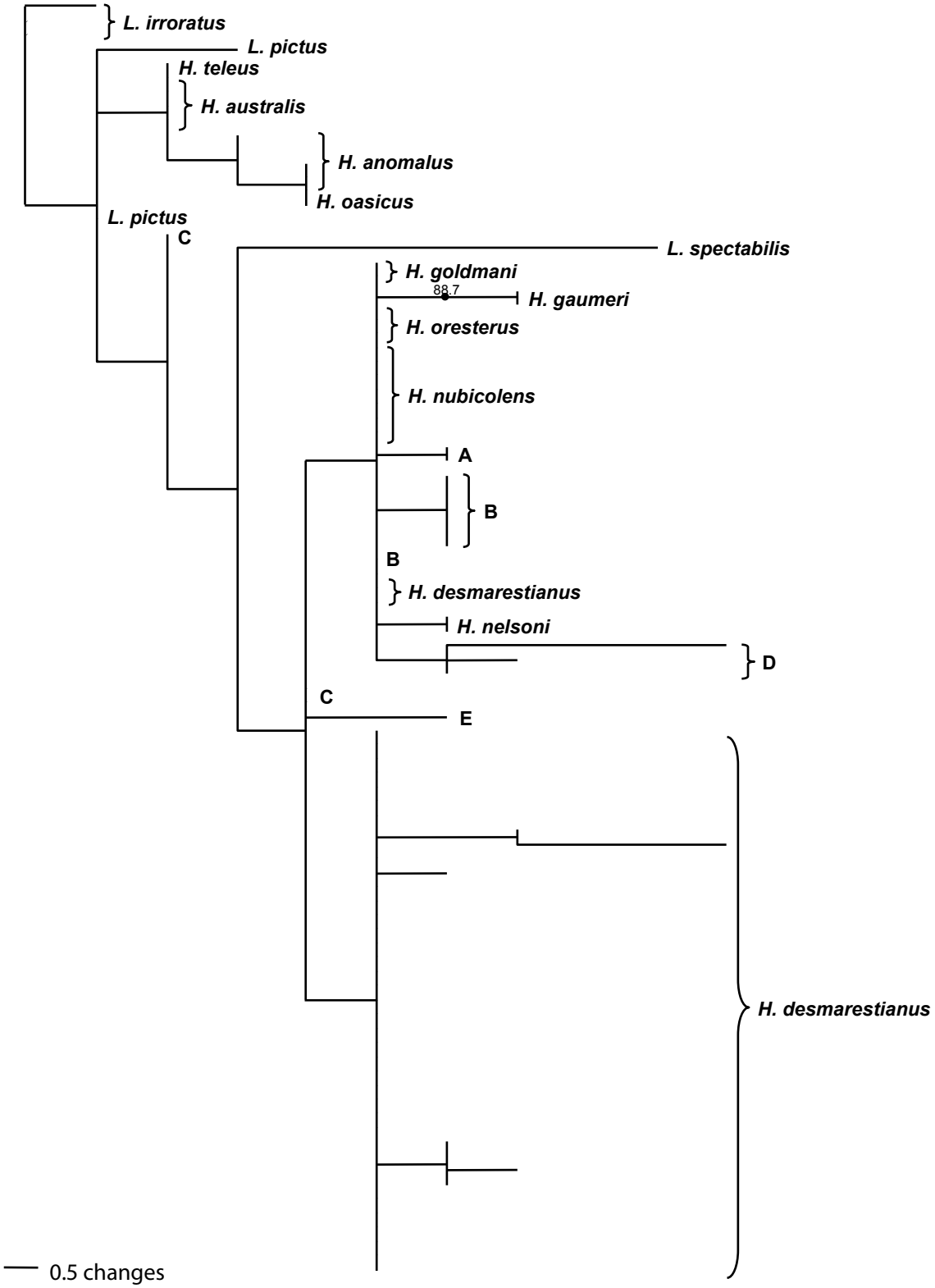
L. irroratus
L. pictus
H. teleus
H. australis
H. anomalus
H. oasicus
L. pictus
C
L. spectabilis
H. goldmani
88.7
H. gaumeri
H. oresterus
H. nubicolens
A
B
B
H. desmarestianus
H. nelsoni
D
C
E
H. desmarestianus
0.5 changes

Figure 6


L. irroratus
L. spectabilis
L. pictus
H. desmarestianus
H. desmarestianus
H. australis
H. desmarestianus
C
H. anomalus
92.8
H. anomalus
H. desmarestianus
H. australis
H. desmarestianus
H. goldmani
H. goldmani
H. anomalus
H. desmarestianus
80.7
E
H. desmarestianus
C
H. oasicus
H. desmarestianus
C
H. nelsoni
74.2
H. gaumeri
H. desmarestianus
71.3
88.3
D
H. anomalus
H. desmarestianus
A
B
H. teleus
B
H. nubicolens
H. oresterus
0.5 changes

Figure 7

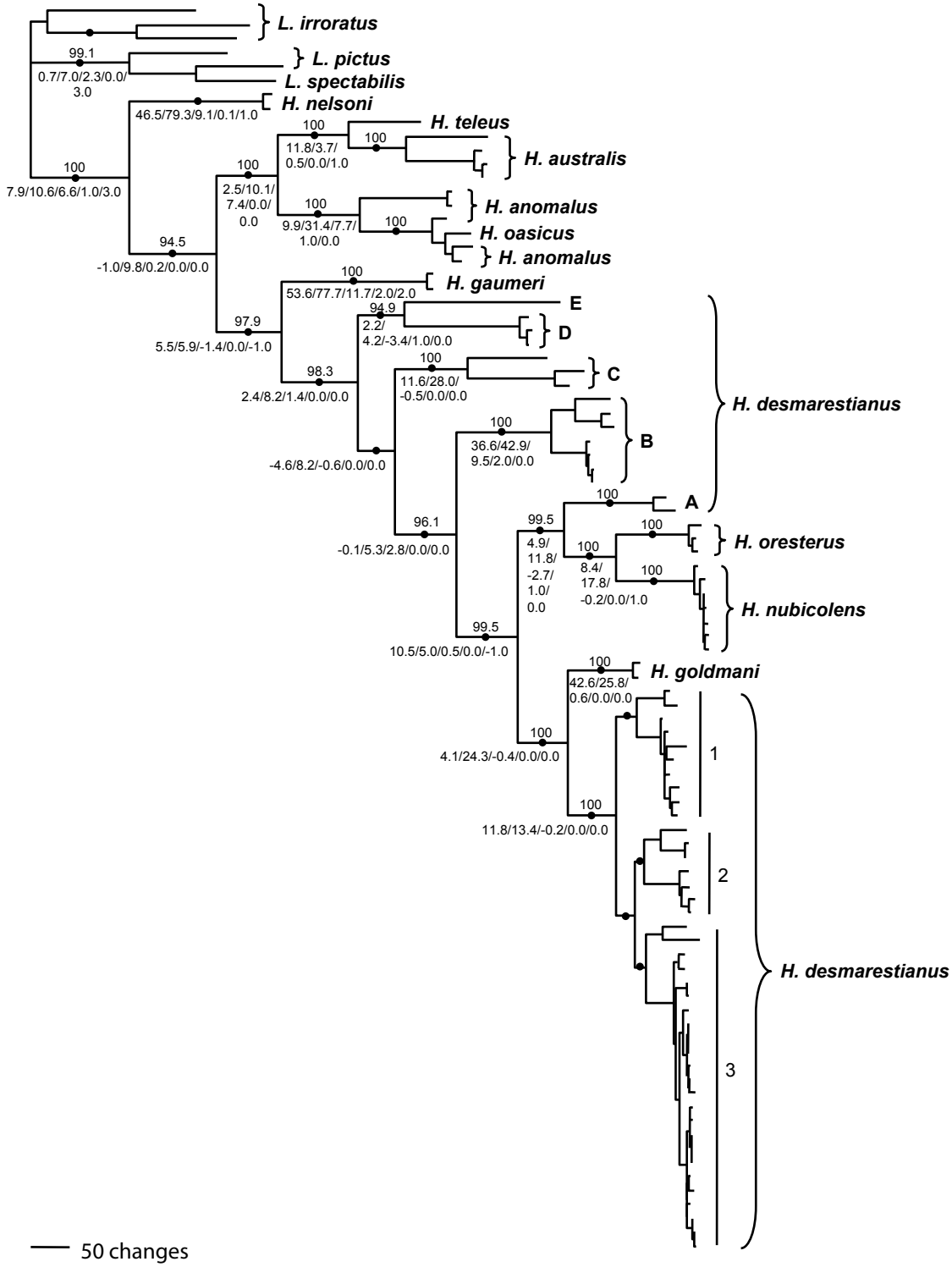
L. irroratus
L. pictus
L. spectabilis
H. nelsoni
H. teleus
H. australis
H. anomalus
H. oasicus
H. anomalus
H. gaumeri
E
D
C
B
A
H. desmarestianus
H. oresterus
H. nubicolens
H. goldmani
H. desmarestianus
1
2
3
99.1
0.7/7.0/2.3/0.0/
3.0
46.5/79.3/9.1/0.1/1.0
100
11.8/3.7/
0.5/0.0/1.0
100
100
7.9/10.6/6.6/1.0/3.0
100
2.5/10.1/
7.4/0.0/
0.0
100
9.9/31.4/7.7/
1.0/0.0
100
94.5
-1.0/9.8/0.2/0.0/0.0
100
53.6/77.7/11.7/2.0/2.0
94.9
2.2/
4.2/-3.4/1.0/0.0
97.9
5.5/5.9/-1.4/0.0/-1.0
100
11.6/28.0/
-0.5/0.0/0.0
98.3
2.4/8.2/1.4/0.0/0.0
100
36.6/42.9/
9.5/2.0/0.0
-4.6/8.2/-0.6/0.0/0.0
100
96.1
-0.1/5.3/2.8/0.0/0.0
99.5
4.9/
11.8/
-2.7/
1.0/
0.0
100
8.4/
17.8/
-0.2/0.0/1.0
100
100
100
99.5
10.5/5.0/0.5/0.0/-1.0
100
42.6/25.8/
0.6/0.0/0.0
100
4.1/24.3/-0.4/0.0/0.0
100
11.8/13.4/-0.2/0.0/0.0
50 changes

Appendix: List of taxa included in this study with locality number, collecting location (Country: Province: locality), and specimen identification numbers. Geographic abbreviations are as follows: BE = Belize; CR = Costa Rica; EC = Ecuador; ES = El Salvador; GU = Guatemala; MX = Mexico; NI = Nicaragua; PN = Panama; VZ = Venezuela. Locality numbers 1-56 are congruent with those of González and Rogers (manuscript in preparation—their locality #51 is not represented in this study), and localities 59-93 are new to this study. Museum abbreviations are as follows: AMNH = American Museum of Natural History; ASNHC = Angelo State Natural History Collections; BYU = Brigham Young University; CM = Carnegie Museum of Natural History; CMC = Collecion de Mamiferos CEAMISH (Centro de Educación Ambiental e Investigación Sierra de Huautla), Universidad Autónoma del Estado de Morelos; EBRG = Estación Biológica Rancho Grande; KU = Museum of Natural History, University of Kansas; LACM = Natural History Museum of Los Angeles County; LSUMZ = Louisiana State University Museum of Zoology; MVZ = Museum of Vertebrate Zoology; ROM = Royal Ontario Museum; TCWC = Texas Cooperative Wildlife Collection, Texas A&M University; USNM = National Museum of Natural History.

Locality No.	Current Name	Sampling Locality	Collector No.	Museum Voucher No.	Karyotype, Field, or Tissue No.
1	*H. anomalus*	VZ: Sucre: 40 km NW Caripito, 250 m, Andres Eloy Blanco	MDE 1999	CM 78166	AK 3411
	"	"	MDE 2033	CM 78167	AK 3436
	"	"	MDE 2034	CM 78168	AK 3437
	"	"	MDE 2062	CM 78169	AK 3449
2a	*H. anomalus*	VZ: Miranda: 25 km N Altagracia de Oricuto, 500 m, Acevedo	MDE 2087	CM 78170	AK 3468
	"	"	MDE 2091	TCWC 37494	AK 3472
	"	"	MDE 2130	CM 78172	AK 3483
2b	"	VZ: Miranda: 40 km N Altagracia de Oricuto, 500 m, Acevedo	MDE 2129	TCWC 39720	AK 3482
3	*H. australis*	PN: Darién: Cerro Pirre, Parque Nacional Darien		ROM 104356	F 38215
	"	"		ROM 104357	F 38216

4	*H. australis*	PN: Darién: abt. 6 km NW Cana, E slope Cerro Pirre, 1200 m	MSH 1187	LSUMZ 25452	TK 22565
5	Candidate species B	MX: Oaxaca: 23 mi. SSW (by road) Tuxtepec, 250 ft	DSR 936	AMNH 254697	AK 3110
6a	Candidate species B	MX: Veracruz: Ojo de Agua, 1400 ft	DSR 921	AMNH 254693	AK 3098
6b	Candidate species B	MX: Veracruz: Ojo de Agua, 600 m	EA 823	BYU 16042	
	"	"	EA 836	BYU 16043	
6c	Candidate species B	MX: Veracruz: Ojo de Agua	MDE 1010	AMNH 254694	
7	Candidate species B	MX: Veracruz: 1 mi. NW Motzorongo, 700 ft	DSR 922	CM 79532	AK 3099
	"	"	DSR 923	CM 79533	AK 3100
8	*H. desmarestianus*	MX: Veracruz: near Los Tuxtlas	HD1	-99	
9a	*H. desmarestianus*	MX: Oaxaca: Vista Hermosa, 1000 m	DSR 934	CM 79530	AK 3108
9b	*"*	MX: Oaxaca: Vista Hermosa, Distrito Ixtlán, 1000 m	DSR 1685	MVZ 161229	
10a	*H. desmarestianus*	MX: Chiapas: 12 km N (by road) Berriozábal	ASK 660	ASNHC 1424	
	"	"	ASK 689	ASNHC 1425	
	"	"	MDE 5003	ASNHC 3515	LAF 1689
10b	"	MX: Chiapas, Pozo de Petroleo, 7 mi. N (by road) Berriozábal	DSR 1686	MVZ 161230	
11a	*H. desmarestianus*	MX: Chiapas: 12.5 km S Palenque		ROM 96096	FN 29887
	"	"		ROM 96105	FN 29896
11b	*H. desmarestianus*	MX: Chiapas: 1.2 km E Ruinas de Palenque	ASK 29	ASNHC 1440	
	"	"	ASK 31	ASNHC 1441	
11c	*H. desmarestianus*	MX: Chiapas: 9 km S Palenque	ASK 49	ASNHC 5826	
11d	*H. desmarestianus*	MX: Chiapas: 6.6 km S Palenque	ASK 51	ASNHC 1426	
12a	*H. desmarestianus*	MX: Chiapas: 6 km E Rayon		ROM 97542	FN 33018
12b	*H. desmarestianus*	MX: Chiapas: 9 km SE Rayon	ASK 589	ASNHC 1431	
	"	"	ASK 591	ASNHC 1432	
13	*H. desmarestianus*	MX: Campeche: 25 km N Xpujil		ROM 96089	FN 29880

14	*H. desmarestianus*	MX: Campeche: 10 km N El Refugio		ROM 97050	FN 30853
	"	"		ROM 97051	FN 30854
	"	"		ROM 97052	FN 30855
	"	"		ROM 97053	FN 30856
15	*H. desmarestianus*	MX: Quintana Roo: 1 km N Noh-Bec		ROM 97520	FN 30995
	"	"		ROM 97521	FN 30996
	"	"		ASNHC 7051	FN 32561
	"	"		ASNHC 7052	FN 32562
16a	*H. desmarestianus*	BE: Stann Creek Dist: 7.7 km WNW Quam Bank, Cockscomb Basin		CM 91960	AK 7664
	"	"		CM 91951	AK 7665
16b	*H. desmarestianus*	BE: Stann Creek Dist: 6.8 km WNW Quam Bank, Cockscomb Basin		CM 91980	AK 7688
16c	*H. desmarestianus*	BE: Stann Creek Dist: 3.4 km WNW Quam Bank, Cockscomb Basin		CM 91988	AK 7663
17a	*H. desmarestianus*	BE: Toledo Dist: 1 km NNE Salamanca, Forestry Camp, Columbio Forest Reserve		CM 91991	AK 7540
17b	*H. desmarestianus*	BE: Toledo Dist: 2.4 km NNW Salamanca, Forestry Camp, Columbio Forest Reserve		CM 91989	AK 7555
17c	*H. desmarestianus*	BE: Toledo Dist: 2.1 km NNE Salamanca, Forestry Camp, Columbio Forest Reserve		CM 91994	AK 7586
	"	"		CM 91993	AK 7588
	"	"		CM 91995	AK 7589
18	*H. desmarestianus*	GU: Baja Verapaz: 5 km E Puruhla		ROM 98405	FN 31394
	"	"		ROM 98406	FN 31395
	"	"		ROM 98407	FN 31396
	"	"		ROM 98408	FN 31397
	"	"		-99	FN 31402
19	*H. desmarestianus*	GU: El Peten: Tikal		ROM 99292	FN 31842

	"	"		ROM 99293	FN 31843
	"	"		ROM 99294	FN 31844
20	*H. desmarestianus*	GU: El Peten: Biotope Cerro Cahui, El Remate		ROM 99639	FN 32211
	"	"		ROM 99603	FN 32272
	"	"		ROM 99604	FN 32273
	"	"		ROM 99605	FN 32274
21	*H. desmarestianus*	GU: El Peten: Campo los Guacamayos, 40 km N Biotopo Laguna del Tigre		ROM 99469	FN 32318
	"	"		ROM 99504	FN 32353
22	*H. desmarestianus*	GU: Sacatepequez: 5 km W San Miguel Duenas		ROM 98265	FN 31254
	"	"		ROM 98266	FN 31255
	"	"		ROM 98267	FN 31256
	"	"		ROM 98269	FN 31258
23	*H. desmarestianus*	ES: Santa Ana: Parque Nacional Montecristo, Bosque Nebuloso, 2,200 m		ROM 101369	F 35547
	"	"		ROM 101389	F 35567
	"	"		ROM 101390	F 35568
24	*H. desmarestianus*	CR: Alajuela: 10 km E Sucre, Parque Nacional, Juan Castro Blanco		ROM 113310	F 48617
	"	"		ROM 113311	F 48618
25	*H. desmarestianus*	CR: Cartago: Iztaru: Cerros de la Carpintera		ROM 113130	F 48436
	"	"		ROM 113131	F 48437
	"	"		ROM 113132	F 48438
26	*H. desmarestianus*	CR: Cartago: Catie: 4 km SE (by road) Turrialba, 600 m	FAR 111	ROM 97324	
	"	"	FAR 112	ROM 97325	
	"	"	FAR 113	ROM 97326	

	"	"	FAR 114	ROM 97327	
27	*H. desmarestianus*	CR: Cartago: Río Reventazón, 5.6 km SE (by road) Turrialba, 450 m	DSR 2153	MVZ 164823	
	"	"	DSR 2154	MVZ 164824	
	"	"	DSR 2166	MVZ 164825	
	"	"	DSR 2167	MVZ 164826	
	"	"	DSR 2246	MVZ 164827	
28	*H. desmarestianus*	CR: Guanacaste: Volcán Santa Maria		ROM 113245	F 48552
29a	*H. desmarestianus*	CR: Guanacaste: 5.0 km NE (by road) Tilarán, 650-675 m	DSR 2121	MVZ 164839	
	"	"	DSR 2122	MVZ 164840	
	"	"	DSR 2145	MVZ 164842	
	"	"	DSR 2235	MVZ 164843	
29b	*H. desmarestianus*	CR: Guanacaste: 4.1 km NE (by road) Tilarán, 650 m	DSR 2123	MVZ 164828	
	"	"	DSR 2124	MVZ 164829	
	"	"	DSR 2125	MVZ 164830	
	"	"	DSR 2134	MVZ 164831	
	"	"	DSR 2138	MVZ 164832	
30	*H. desmarestianus*	CR: Puntarenas: 1 km N, 5 km W Palmar Norte	MSH 1260	LSUMZ 28354	M-1833
31	*H. desmarestianus*	CR: San José: Bajo de Iglesia, SW Volcán Irazu, Cascajal de Coronado	EA 21	BYU 15197	
	"	"	EA 22	BYU 15198	
32	*H. desmarestianus*	CR: San José: Parque Nacional Braulio Carillo, Moravia Cerro Honduras	EA 78	BYU 15195	
	"	"	EA 79	BYU 15196	
33	*H. desmarestianus*	CR: Guanacaste, Area de Conservación Guanacaste, ca. 20 km NNE Liberia, Pailas, Sendro Palas near Rio Colorado, 800 m	MK 00-112	KU 158615	

34	*H. desmarestianus*	NI: Esteli		ROM 112284	F 48170
35	*H. goldmani*	MX: Chiapas: 15.5 mi SE (by road) Mapastepec, 150 ft	MDE 1224	CM 79529	AK 3150
36	*H. desmarestianus*	MX: Chiapas: El Triunfo, 10 km SSE Finca Prusia	LJB 3108	LACM 74200	LAF 1773
	H. goldmani	"	LJB 3109	LACM 74201	LAF 1774
	"	"	MDE 5049	ASNHC 3523	LAF 1790
37	*H. oresterus*	CR: Cartago: Catie: 4 km (by road; Pan American Hwy) Villa Mills		ROM 102753	
38	*H. oresterus*	CR: San José: 2.2 km E (by road) La Trínidad de Dota, 2600 m	DSR 2092	MVZ 164861	
	"	"	DSR 2107	MVZ 164863	
	"	"	DSR 2244	MVZ 165786	
39	*H. oresterus*	CR: San José: Cerro la Muerte, San Gerardo de Dota		ROM 113208	F 48514
	"	"		ROM 113229	F 48535
40	*H. nubicolens*	CR: Guanacaste: Monteverde, Campbell's Woods	DSR 1744	MVZ 161224	
	"	"	DSR 1745	MVZ 161225	
41	*H. nubicolens*	CR: Puntarenas, Monte Verde Biological Station, elevation 1,655 m		ROM 113257	F 48564
42	Candidate species A	CR: Limón: 4.6 km W (by road) Limón, 25 m	DSR 2150	MVZ 164844	
	"	"	DSR 2151	MVZ 164845	
	"	"	DSR 2155	MVZ 164846	
	"	"	DSR 2163	MVZ 164847	
	"	"	DSR 2165	MVZ 164849	
	"	"	DSR 2245	MVZ 164851	
43	Candidate species A	CR: Alajuela: 7 km NE (by road) Quesada, 2297 m	DJH 2469	LSUMZ 26357	M-607

44	Candidate species C	CR: Puntarenas: 1.1 km SE (by road) Ciudad Nielly, 25 m	DSR 2193	MVZ 164852	
	"	"	DSR 2195	MVZ 164854	
	"	"	DSR 2222	MVZ 164865	
	"	"	DSR 2242	MVZ 164856	
45	Candidate species C	PN: Chiriqui: Ojo de Agua, 2 km N Santa Clara		ROM 104296	F 38147
	"	"		ROM 104297	F 38148
	"	"		ROM 104307	F 38158
	"	"		ROM 104308	F 38159
	"	"		ROM 104324	F 38175
	"	"		ROM 104325	F 38176
	"	"		-99	F 38177
	"	"		ROM 104326	F 38178
46	Candidate species D	PN: Darién: abt. 6 km NW Cana, E slope Cerro Pirre, 1400 m	DJH 2427	LSUMZ 25451	
47	*H. gaumeri*	MX: Quintana Roo: 7 km NE Xul-Ha		ASNHC 7127	FN 32575
	"			ASNHC 7128	FN 32576
48	*H. gaumeri*	MX: Campeche: 7 km N Escarcega		ASNHC 7118	FN 32736
49	*H. gaumeri*	MX: Quintana Roo: Puerto Morelos		ASNHC 7127	AJ 389536
50	*H. nelsoni*	MX: Chiapas: Cerro Mozotal, 2930 m	DSR 7181	CMC 391	
	"	"	DSR 7187	BYU 20643	
	"	"	DSR 7189	BYU 20644	
	"	"	DSR 7191	CMC 396	
	"	"	DSR 7212	CMC 398	
52	*L. irroratus*	MX: Puebla: 4 mi. SW Xicotepec de Juarez	MDE 986	CM 79450	AK 3083
53	*L. irroratus*	MX: Tamaulipas: 2.2 mi. N Soto la Marina	MDE 3280	TCWC 42044	AK 4335
	"	"	MDE 3284	TCWC 42048	AK 4339

54	*L. irroratus*	MX: San Luis Potosi: Rancho La Laja, 6 km W Xilitla, 785 m, Mpio. Xilitla	EA 223	BYU 15266	
55	*L. irroratus*	MX: Jalisco: Ameca	EA 816	BYU 16047	
56	*L. irroratus*	MX: Michocán: 10 km S (by road) Pátzcuro, 2200 m	DSR 5215	BYU 16052	
59a	*H. anomalus*	VZ: Falcón: Serranía de San Luis; Parque Nacional J.C. Falcón, Sector Cerro Galicia, ca. 10 km W 4 km N Cabure	JOG 4522	AMNH 276507 / EBRG 25308	
	"	"	RPA 253	EBRG 25386	
	"	"	RPA 261	EBRG 25311	
	"	"	RPA 265	AMNH 276557 / EBRG 25391	
59b	*H. anomalus*	VZ: Falcón: Serranía de San Luis; Parque Nacional J. C. Falcón, Sector El Haitón, ca. 8 km W 1 km N Cabure	JOG 4535	EBRG 25377	
	"	"	RPA 248	EBRG 25384	
	"	"	RPA 257	AMNH 276555 / EBRG 25388	
	"	"	RPA 264	AMNH 276556 / EBRG 25390	
59c	*H. anomalus*	VZ: Falcón: Serranía de San Luis; Parque Nacional J. C. Falcón, Sector El Chorro, ca. 9 km N Cabure	JOG 4560	EBRG 25309	
	"	"	JOG 4573	EBRG 25399	
	"	"	JOG 4574	AMNH 276521 / EBRG 25400	
	"	"	JOG 4575	EBRG 25401	
	"	"	JOG 4576	EBRG 25402	
	"	"	JOG 4583	AMNH 276524 / EBRG 25408	

59d	*H. anomalus*	VZ: Falcón: Serranía de San Luis; Parque Nacional J. C. Falcón, Sector Cumbres de Uria, ca. 9 km N Cabure	JOG 4570	AMNH 276519 / EBRG 25310	
	"	"	JOG 4571	EBRG 25397	
	"	"	JOG 4572	AMNH 276520 / EBRG 25398	
	"	"	JOG 4578	EBRG 25404	
	"	"	RPA 300	AMNH 276574 / EBRG 25419	
	"	"	RPA 301	EBRG 25312	
	"	"	RPA 302	AMNH 276575 / EBRG 25313	
	"	"	RPA 303	no catalog #	
	"	"	RPA 316	AMNH 276583 / EBRG 25428	
	"	"	RPA 317	EBRG 25314	
	"	"	RPA 318	EBRG 25315	
	"	"	RPA 319	EBRG 25429	
	"	"	RPA 325	EBRG 25434	
	"	"	RPA 326	AMNH 276587 / EBRG 25316	
	"	"	RPA 327	EBRG 25317	
	"	"	RPA 328	AMNH 276588 / EBRG 25318	
60	*H. australis*	EC: Esmeraldas: 2 km S Alto Tambo		ROM 105784	F 40077
61	*H. australis*	PN: Darién: Cana		ROM 116253	F 48794
	"	"		ROM 116302	F 48843
62	*H. desmarestianus*	ES: Santa Ana: Parque Nacional Montecristo, Los Planes		ROM 101505	F 35683
	"	"		ROM 101510	F 35688
63	*H. desmarestianus*	CR: Guanacaste: Volcán Santa Maria		ROM 113246	F 48553
64	*H. desmarestianus*	CR: Alajuela: 12.7 km NE Zarcero		ROM 113293	F 48600

65	*H. nubicolens*	CR: Puntarenas: Sainta Elena, Monte Verde Station		ROM 114272	F 48710
66a	Candidate species D	PN: Darién: Mount Pirre		ROM 116257	F 48798
	"	"		ROM 116258	F 48799
	"	"		ROM 116259	F 48800
	"	"		ROM 116260	F 48801
	"	"		ROM 116261	F 48802
	"	"		ROM 116262	F 48803
	"	"		ROM 116263	F 48804
	"	"		ROM 116264	F 48805
	"	"		ROM 116265	F 48806
	"	"		ROM 116266	F 48807
	"	"		ROM 116267	F 48808
	"	"		ROM 116268	F 48809
	"	"		ROM 116269	F 48810
	"	"		ROM116270	F 48811
	"	"		ROM 116271	F 48812
66b	*H. desmarestianus*	PN: Darién: Cerro Pirre		ROM 116273	F 48814
67a	*H. desmarestianus*	BE: Orange Walk: 4 km S Las Milpas Camp, 12 m mark, Rio Bravo area		-99	FN 29952
67b	*H. desmarestianus*	BE: Orange Walk: 8 km S Las Milpas, Rio Bravo		-99	FN 29971
68	*H. desmarestianus*	GU: El Peten: 1.5 km S, 1 km W Poptun		ROM 99230	FN 31780
69	*H. desmarestianus*	GU: El Peten: 10 km N of Tikal		ROM 99409	FN 31859
	"	"		ROM 99410	FN 31960
70	*H. desmarestianus*	GU: El Peten: Campo los Guacamayos, Biotopo Laguna del Tigre, 40 km N El Naranjo		ROM 99529	FN 32378
	"	"		ROM 99538	FN 32387

71	*H. desmarestianus*	MX: Quintana Roo: 6 km S, 1.5 km W Tres Garantias		ASNHC 7053	FN 32683
	"	"		ASNHC 7059	FN 32686
72	*H. desmarestianus*	CR: Guanacaste: Liberia, ~39 km N Pitilla, Sendero Orosilito	KM 99-091	KU 158510	
	"	"	KM 99-092	KU 158511	
	"	"	KM 99-093	KU 158512	
	"	"	KM 99-094	KU 158513	
	"	"	KM 99-102	KU 158514	
	"	"	KM 99-095	KU 158711	
73	Candidate species E	PN: Bocas Del Toro: Isla Popa, 1 km SE Deer Island Channel	J-501	USNM 464382	
	"	"	COH 14867	USNM 464383	
	"	"	COH 14887	USNM 464384	
	"	"	COH 14890	USNM 464385	
74	*H. desmarestianus*	GU: Quetzaltenango: 4 km SE Zunil, Finca la Chingada	WB 8425	USNM 569675	
75	*H. desmarestianus*	GU: Alta Verapaz: Chelemha, Yalijux Mountain		USNM 569852	TK 151027
	"	"		USNM 569866	TK 151041
	"	"		USNM 569945	TK 151134
	"	"		USNM 569949	TK 151139
	"	"		USNM 569956	TK 151150
	"	"		USNM 569981	TK 151178
	"	"		USNM 569984	TK 151183
	"	"		USNM 569985	TK 151184
	"	"		USNM 569991	TK 151190
	"	"		USNM 570003	TK 151126
	"	"		USNM 570007	TK 151140

76	*H. desmarestianus*	GU: Zacapa: Gualan Municipality: 9.5 km NW Gualan, El Limo, Sierra de las Minas	WB 8477	USNM 570034	
	"	"	WB 8478	USNM 570035	
	"	"	WB 8479	USNM 570036	
	"	"	WB 8517	USNM 570073	
	"	"	WB 8518	USNM 570074	
	"	"	WB 8546	USNM 570097	
	"	"	WB 8549	USNM 570131	
77	*H. desmarestianus*	GU: Baja Verapaz: 9 km S of Pasmola, btwn km 166 & 167 on CA-14, Hotel Country Delights	NW 1293	USNM 570134	
78	Candidate species E	PN: Bocas Del Toro: Nuri	FMG 2793	USNM 575655	
79	Candidate species E	PN: Bocas Del Toro: Peninsula Valiente, Quebrada Hido	FMG 2623	USNM 578383	
80a	Candidate species B	MX: Veracruz: 13.0 km NW (by road) Sontecomapan, Estacion Los Tuxtlas, IBUNAM, 40 m	DSR 8546	CMC 2004	
	"	"	DSR 8547	CMC 2005	
	"	"	DSR 8548	CMC 2006	
	"	"	DSR 8549	CMC 2007	
	"	"	DSR 8550	CMC 2008	
	"	"	DSR 8551	CMC 2009	
	"	"	DSR 8552	CMC 2010	
	"	"	DSR 8553	CMC 2011	
80b	Candidate species B	MX: Veracruz: 12.1 km NW (by road) Sontecomapán, 150 m	DSR 8561	CMC 2002	
	"	"	DSR 8562	CMC 2003	
81	*H. goldmani*	MX: Chiapas: 18.5 km S Frontera Comalapa		ROM 97673	FN 33154

	"	"		ROM 97674	FN 33155
82a	*H. nubicolens*	CR: Puntarenas: Monteverde Biological Station		ROM 113258	F 48565
	"	"		ROM 113259	F 48566
	"	"		ROM 113260	F 48567
	"	"		ROM 113261	F 48568
	"	"		ROM 113262	F 48569
	"	"		ROM 113263	F 48570
	"	"		ROM 113264	F 48571
	"	"		ROM 113265	F 48572
	"	"		ROM 113282	F 48589
82b	*H. nubicolens*	CR: Puntarenas: Monteverde, Cerro Amigos	TRM 3746	KU 142057	
82c	*H. nubicolens*	CR: Puntarenas: Monteverde, Cerro Amigos, Puntarenas-Guanacaste border	TRM 3869	KU 143455	
82d	*H. nubicolens*	CR: Puntarenas: Monteverde, Monteverde Cloud Forest Reserve, investigator trail	RMT 4461	KU 159022	
		"	RMT 4462	KU 159023	
		"	RMT 4467	KU 159024	
		"	RMT 4468	KU 159025	
		"	RMT 4469	KU 159026	
		"	RMT 4471	KU 159027	
83a	*H. nubicolens*	CR: Alejuela: Monteverde, Monteverde Cloud Forest Reserve, Cerro Amigos	CMM 222	KU 159101	
83b	*H. nubicolens*	CR: Alejuela: Monteverde, Monteverde Cloud Forest Reserve, Camino a Penas Blancas	CMM 245	KU 159102	
	"	"	CMM 258	KU 159103	

84	*H. oasicus*	VZ: Falcón: Península de Paraguaná; Cerro Santa Ana, ca. 4 km N Santa Ana	JOG 4460	EBRG 25450	
	"	"	JOG 4505	AMNH 276500 / EBRG 25485	
	"	"	JOG 4550	EBRG 25532	
	"	"	JOG 4554	EBRG 25533	
	"	"	RPA 209	AMNH 276534 / EBRG 25339	
85	*H. teleus*	EC: Los Rios: Rio Palenque Biological Station	ATS 183	KU 149134	
86	*H. desmarestianus*	CR: Alajuela: Parque Nacional Volcán Poas		ROM 113332	F 48640
87	*H. anomalus*	VZ: Zulia	RSV 1124	USNM 448559	
89	*L. pictus*	MX: Chiapas: 7.5 km SW of Ixtapa	MDE 2420	TCWC 37059	AK 4200
90	*L. pictus*	MX: Nayarit: 4.6 km NE Jalcocotán	ASK 1701	ASNHC 3260	
91	*L. pictus*	MX: Colima: 5 km S Alzada	ASK 2034	ASNHC 3072	
93	*L. spectabilis*	MX: Jalisco: 3 mi NE of Contla	MDE 3012	TCWC 42412	AK 5884
	"	"	MDE 3014	TCWC 42413	AK 5885
	"	"		TCWC 42405	AK 5894

CHAPTER 2

SYSTEMATICS OF THE SUBFAMILY HETEROMYINAE

Introduction

The rodent family Heteromyidae (pocket mice) consists of three subfamilies (Alexander and Riddle 2005; Hafner *et al*. 2007) and is endemic to the New World, with its origin in western North America (Wahlert 1993). The Perognathinae (silky pocket mice) and Dipodomyinae (kangaroo rats and kangaroo mice) inhabit grasslands, deserts, and other semiarid environments in the western United States and Mexico. Members of the third subfamily, Heteromyinae (spiny pocket mice), occur from southern Texas to Ecuador (Schmidly *et al*. 1993; Williams *et al*. 1993). Species of heteromyines tend to demonstrate strong specificity to particular habitats, which collectively constitute an array of tropical environments including thorn scrub, pluvial rainforest, and montane cloud forests (Genoways 1973; Schmidly *et al*. 1993; Anderson 1999; 2003). Moreover, the number of species-level taxa of heteromyines likely is underestimated (González 2005; Rogers and Vance 2005).

Heteromyines also represent one of many mammal groups to have dispersed across the Central American isthmus after the land bridge closed completely during the Pliocence, about 3 million years ago (Marshall *et al*. 1982; Coates *et al*. 1992; Graham 1992; Hooghiemstra 1994; Webb and Rancy 1996). Wallace first recognized this and other dispersal events—known collectively as the Great American Biotic Interchange between North and South America—in 1876. Unlike many other North American mammal groups that dispersed broadly, spiny pocket mice only colonized the northwestern reaches of South America. Due to lack of a fossil record in this region

(Wahlert 1993), they are generally considered to be among the most recent immigrants into the area (Patterson and Pascual 1968; Hershkovitz 1972; Marshall *et al*. 1982; Webb and Marshall 1982; Stehli and Webb 1985). Although their history of diversification and restricted colonization remains unclear, molecular phylogenetic data may help to address biotic dispersal patterns in the subfamily Heteromyinae by providing objective data for testable hypotheses.

Two genera, *Liomys* and *Heteromys*, comprise the subfamily Heteromyinae (but see Hafner *et al*. 2007), with five and 11 recognized species, respectively (Williams *et al*. 1993; Patton 2005; Anderson *et al*. 2006; Anderson and Gutiérrez in press). Members of the genus *Liomys* inhabit arid and semiarid thorn-scrub regions in Central and South America and are replaced by *Heteromys* in more mesic tropical habitats (Alexander and Riddle 2005).

Currently, the genus *Liomys* contains five species*: L. adspersus, L. irroratus, L. pictus, L. salvini,* and *L. spectabilis* (as revised by Genoways 1973). Genoways' (1973) hypothesis of relationships was as follows: (((*L. pictus*, *L. spectabilis*), *L. irroratus*) (*L. adspersus, L. salvini*)). Von Lehmann and Schaefer (1979) suggested that *L. adspersus* and *L. salvini* were phylogenetically distinct and should be placed in a separate subgenus (*Schaeferia*), but this recommendation was only recently appreciated in the context of potential nomenclatural implications (Anderson and Gutiérrez in press). Rogers (1990) confirmed the relationships defined by Genoways (1973) with allozyme data but concluded that *L. pictus* was paraphyletic. With further analyses of genetic differentiation in the *L. pictus* species group using mtDNA sequence data, Rogers and Vance (2005) confirmed that *L. pictus*, as presently defined, is a composite taxon and is

paraphyletic relative to *L. spectabilis*. Moreover, *L. pictus* likely is comprised of at least three candidate species (see also Vance 2006).

The genus *Heteromys* is comprised of 11 species: *H. anomalus, H. australis, H. catopterius, H. desmarestianus, H. gaumeri, H. goldmani, H. nelsoni, H. nubicolens, H. oasicus, H. oresterus*, and *H. teleus* (Anderson *et al*. 2006; Anderson and Gutiérrez in press; González 2005). Studies based on sequence data and morphology have determined that *Heteromys* is a monophyletic taxon (Anderson *et al.* 2006; Hafner *et al.* 2007; Rogers and Vance 2005).

However, molecular data suggest that *Liomys* is paraphyletic relative to *Heteromys* (Hafner *et al*. 2007; Rogers and Vance 2005), and allozyme and morphological data do not contradict this (Anderson *et al*. 2006; Rogers 1990). In the recent study by Hafner *et al*. (2007), sequence data from three mtDNA genes were used to demonstrate strong nodal support for *Liomys* paraphyly. These authors also showed that the *L. pictus* group ((*L. pictus, L. spectabilis*), *L. irroratus*) formed the sister group to *Heteromys* rather than to the *L. salvini* group (*L. adspersus, L. salvini*). As a taxonomic solution to paraphyly among species in the genus *Liomys,* Hafner *et al*. (2007) proposed that *Liomys* be synonymized with *Heteromys*.

My study aims to address this taxonomic problem. I include representatives of all described species of heteromyines with the exception of *H. catopterius* from Venezuela (Anderson and Gutiérrez in press), and develop sequence data for mtDNA (Cytochrome *b* [cyt *b*] and Cytochrome oxidase I [CoI]), and nucDNA (Beta fibrinogen [*Fgb-17*], Engrailed II [*En2*], and Myosin heavy chain II [*Myh2*]) to test the current hypothesis of relationships for the subfamily Heteromyinae.

Materials and Methods

Taxon Sampling:

Mice used in this study were collected from natural populations and were preserved as museum voucher specimens. Liver, spleen, kidney, heart, or lung tissue was removed from each individual and maintained in ultralow freezers at -80°C or in 95% ethanol at -20°C. The sample representing *H. teleus* was a skin clip. Tissue samples of some individuals were obtained through tissue loans from cooperating museums and universities. Sequence data for specimens representing the subfamily Heteromyinae were generated from 294 individuals representing 10 described species in the genus *Heteromys*; including several candidate species identified by a previous investigator (González 2005), as well as all five species currently recognized in the genus *Liomys* (Appendix). These specimens represent collecting localities from throughout Mexico, Belize, Guatemala, El Salvador, Nicaragua, Costa Rica, Panama, Venezuela, and Ecuador. Figure 1 is a map of collecting localities showing the sampling sites included in this study; numbers correspond to localities as numbered in the Appendix.

Dipodomys ordii from the subfamily Dipodomyinae as well as *Chaetodipus pencillatus* and *Perognathus apache* from the subfamily Perognathinae were used as outgroup taxa for this study, as these two subfamilies, with Heteromyinae, make up the family Heteromyidae (Hafner *et al*. 2007; González 2005; Rogers and Vance 2005).

Molecular Data Collection:

Whole genomic DNA was extracted for each individual from tissue (or skin from a single representative of *H. teleus*) using the Qiagen (Valencia, CA) DNeasy™ Tissue Kit (Cat. No. 69504) and following the protocol for animal tissues (July 2006, pp 18-20).

DNA was eluted with the manufacturer's AE buffer at a final volume of 200µl. Four microliters of DNA extraction product was electrophoresed on a 2.0% agarose gel stained with SYBR green to estimate the quality and amount of genomic DNA present.

PCR technique was used to amplify the entire cyt *b* gene using primers L14724 and H15915 (Irwin *et al*. 1991). Four internal primers were also used for amplification and sequencing: CB3H (Palumbi 1996), MVZ16 (Smith and Patton 1993), H15149 (Irwin *et al*. 1991), and F1 (Whiting *et al*. 2003). Table 1 describes the PCR conditions employed for all five genes or gene segments used in this study. For a subset of individuals that represent the major clades based on cyt *b* sequence data analyses, additional genes or gene segments were sequenced. A second mtDNA marker, CoI, was amplified via PCR using primers CoI-5285F and CoI-6929R (Spradling *et al*. 2004). Five internal primers also were used for amplification and sequencing: MCo-173F, MCo-1345R, MCo-1480R (Hafner *et al*. 2007), CoI-R1, and CoI-F3 (this study). For both mtDNA markers, standard Taq polymerase (Promega –Madison, WI) was used with its accompanying salts and buffer.

Sequence data for three nuclear introns also were obtained for the same subset of individuals using PCR technique. The seventh intron of the β-fibrinogen gene (*Fgb-17*) was amplified with primers B17 (Wickliffe *et al*. 2003) and Fgb-571F (this study). Members of the genus *Heteromys* (and possibly more members of the heteromyid family) possess large, variably sized indels in *Fgb-17*, so specific primers were designed (Table 1) to amplify the portion of the intron that is homologous to other rodent *Fgb-17*. β-fibrinogen amplifications used Platinum Taq (Invitrogen – Carlsbad, CA) with pre-mixed buffer and salts. Engrailed protein 2 (*En2*) was amplified using 1:10 diluted DNA and

the following primers, also diluted at a 1:10 ratio: EN2-F and EN2-R (Lyons *et al*. 1997). Similarly, myosin heavy chain 2 (*Myh2*) required 1:10 diluted DNA and primers: MYH2-F and MYH2-R (Lyons *et al*. 1997). For these last two PCRs, HotMaster Taq (Eppendorf – Westbury, NY), with its accompanying buffer and salts, worked best for amplification. Positive and negative controls were run with all amplifications.

Four microliters of double-stranded PCR product were assayed by electrophoresis on a 2% agarose gel. The remaining product (ca. 21µl) was purified using the Millipore (Billerica, MA) Multiscreen^{TM} PCR 96-Well Filtration System (Cat. No. MANU03050), and rehydrated with 25µl HPLC-H_20. All purified PCR products were then cycle sequenced using the Big Dye v3.1 Dye Terminator Cycle Sequencing Ready Reaction Kit (Applied Biosystems – Foster City, CA) with the same primers listed above for PCR amplification, all at a 1:10 dilution. Excess dye terminator was removed using a separation column made of a solution of Sephadex G50 in conjunction with Millipore (Billerica, MA) Multiscreen^{TM} Filter Plates for High Throughput Separations (Cat. No. MAHVN4510). Both strands of DNA fragments were sequenced in order to verify the accuracy of the sequenced nucleotides. Sequences were determined using the ABI 570 Genetic Analyzer (Applied Biosystems – Foster City, CA) located in the DNA Sequencing Center at Brigham Young University.

Sequence Alignment:

All sequences were compiled and edited using Sequencher v4.7 (Gene Codes Corporation, 2006). Base pairs exhibiting multiple peaks in the chromatographs of the nuclear markers were interpreted as heterozygous sites and coded as ambiguous characters. Manual alignment was possible with the Sequencher software for the cyt *b*

gene and the *En2* intron, as there were no insertion-deletions (indels) present. The CoI, *Myh2*, and *Fgb-17* sequences each contained at least one indel. As a result, MAFFT (Katoh *et al*. 2005) and MUSCLE (Edgar 2004) programs were used to align these sequences. MAFFT multiple alignment software offers three general ways to align sequences, each differing in speed and accuracy. I employed the strategy that maximized accuracy rather than speed to obtain my *Fgb-17* alignment, and the iterative refinement method (L-INS-i) using the weighted sum-of-pairs (WSP) and consistency scores was selected by the automated program. This method (Katoh *et al*. 2005) undergoes four stages of alignment: (1) a distance matrix is made based on all pairwise alignments, (2) a guide tree is constructed, (3) progressive alignment, and (4) iterative refinement of the alignment using WSP scores (Gotoh 1995) and COFFEE-like scores (Notredame *et al*. 2000). MUSCLE is another multiple sequence alignment program that implements three stages of alignment: (1) an initial progressive alignment generated from a distance matrix, (2) refinement of the progressive alignment by generation of alternative trees and comparison of tree scores, and (3) refinement of the alignment using a profile-profile alignment (Edgar 2004). MAFFT and MUSCLE produced very similar alignments, and I used the MAFFT alignment for all subsequent analyses.

Phylogenetic Analyses:

Collapse v1.2 (available from http://darwin.uvigo.es) was used to identify non-redundant haplotypes in the cyt *b* data set and to remove redundant haplotypes. However, if redundant haplotypes represented different localities, at least one sequence was retained for each collecting location. In total, the cyt *b* data set was reduced from 301 to 170 individuals. Models of evolution were determined among 56 different models

using ModelTest v3.7 (Posada and Crandall 1998) for cyt *b*, CoI, *Fbg-17*, *En2*, and *Myh2*. The Akaike information criterion (AIC) was used to obtain the best model and likelihood settings for each gene separately, as well as the combined data set consisting of all five gene segments (see below). Indels in the *Fgb-17* and *Myh2* markers were coded according to the simple indel coding (SIC) scheme outlined by Simmons and Ochoterena (2000) in the gap coding program SeqState (Müller 2005). Each SIC matrix was appended to its corresponding data matrix (*Fgb-17* and *Myh2*) for use in Bayesian and parsimony analyses.

Maximum parsimony (MP) analyses were conducted in PAUP* v4.0 (Swofford 2002) as unweighted heuristic searches with 1000 random additions and TBR branch swapping. Separate analyses were conducted for each of the genetic markers individually, and also for a combined data set in which all five markers were concatenated into one data matrix. Two cyt *b* data sets were used for comparative analyses: the 170-taxon data set representing all unique haplotypes, and a 97-taxon data set that contained only specimens for which nuclear data also were available. All other single and multi-gene data sets were congruent, in that each represented the same 97 individuals. Nonparametric bootstrap values (Felsenstein 1985) also were obtained in PAUP* for each data set using 1000 pseudoreplicates and 100 random additions. Bootstrap values $\geq$70% were considered well supported (Hillis and Bull 1993). Partitioned Bremer supports (PBS) were generated for the most optimal five-gene MP tree in TreeRot v3 (Sorenson and Franzosa 2007). For the final parsimony search of 20 repetitions in the TreeRot protocol, the "maxtrees" setting was increased from its 100-tree default to 500 trees.

A maximum likelihood (ML) approach also was used to analyze the genetic markers for the independent and combined data sets. ML analyses were performed using Garli v0.94 software (Zwickl 2006), and were set to autoterminate when resolution in log likelihood scores was <0.001 after 500 generations. The AIC model of evolution obtained from ModelTest v3.7 (Posada and Crandall 1998) was used in these analyses, and the parameters were estimated in Garli. As the ML algorithm allows only one model of evolution, the most complex model, GTR+I+Γ, was employed for the combined analysis. Bootstrap nodal support values were estimated in PhyML (Guindon and Gascuel 2003) using 1000 replicates.

Additionally, Bayesian inference (BI) was performed on individual genetic markers and on the combined data set using MrBayes v3.1 (Huelsenbeck and Ronquist 2001; Nylander *et al*. 2004). The appropriate AIC model of evolution was assigned for each analysis, as determined in ModelTest v3.7 (Posada and Crandall 1998). For the combined data set, a mixed-model Bayesian analysis was run using the appropriate model of evolution for each gene partition (see Results). Each data set was run twice for 20 million generations using Markov Chain Monte Carlo (MCMC) with four chains per run. Each run began with a random starting tree and trees were sampled every 2000 generations. Log-likelihood scores and standard errors from the log file were examined in Tracer v1.4 (Rambaut and Drummond 2007) to determine stationarity, and the first 20% of trees were discarded as burn-in. Posterior probabilities were generated from the remaining trees in PAUP* v4.0 (Swofford 2002), using the 50% majority rule consensus tree function.

Hypothesis Testing:

Alternative phylogenetic hypotheses were evaluated for statistical significance using the one-tailed Shimodaira-Hasegawa (S-H) test (Shimodaira and Hasegawa 1999) with restricted likelihood as implemented in PAUP* 4.0 (Swofford 2002). Ten thousand bootstrap replicates were performed using the S-H topology test by resampling the partial likelihoods for each site (RELL model).

Results

Sequence Analysis:

The entire cyt *b* gene was sequenced for all 301 specimens represented in this study, including seven outgroup taxa. Elimination of redundant haplotypes reduced the number of individuals to 170 for the cyt *b* data set. Sequence data also was obtained for the entire CoI gene, and for *Fgb-17*, *En2*, and *Myh2* introns for a total of 97 individuals, inclusive of three outgroup specimens.

Alignment of the cyt *b* gene (1140 bp) was trivial and yielded 512 parsimony-informative characters and 21 variable non-informative characters. The ingroup heteromyines exhibited no gaps for the CoI gene, however the two *Chaetodipus pencillatus* outgroup individuals contained a 3 bp gap near the 3' end of this gene. This indel is consistent with the findings of Light and Hafner (2008), who also documented a 3 bp deletion in CoI for *Chaetodipus* mice, relative to other heteromyids. The CoI alignment resulted in 1548 bp, with 578 parsimony-informative characters and 37 variable non-informative characters. For a number of *Heteromys* specimens (16 of 97), the β-fibrinogen intron contained a large insertion adjacent to a poly-A region of hypervariable length. The varying poly-A lengths among taxa introduced gaps of different sizes and made statements of homology less clear. To clarify coding and alignment in this region, I removed a 10-character segment from all *Fgb-17* sequences adjacent to the poly-A region so that the lowest common denominator of repeating adenines was still represented, but without the ambiguous alignment caused by differently sized gaps. There were 32 indels [SeqState Simple Indel Coding (SIC) results] after the 10-character segment adjacent to the hypervariable poly-A region was

removed. The aligned length of the *Fgb-17* intron was 899 bp, with 219 parsimony-informative characters and 79 variable non-informative characters. A data matrix with the 32 coded indels also was made for parsimony and Bayesian analyses, and for this mixed-data matrix there were 931 characters, 240 of which were parsimony-informative and 91 were variable non-informative. The gene segment *En2* contained no indels, and was 146 bp in length with 16 parsimony-informative characters and 10 non-informative variable characters. The *Myh2* gene segment contained six indels (SeqState SIC results), and had an aligned length of 205 bp, with 40 parsimony-informative characters and 29 variable non-informative characters. A mixed-data matrix with the six coded indels for *Myh2* was made for parsimony and Bayesian analyses, and this resulted in 211 characters, with 44 of these being parsimony-informative and 31 being variable non-informative characters. The combined data set, with the concatenation of all five genetic markers (without the SIC matrices), generated a total alignment length of 3938 bp.

Phylogenetic analysis of individual genes:

The cyt *b* data set generated a GTR+I+Γ model of evolution. The base frequencies were A=0.3357, C=0.3179, G=0.0526, and T=0.2938; transversion (tv) rates were (A-C)=0.3095, (A-G)=10.9957, (A-T)=0.6564, (C-G)=0.6514, (C-T)=6.5711, (G-T)=1.0000; the proportion of invariable sites (I) was 0.5009, and the gamma distribution shape parameter (Γ) was 0.8524. ML analysis of the 170-individual cyt *b* data set yielded a single tree (lnL= -15564.98) with high bootstrap support (≥70) for monophyly of the subfamily Heteromyinae with respect to outgroup taxa (Figure 2). This tree also demonstrated high support for *Liomys* paraphyly, in that the *L. pictus* group ((*L. pictus, L. spectabilis*), *L. irroratus*) formed a sister group to the genus *Heteromys* rather than to the

L. salvini group (*L. adspersus*, *L. salvini*). ML analysis of the cyt *b* data set containing 97 specimens, each represented by the four additional genetic markers, generated a tree (not shown) with the same topology and similar bootstrap support values as the 170-terminal data set. MP analysis of the 170-individual cyt *b* data set generated a single best tree (3310 steps; consistency index [CI]=0.263, retention index [RI]=0.852) analogous to the likelihood topology. Similarly, the 50% majority rule BI tree also was congruent in resolving the same major clades with high nodal supports [posterior probability (pP) $\geq$0.95] for monophyly of the subfamily Heteromyinae and paraphyly of the genus *Liomys*. Figure 2 depicts the ML tree for cyt *b* with ML bootstrap and Bayesian pP support values mapped onto the major nodes.

The CoI gene also was determined to have a GTR+I+Γ evolutionary model. (A=0.3346, C=0.2377, G=0.0978, and T=0.3298; tv rates [A-C]=0.6479, [A-G]=13.5460, [A-T]=1.1534, [C-G]=0.3841, [C-T]=10.7976, [G-T]=1.0000; I=0.6025; Γ=1.4551.) ML analysis of this gene produced a topology (lnL= -15877.24) similar to the cyt *b* gene tree, but with several important differences (Figure 3). First, *L. salvini* was arranged as sister to the *Dipodomys* outgroup taxon, rather than with the rest of the subfamily Heteromyinae. Secondly, bootstrap support values for the most basal clades in the CoI tree were lower than they were for the cyt *b* tree. Unlike the ML tree, the BI topology for CoI (not shown) generated high nodal support for the monophyly of the heteromyines and paraphyly of the genus *Liomys*; and as such was more similar to the cyt *b* gene tree topology. Figure 3 shows the ML tree for CoI with ML bootstrap and Bayesian pP values mapped onto the nodes, where nodal support was high. The MP tree (not shown; 3329 steps; CI=0.293, RI=0.775) depicts an unresolved trichotomy among the outgroup

genera, the *L. salvini* group, and the remaining *Liomys* and *Heteromys* taxa ((((*L. pictus*, *L. spectabilis*), *L. irroratus*), *Heteromys nelsoni*) (all other *Heteromys*)).

The β-fibrinogen gene segment was analyzed using ML and BI approaches under the GTR+Γ model of evolution. (A=0.2824, C=0.2320, G=0.2165, and T=0.2691; tv rates [A-C]=1.7847, [A-G]=4.8225, [A-T]=1.0700, [C-G]=2.0396, [C-T]=6.4067, [G-T]=1.0000; Γ=0.9373.) Both these criteria produced similar trees with high nodal supports for the most basal clades within the Heteromyinae. Figure 4 illustrates the ML topology (lnL= -3818.82) with ML bootstrap and pP values mapped onto the major nodes. Under both ML and BI criteria, *Fgb-17* clearly supports the monophyly of the subfamily Heteromyinae and the paraphyly of the genus *Liomys*, again with the *L. pictus* group clustering sister to members of the genus *Heteromys*. Bayesian analyses with and without the SIC matrix did not differ in topologies, and only slightly in some pP values. The MP analysis, however, generated different topologies based on the *Fgb-17* data set with and without the appended SIC matrix. Without the indel-coding matrix, the single best MP tree (not shown; 444 steps; CI=0.786, RI=0.924) arranged *H. nelsoni* sister to *H. gaumeri*, which also appeared in the ML and BI topologies at low support values, but this relationship was not recovered with the two mtDNA genes. The *Fgb-17* data set with the SIC matrix generated a single MP tree (not shown; 486 steps; CI=0.788, RI=0.925) that placed *H. nelsoni* more basal, and sister to the *H. anomalus* group; this is more congruent with the phlyogentic relationships recovered with the cyt *b* and CoI gene trees.

The *En2* data set generated a K81uf+I+Γ model of evolution. (A=0.2636, C=0.3192, G=0.3026, and T=0.1145; tv rates [A-C]=1.0000, [A-G]=5.5079, [A-T]=2.2816, [C-G]=2.2816, [C-T]=5.5079, [G-T]=1.0000; I=0.9072; Γ=0.7251.) Under

ML analysis a single tree was produced (lnL= -462.37) with high bootstrap support for the monophyly of the subfamily Heteromyinae and paraphyly of *Liomys* (Figure 5). However, with so few phylogenetically informative characters in this short nuclear intron (146 bp), the ability to clearly define lower level relationships was diminished. Bayesian analysis yielded similar results, with high pP support values for the higher-level relationships. The *En2* gene segment possessed only a few parsimony-informative characters, resulting in the inability to develop a MP tree due to excessively lengthy computation time.

The *Myh2* sequence data was analyzed using ML and BI criteria under a TrN+Γ model of evolution. (A=0.2706, C=0.2697, G=0.3117, and T=0.1479; tv rates [A-C]=1.0000, [A-G]=3.6270, [A-T]=1.0000, [C-G]=1.0000, [C-T]=10.0306, [G-T]=1.0000; Γ=0.4071.) ML analysis of the *Myh2* gene segment produced a tree (lnL= -824.34) that confirmed the monophyly of the genus *Heteromys* and paraphyly of the genus *Liomys*. However, this gene tree did not resolve a monophyletic heteromyine subfamily; the ML tree (Figure 6) showed the outgroup taxon *Dipodomys* clustering with *Liomys* taxa. However, the Bayesian tree (not shown) recovered the subfamily Heteromyinae as monophyletic (pP = 0.87). BI analysis also generated high support for the monophyly of the genus *Heteromys* and arranged the genus *Liomys* to be paraphyletic. For the *Myh2* data sets with and without the SIC matrix, there was no notable difference in BI topologies or pP nodal supports. MP analysis was not conducted for *Myh2* due to the excessive computation time required.

Phylogenetic analysis of the combined data set:

The combined data set contained 97 individuals with a total aligned sequence length of 3938 bp. The most complex model of evolution, GTR+I+Γ, was applied to this data set for ML analysis (A=0.3041, C=0.2669, G=0.1433, and T=0.2857; tv rates [A-C]=1.5331, [A-G]=11.8479, [A-T]=2.6823, [C-G]=1.4379, [C-T]=21.7754, [G-T]=1.0000; I=0.5155; Γ=0.7611). BI utilized a mixed-model analysis wherein each gene partition was assigned its own model of evolution (cyt *b* and CoI = GTR+I+Γ; *Fgb-17* = GTR+Γ; *En2* = K81uf+I+Γ; *Myh2* = TrN+Γ). Figure 7 is the ML phylogram (lnL= -35727.57) with bootstrap and pP values mapped onto the nodes. Under both likelihood and Bayesian criteria, the same topology was generated with high nodal support values. MP analysis produced 32 equally parsimonious trees (not shown; 6819 steps; CI=0.331, RI=0.778), which were congruent with the ML and BI topologies. In addition to bootstrap and pP supports, Partitioned Bremer Support (PBS) values also were mapped onto the nodes (Figure 7 – cyt *b*/CoI/*Fgb-17*/*En2*/*Myh2*). The phylogenetic relationships estimated from the five-gene tree were most similar to the cyt *b* tree described above, but with better resolution among the basal and interior nodes of the tree.

Hypothesis testing:

A-priori hypotheses were tested using topology constraints and the Shimodara-Hasegawa statistical test. A constraint resulting in a significantly worse tree score ($P \leq 0.05$) was understood to depict an invalid relationship. Two topological constraints were tested: (1) the existing taxonomy, forcing the *Liomys irroratus* and *L. salvini* species groups to be sister clades and (2) monophyly of the species *L. pictus*. Both constraints resulted in significantly less likely trees; (1) $P<0.0001$, (2) $P<0.0001$.

Discussion

Phylogenetic analyses described herein support the findings of Vance (2006), Rogers and Vance (2005), and Hafner *et al*. 2007, all of whom documented paraphyly among members of the genus *Liomys*. Specifically, *L. irroratus*, *L. pictus* and *L. spectabilis* were more closely related to members of the genus *Heteromys* than to *Liomys salvini* (and by extension *L. adspersus*). Likewise, Rogers and Vance (2005) and Vance (2006) failed to recover *Liomys pictus* as a monophyletic group relative to *L. spectabilis*. Using three presumably unlinked markers and heavy sampling in the *L. pictus-spectabilis* complex, Vance (2006) hypothesized that six species-level taxa exist in this clade, rather than the two that are presently recognized. The current study uses sequence data from two additional genes and provides further evidence for these two instances of paraphyly within taxa currently assigned to the genus *Liomys*.

The three basal clades recovered in this study—(*L. adspersus*, *L. salvini*), ((*L. pictus*, *L. spectabilis*), *L. irroratus*), and (*Heteromys*)—also were recognized as monophyletic by Hafner *et al*. (2007) in their paper discussing phylogenetic relationships within the family Heteromyidae. As in previous studies based on sequence data (Rogers and Vance 2005; Vance 2006), Hafner *et al.* (2007) also recovered the genus *Liomys* as paraphyletic. To resolve this paraphyly, these authors suggested recognizing only a single genus within the subfamily Heteromyinae, with *Heteromys* having name priority. Hafner *et al*. (2007) further recommended that the morphological and ecological differentiation evident in heteromyines be reflected by a series of subgenera, although they did not propose any taxonomic changes.

In a paper that was largely overlooked for several decades, Von Lehmann and Schaefer (1979) recommended that *L. salvini* (and by extension *L. adspersus*) be assigned to a newly named subgenus *Schaeferia*. One justification for this change involved a detailed description of the sperm morphology possessed by *L. salvini* together with a summary of Genoways' (1973) drawings of sperm heads for all five *Liomys* species. Von Lehmann and Schaefer (1979) reiterated the observation by Genoways (1973) that *L. adspersus* and *L. salvini* possess blunt and rounded sperm heads compared to other species of *Liomys* (*irroratus, pictus* and *spectabilis*), which have elongate and tapered heads (Figure 57—Genoways 1973). Von Lehmann and Schaefer (1979) also remarked that *L. adspersus* and *L. salvini* possess similar karyotypes that together, differ from other species of heteromyines (Genoways 1973). Under their recommendations, the genus *Liomys* would encompass two subgenera: *Liomys*, which would include *L. irroratus*, *L. pictus*, and *L. spectabilis*, and *Schaeferia*, which would include *L. adspersus* and *L. salvini* (Von Lehmann and Schaefer 1979).

Taxonomic Recommendations

Given that the genus *Liomys* is paraphyletic, I agree with Hafner *et al.* (2007) that the existing taxonomy is unsatisfactory. As suggested by Anderson *et al*. (2006), a second option in dealing with this paraphyly would be to split *Liomys* into two generic-level entities and then retain *Heteromys* as currently configured. The ((*L. pictus*, *L. spectabilis*), *L. irroratus*) clade has name priority for *Liomys*. Therefore, this approach would place *L. adspersus* and *L. salvini* in *Schaeferia*, which would be elevated to the generic level (Von Lehmann and Schaefer 1979).

I favor the latter approach for two reasons. First, this classification would convey greater genealogical information and more accurately reflect the biodiversity that exists in the heteromyine subfamily. Second, it would require fewer name changes and therefore would provide more nomenclatural stability. Table 2 summarizes my taxonomic recommendations.

Literature Cited

Alexander, L. F., and B. R. Riddle. 2005. Phylogenetics of the New World rodent family Heteromyidae. Journal of Mammalogy 86:366-379.

Allen, J. A., and F. M. Chapman. 1897. On mammals from Yucatan with descriptions of new species. Bulletin of the American Museum of Natural History 9:1-12.

Anderson, R. P. 1999. Evaluating predictive models of species' distributions: criteria for selecting optimal models. Ecological Modeling 162:211-232.

Anderson, R. P. 2003. Taxonomy, distribution, and natural history of the genus *Heteromys* (Rodentia: Heteromyidae) in western Venezuela, with the description of a dwarf species from the Peninsula de Paraguana. American Museum Novitates 3396:1-43.

Anderson, R. P., M. Weksler, and D. S. Rogers. 2006. Phylogenetic analyses of spiny pocket mice (Heteromyidae: Heteromyinae) based on allozymic and morphological data. Journal of Mammalogy 87:1218-1233.

Coates, A. G., J. B. C. Jackson, L. S. Collins, T. M. Cronin, H. J. Dowsett, L. M.Bybell, P. Jung, and J. A. Orbando. 1992. Closure of the Isthmus of Panama: the near-shore marine record of Costa Rica and western Panama. Geological Society of America Bulletin 104:814-828.

Edgar, R. C. 2004. MUSCLE: multiple sequence alignment with high accuracy and high throughput. Nucleic Acids Research 32:1792-1797.

Engstrom, M. D., H. H. Genoways, and P. K. Tucker. 1987. Morphological variation, karyology, and systematic relationships of *Heteromys gaumeri* (Rodentia: Heteromyidae). Pages 289-303 *in* Studies in Neotropical mammalogy: essays in

honor of Philip Hershkovitz. Fieldiana: Zoology, new series (B. D. Patterson, and R. M. Timm, eds.).

Felsenstein, J. 1985. Confidence-limits on phylogenies: an approach using the bootstrap. Evolution 39:783-791.

Genoways, H. H. 1973. Systematics and evolutionary relationships of spiny pocket mice, genus *Liomys*. Special Publications of the Museum, Texas Tech University 5:1-368.

Goldman, E. A. 1911. Revision of the spiny pocket mice (genera *Heteromys* and *Liomys*). North American Fauna, 34:1-70.

González, M. 2005. Phylogenetic relationships of forest spiny pocket mice (Genus *Heteromys*) inferred from mitochondrial and nuclear markers with implications for species boundaries. M.S. thesis. Brigham Young University, Provo, Utah.

Gotoh, O. 1995. A weighting system and algorithm for aligning many phylogenetically related sequences. Computer Applications in the Biosciences 11:543-551.

Graham, A. 1992. Utilization of the isthmian land bridge during the Cenozoic—paleobotanical evidence for timing, and the selective influence of altitudes and climate. Review of Paleobotany and Palynology 72:119-128.

Gray, J. E. 1868. Synopsis of the species of Saccomyinae, or pouched mice in the collection of the British Museum. Proceedings of the Zoological Society of London 1868:199-206.

Guindon, S., and O. Gascuel. 2003. PhyML: A simple, fast, and accurate algorithm to estimate large phylogenies by maximum likelihood. Systematic Biology 52:696-704.

Hafner, J. C., and M. S. Hafner. 1983. Evolutionary relationships of heteromyid rodents. Great Basin Naturalist 7:3-29.

Hafner, J. C., J. E. Light, D. J. Hafner, M. S. Hafner, E. Reddington, D. S. Rogers, and B. R. Riddle. 2007. Basal clades and molecular systematics of Heteromyid rodents. Journal of Mammalogy 88:1129-1145.

Harris, W. P., Jr. 1932. Four new mammals from Costa Rica. Occasional Papers of the Museum of Zoology, University of Michigan 248:1-6.

Hershkovitz, P. 1972. Notes on New World monkeys. London: Zoological Society of London.

Hillis, D. M., and J. J. Bull. 1993. An empirical test of bootstrapping as a method for assessing confidence in phylogenetic analysis. Systematic Biology 42:182-192.

Homan, J. A., and H. H. Genoways. 1978. An analysis of hair structure and its phylogenetic implications among heteromyid rodents. Journal of Mammalogy 59:740-760.

Hooghiemstra, H. 1994. Pleistocene-Quaternary floral migration, evolution of northern Andean ecosystems and climatic change: implications from the closure of the Panamanian isthmus. Profile 7:413-425.

Huelsenbeck, J. P., and F. Ronquist. 2001. MRBAYES: Bayesian inference of phylogenetic trees. Bioinformatics 17:754-755.

Irwin, D. M., T. D. Kocher, and A. C. Wilson. 1991. Evolution of the cytochrome *b* gene in mammals. Journal of Molecular Evolution 32:128-134.

James, G. T. 1963. Paleontology and nonmarine stratigraphy of the Cuyama Valley Badlands, California. Part I. Geology, faunal interpretations, and systematic

descriptions of Chiroptera, Insectivora and Rodentia. University of California Publications in Geological Sciences 45:i-iv, 1-171.

Katoh, K., K. Kuma, H. Toh, and T. Miyata. 2005. MAFFT version 5: improvement in accuracy of multiply sequence alignment. Nucleic Acids Research 33:511-518.

Kishino, H., J. L. Thorne, and W. J. Bruno. 2001. Performance of a divergence time estimation method under a probabilistic model of rate estimation. Molecular Biology and Evolution 18:352-361.

Light, J. E., and M. S. Hafner. 2008. Codivergence in heteromyid rodents (Rodentia: Heteromyidae) and their sucking lice of the genus Fahrenholzia (Phthiraptera: Anoplura). Systematic Biology 57:449-465.

Lyons, L. A., T. F. Laughlin, N. G. Copeland, N. A. Jenkins, J. E. Womack, and S. J. O'Brien. 1997. Comparative anchor tagged sequences (CATS) for integrative mapping of mammalian genomes. Nature Genetics 15.

Marshall, L. G., S. D. Webb, J. J. Sepkoski, Jr., and D. M. Raup. 1982. Mammalian evolution and the Great American Interchange. Science 215:1351-1357.

Merriam, C. H. 1902. Twenty new pocket mice (*Heteromys* and *Liomys*) from Mexico. Proceedings of the Biological Society of Washington 15:41:50.

Müller, K. 2005. SeqState: Primer design and sequence statistics for phylogenetic DNA datasets. Applied Bioinformatics 4:65-69.

Notredame, C., D. G. Higgins, and J. Heringa. 2000. T-Coffee: a novel method for fast and accurate multiple sequence alignment. Journal of Molecular Biology 302:205-217.

Nylander, J. A. A., F. Ronquist, J. P. Huelsenbeck, and J. L. Nieves-Aldrey. 2004. Bayesian phylogenetic analysis of combined data. Systematic Biology 53:47-67.

Palumbi, S. R. 1996. Nucleic acids I: The polymerase chain reaction. Pages 205-247 *in* Molecular systematics, 2nd ed. (D. M. Hillis, C. Moritz, and B. K. Mable, eds.). Sinauer, Sunderland, Massachusetts.

Patterson, B., and R. Pascual. 1968. The fossil fauna of South America. Quarterly Review of Biology 43:409-451.

Patton, J. L. 2005. Family Heteromyidae. Pages 477-485 *in* Mammal Species of the World: a taxonomic and geographic reference, 2nd ed. (D. E. Wilson, and D. M. Reeder, eds.). Washington, DC: Smithsonian Institution Press.

Posada D., and K. A. Crandall. 1998. Modeltest: testing the model of DNA substitution. Bioinformatics 14:817-818.

Rambaut, A., and A. J. Drummond. 2007. Tracer v1.4: MCMC trace analysis tool. University of Edinburgh and University of Auckland. (http://tree.bio.ed.ac.uk/software/tracer/)

Rogers, D. S. 1990. Genic evolution, historical biogeography, and systematic relationships among spiny pocket mice (subfamily Heteromyinae). Journal of Mammalogy 71:668-685.

Rogers, D. S., and V. L. Vance. 2005. Phylgenetics of spiny pocket mice (genus *Liomys*): analysis of cytochrome *b* based on multiple heuristic approaches. Journal of Mammalogy 86:1085-1094.

Schmidly, D. J., K. T. Wilkens, and J. N. Derr. 1993. Biogeography. Pages 319-356 *in* Biology of the Heteromyidae. Special Publications, American Society of Mammalogists (H. H. Genoways, and J. H. Brown, eds.).

Shimodaira, H., and M. Hasegawa. 1999. Multiple comparisons of log-likelihoods with applications to phylogenetic inference. Molecular Biology and Evolution 16:1114-1116.

Simmons, M. P., and H. Ochoterena. 2000. Gaps as characters in sequence-based phylogenetic analyses. Systematic Biology 49:369-381.

Smith, M. F., and J. L. Patton. 1993. The diversification of South American muroid rodents: evidence from mitochondrial DNA sequence data for the akodontine tribe. Biological Journal of the Linnaean Society 50:149-177.

Sorensen, M. D., and E. A. Franzosa. 2007. TreeRot, version 3. Boston University, Boston, MA.

Spradling T. A., S. V. Brant, M. S. Hafner, and C. J. Dickerson. 2004. DNA data support a rapid radiation of pocket gopher genera (Rodentia: Geomyidae). Journal of Mammalian Evolution 11:105-125.

Stehli, F. G., and S. D. Webb. 1985. The Great American Biotic Interchange. Plenum Press, New York.

Swofford, D. L. 2002. PAUP*: Phylogenetic analysis using parsimony (*and other methods). Version 4.0b10. Sinauer Associates, Sunderland, Massachusetts, USA.

Thomas, O. 1901. New South American *Sciuri*, *Heteromys*, *Cavia*, and *Caluromys*. Annals and Magazine of Natural History 7:192-196.

Thompson, J. W. 1815. Description of a new species of the genus *Mus*, belonging to the section of pouched rats. Transactions of the Linnaean Society, London 11:161-163.

Thorne, J. L., and H. Kishino. 2002. Divergence time and evolutionary rate estimation with multilocus data. Systematic Biology 51:689-702.

Vance, V. L. 2006. Delimiting species boundaries within the *Liomys pictus-spectablis* complex (Rodentia: Heteromyidae). M.S. thesis. Brigham Young University, Provo, Utah.

Von Lehmann, E., and H. E. Schaefer. 1979. Cytological-taxonomic studies on rodents from Honduras (sperm morphology and comparative cytochemics). Zeitschrift fur Zoologische Systemakik und Evolutionsforschung 17:226-236.

Wahlert, J. H. 1993. The fossil record. Pages 1-37 *in* Biology of the Heteromyidae. Special Publication, American Society of Mammalogists (H. H. Genoways, and J. H. Brown, eds.).

Wallace, A. R. 1876. The Geographic Distribution of Animals. Harper and Borthers, New York, Vol. 1.

Webb, S. D., and L. G. Marshall. 1982. Historical biogeography of recent South American land mammals. Pages 39-52 *in* Mammalian biology in South America. Special Publication Series, Pymatuning Laboratory of Ecology, University of Pittsburgh (M. A. Mares and H. H. Genoways, eds.).

Webb, S. D., and A. Rancy. 1996. Late Cenozoic evolution of the Neotropical mammal fauna. Pages 335-358 *in* Evolution and environment in tropical America. (B. C.

Jackson, A. F. Budd, and A. G. Coates, eds.). University of Chicago Press, Chicago, Illinois.

Whiting, A. S., A. M. Bauer, and J. W. Sites, Jr. 2003. Phylogenetic relationships and limb loss in sub-Saharan African scincine lizards (Squamata: Scincidae). Molecular Phylogenetics and Evolution 29:583-598.

Wickliffe, J. K., F. G. Hoffmann, D. S. Carroll, Y. V. Dunina-Barkovshaya, R. D. Bradley, and R. J. Baker. 2003. Intron 7 (*FGB*): a nuclear DNA phylogenetic marker for mammals. Occasional Papers, Museum Texas Tech University 219:1-6.

Williams, D. F., H. H. Genoways, and J. K. Braun. 1993. Taxonomy. Pages 38-196 *in* Biology of the Heteromyidae. Special Publications, American Society of Mammalogists (H. H. Genoways, and J. H. Brown, eds.).

Wood, A. E. 1935. Evolution and relationships of the heteromyid rodents with new forms from the Tertiary of western North America. Annals of Carnegie Museum 24:73-262.

Yang, Z. 1997. PAML: a program package for phylogenetics analysis by maximum likelihood. Computer Applications in the Biosciences 13:555-556.

Zwickl, D. J. 2006. Genetic algorithm approaches for the phylogenetic analysis of large biological sequence datasets under the maximum likelihood criterion. Ph.D. dissertation, The University of Texas at Austin. www.bio.utexas.edu/faculty/antisense/garli/Garli.html

Table 1: PCR conditions used for cytochrome *b* (cyt *b)*, cytochrome oxidase I (CoI), β-fibrinogen (*Fgb-17*), Engrailed protein II (*En2*), and Myosin heavy chain II (*Myh2*). Final volume = 25µl. MM = Master Mix. See text for primer sources.

Gene	PCR conditions	Primer	Primer sequence
cyt *b*	94°/3min | 39 cycles: 94°/1min; 50°/1min, 72°/1min | 72°/3min 24µl MM + 1µl DNA	L14724 H15915 CB3H MVZ16 H15149 F1	5'-CGA AGC TTG ATA TGA AAA ACC ATC GTT G-3' 5'-AAC TGC AGT CAT CTC GGG TTT ACA AGA C-3' 5'-GGC AAA TAG GAA RTA TCA TTC-3' 5'-TAG GAA RTA TCA YTC TGG TTT RAT-3' 5'-AAA CTG CAG CCC CTC AGA ATG ATA TTT GTC CTC A-3' 5'-TGA GGA CAR ATA TCH TTY TGR GG-3'
CoI	94°/2min | 4 cycles: 94°/1min; 47°/1min, 72°/1min | 34 cycles: 94°/1min; 54°/1min, 72°/1min | 72°/10min 24µl MM + 1µl DNA	CoI-5285F CoI-6929R MCo-173F MCo-1345R MCo-1480R CoI-R1 CoI-F3	5'-CCY CTG TNY TTA GAT TTA CAG TCT A-3' 5'-ACA ARG TTA TGT AAT DDT TTT ACT A-3' 5'-TAT TAG GNG AYG AYC ARA T-3' 5'-TGT TGW GGG AAR AAD GTT A-3' 5'-GCT TCT CAR ATT ATR WAR ATT AT-3' 5'-ATG TAR ACT TCA GGG TGA C-3' 5'-GAT CWT TMT TAA TTA CTG CTG-3'
Fgb-17	85° Hot Start | 94°/10min | 32 cycles: 94°/1min; 65°/1min, 72°/1min 19.36µl MM + 3µl DNA + 2.64µl dNTP Mix	B17 Fgb-571F	5'-ACC CCA GTA GTA TCT GCC GTT TGG AT-3' 5'-CGT AGC CTT GTG CTT GCA ATA G-3'
En2	94°/10min | 32 cycles: 94°/1min; 57°/1min, 72°/1min 12.5µl MM + 12.5µl DNA (1:10)	EN2-F EN2-R	5'-CCC GAA AAC CAA AGA AGA AG-3' 5'-GTT CTG GAA CCA AAT CTT GAT C-3'
Myh2	85° Hot Start | 94°/10min | 32 cycles: 94°/1min; 62°/1min, 72°/1min 9.85µl MM + 12.5µl DNA (1:10) + 2.64µl dNTP Mix	MYH2-F MYH2-R	5'-GAA CAC CAG CCT CAT CAA CC-3' 5'-TGG TGT CCT GCT CCT TCT TC-3'

Table 2: Taxonomic arrangements among members of the subfamily Heteromyinae by Hall (1981) and this study. Given paraphyly within *Liomys*, Hafner *et al*. (2007) proposed that all heteromyines be recognized under the name *Heteromys*. See text for additional information.

Hall 1981	This study
Subfamily Heteromyinae	**Subfamily Heteromyinae**
Genus *Heteromys*	Genus *Heteromys*
Subgenus *Heteromys*	Subgenus *Heteromys*
H. anomalus group	*H. anomalus* group
H. anomalus	*H. anomalus* (*H. a. anomalus* & *H. a. oasicus*)
H. australis	*H. australis*
H. desmarestianus group	*H. catopterius**
H. desmarestianus	*H. teleus*
H. gaumeri	*H. desmarestianus* group
H. goldmani	*H. desmarestianus*
H. lepturus	*H. goldmani*
Subgenus *Xylomys*	*H. nubicolens*
H. nelsoni	*H. oresterus*
H. oresterus	Candidate species A, B, C, D, E
	H. gaumeri group
	H. gaumeri
	Subgenus *Xylomys*
	H. nelsoni
Genus *Liomys*	Genus *Liomys*
L. pictus group	*L. irroratus*
L. irroratus	*L. pictus***
L. pictus	*L. spectabilis*
L. spectabilis	Genus *Schaeferia*
L. salvini group	*S. adspersus****
L. adspersus	*S. salvini*
L. salvini	

*No sequence data were available for *H. catopterius*; placement is tentative pending future phylogenetic investigations. **Rogers and Vance (2005) and Vance (2006) proposed several candidate species within *L. pictus*. ***No nuclear sequence data were available for *S. adspersus* in this study, but based on mitochondrial sequence data (this study) and morphological evidence (Anderson *et al*. 2006), *S. adspersus* is sister to *S. salvini*.

Figure 1: Map of Mexico and Central America with an insert of northern South America. Dots indicate collecting sites of *Heteromys*; triangles represent collecting localities of *Liomys.* Collecting sites of *H. teleus* (locality 60), a single *H. australis* from Ecuador (locality 85), and outgroup taxa are not shown. Numbers correspond to localities as listed in the Appendix.

Figure 2: Phylogram (lnL= -15564.98) generated from ML analysis of the cyt *b* data set with 170 samples (redundant haplotypes omitted from this analysis) representing the subfamily Heteromyinae as well as outgroup taxa *Chaetodipus pencillatus*, *Dipodomys ordii*, and *Perognathus apache*. ML bootstrap support (Bp) values (based on 1000 iterations) and BI posterior probabilities (pP) values (based on 50% majority rule for the consensus tree) have been mapped onto the major nodes (Bp values $\geq$70 are above branches; pP values $\geq$0.95 are represented by a dot).

Figure 3: Phylogram (lnL= -15877.24) generated from ML analysis of the CoI data set with 97 taxa representing the subfamily Heteromyinae as well as these outgroup taxa *Chaetodipus pencillatus*, and *Dipodomys ordii*. ML and BI support values are depicted as in Fig. 2.

Figure 4: Phylogram (lnL= -3818.82) generated from ML analysis of the 7th intron of the β-fibrinogen (*Fgb-17*) data set with 97 samples representing the subfamily Heteromyinae as well as outgroup taxa as listed in Fig. 3. Clades labeled A-E correspond

to the five *H. desmarestianus* lineages, as denoted in Figs. 2 and 3. ML and BI support values are depicted as in Fig. 2.

Figure 5: Phylogram (lnL= -462.37) generated from ML analysis of the *En2* data set with 97 taxa representing the subfamily Heteromyinae as well as outgroup taxa as listed in Fig. 3. Clades labeled A-E correspond to the five *H. desmarestianus* lineages, as denoted in Figs. 2 and 3. ML and BI support values are depicted as in Fig. 2.

Figure 6: Phylogram (lnL= -824.34) generated from ML analysis of the *Myh2* data set with 97 taxa representing the subfamily Heteromyinae as well as outgroup taxa as listed in Fig. 3. Clades labeled A-E correspond to the five *H. desmarestianus* lineages, as denoted in Figs. 2 and 3. ML and BI support values are depicted as in Fig. 2.

Figure 7: Phylogram (lnL= -35727.57) generated from ML analysis of the combined (5-gene) data set with 97 taxa representing the subfamily Heteromyinae as well as outgroup taxa as listed in Fig. 3. ML and BI support values are depicted as in Fig. 2. Additionally, partitioned Bremmer support (PBS) values are below each node (cyt *b*/CoI/*Fgb-17*/*En2*/*Myh2*). Boxes mapped onto the nodes represent indels in the *Myh2* sequence alignment. One additional indel (not mapped) was a one-bp deletion in two of the Candidate D samples.

Figure 1

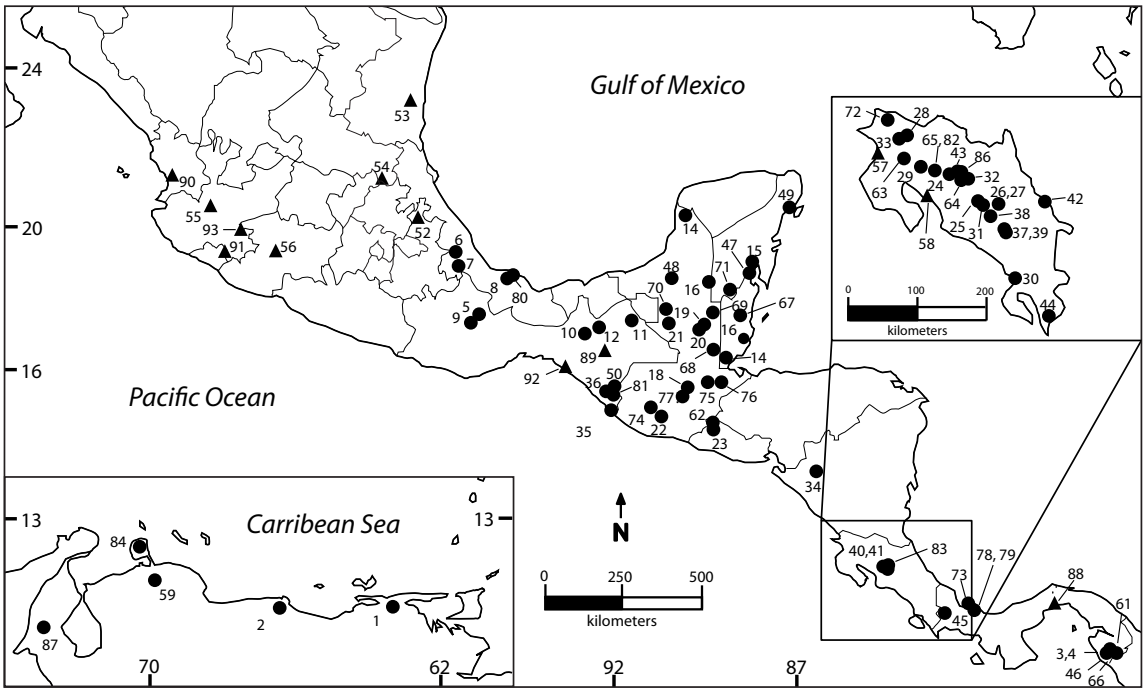
Gulf of Mexico
Pacific Ocean
Carribean Sea
N
0 250 500
kilometers
0 100 200
kilometers
24
20
16
13
70
62
92
87

Figure 2

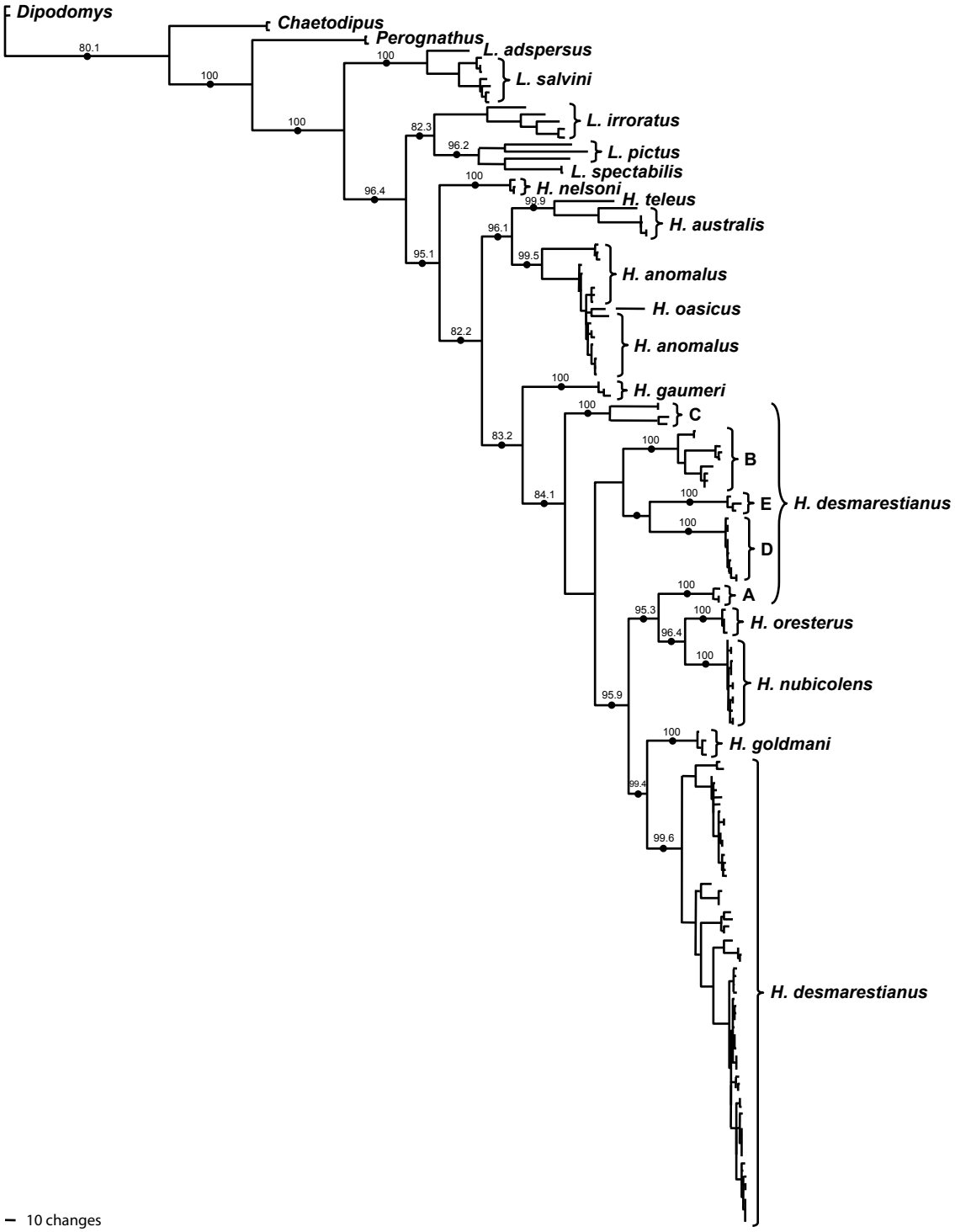
Dipodomys
Chaetodipus
Perognathus
L. adspersus
L. salvini
L. irroratus
L. pictus
L. spectabilis
H. nelsoni
H. teleus
H. australis
H. anomalus
H. oasicus
H. anomalus
H. gaumeri
C
B
E
D
A
H. desmarestianus
H. oresterus
H. nubicolens
H. goldmani
H. desmarestianus
80.1
100
100
100
82.3
96.2
100
96.4
99.9
96.1
95.1
99.5
82.2
100
100
83.2
100
84.1
100
100
100
100
95.3
96.4
100
95.9
100
99.4
99.6
10 changes

Figure 3

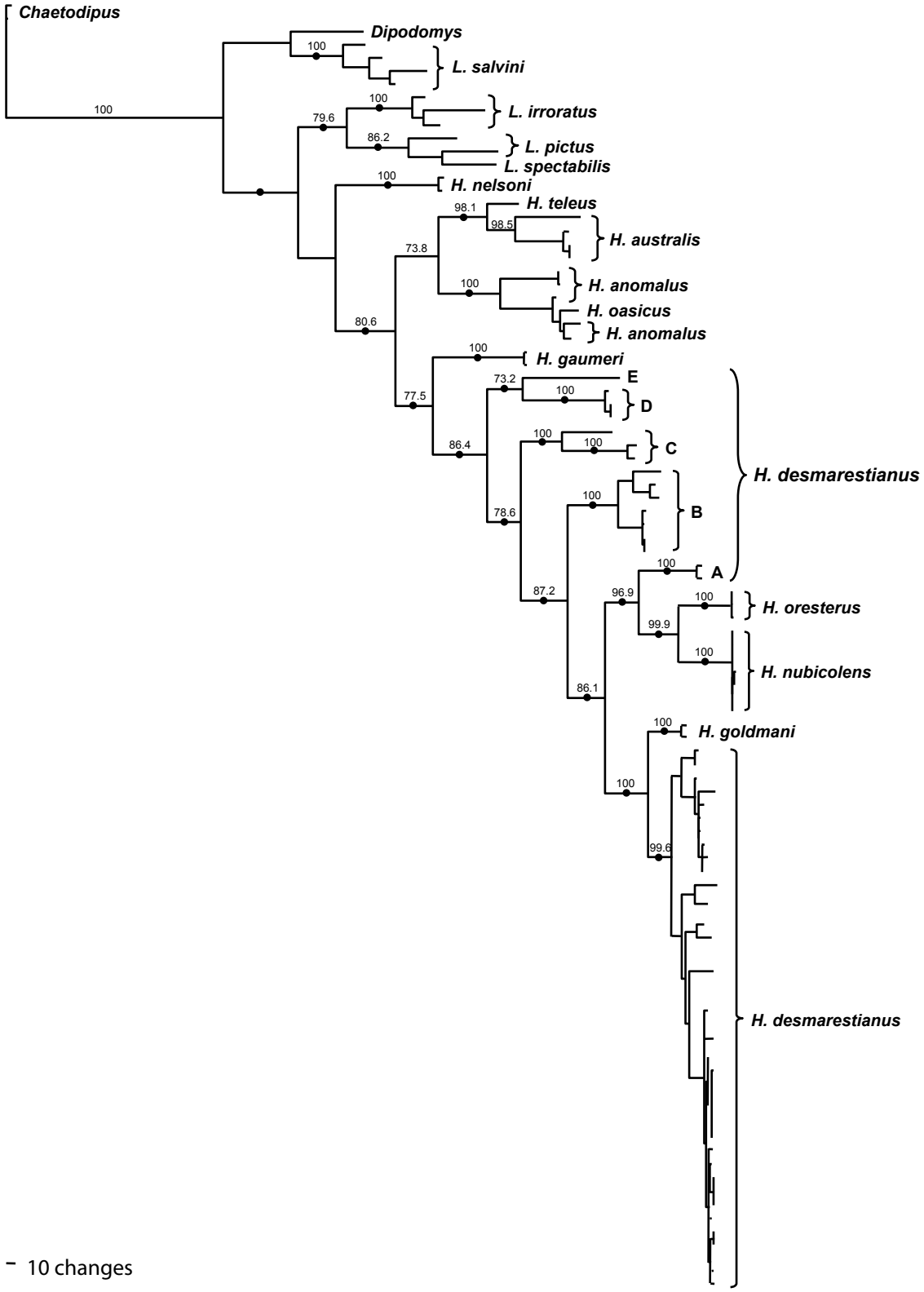
Chaetodipus
Dipodomys
L. salvini
L. irroratus
L. pictus
L. spectabilis
H. nelsoni
H. teleus
H. australis
H. anomalus
H. oasicus
H. anomalus
H. gaumeri
E
D
C
B
A
H. desmarestianus
H. oresterus
H. nubicolens
H. goldmani
H. desmarestianus
100
79.6
86.2
98.1
98.5
73.8
80.6
73.2
77.5
86.4
78.6
87.2
96.9
99.9
86.1
99.6
10 changes

Figure 4


Chaetodipus
Dipodomys
L. salvini
L. irroratus
L. pictus
L. spectabilis
H. teleus
H. australis
H. anomalus
H. oasicus
H. anomalus
H. nelsoni
H. gaumeri
H. desmarestianus
E
D
C
C
H. oresterus
H. nubicolens
A
H. desmarestianus
A
H. oresterus
B
H. desmarestianus
D
H. desmarestianus
H. goldmani
H. desmarestianus
100
100
100
99.7
97.5
77.2
82.4
99.7
98.9
100
100
99.8
82.7
99.7
100
76.1
1 change

Figure 5


Chaetodipus
Dipodomys
L. salvini
L. spectabilis
84.5
L. pictus
C
78.3
L. irroratus
L. pictus
H. teleus
H. australis
H. anomalus
H. oasicus
H. anomalus
H. nelsoni
H. nubicolens
90.4
H. gaumeri
H. nubicolens
H. oresterus
H. nubicolens
H. desmarestianus
H. goldmani
H. nubicolens
B
H. oresterus
H. nubicolens
A
H. desmarestianus
H. nubicolens
D
B
H. goldmani
E
C
H. desmarestianus
0.5 changes

Figure 6

- 0.5 changes

Figure 7

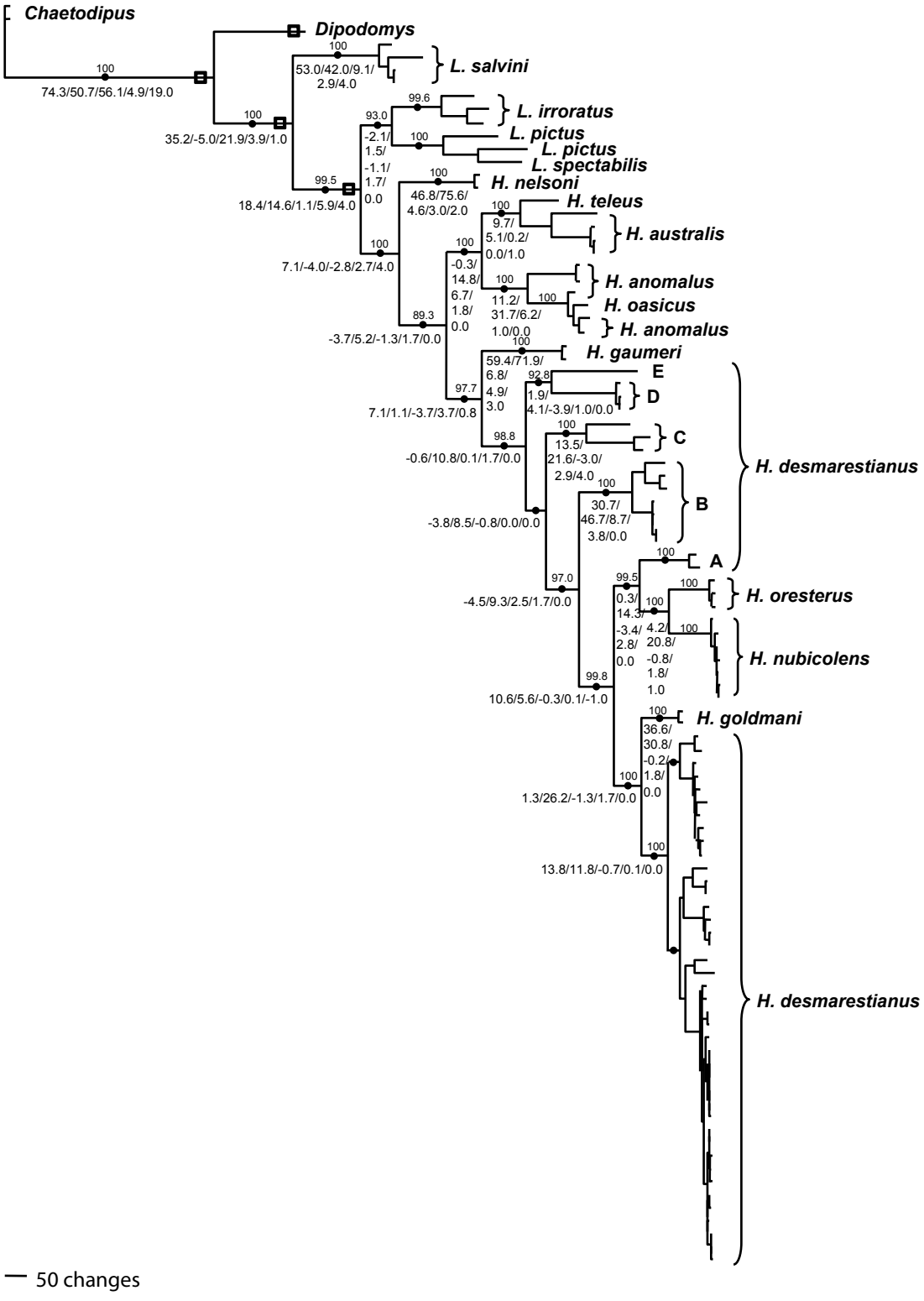
Chaetodipus
Dipodomys
L. salvini
L. irroratus
L. pictus
L. pictus
L. spectabilis
H. nelsoni
H. teleus
H. australis
H. anomalus
H. oasicus
H. anomalus
H. gaumeri
E
D
C
B
A
H. desmarestianus
H. oresterus
H. nubicolens
H. goldmani
H. desmarestianus
74.3/50.7/56.1/4.9/19.0
53.0/42.0/9.1/ 2.9/4.0
35.2/-5.0/21.9/3.9/1.0
-2.1/ 1.5/ -1.1/ 1.7/ 0.0
18.4/14.6/1.1/5.9/4.0
46.8/75.6/ 4.6/3.0/2.0
9.7/ 5.1/0.2/ 0.0/1.0
7.1/-4.0/-2.8/2.7/4.0
-0.3/ 14.8/ 6.7/ 1.8/ 0.0
11.2/ 31.7/6.2/ 1.0/0.0
-3.7/5.2/-1.3/1.7/0.0
59.4/71.9/ 6.8/ 4.9/ 3.0
1.9/ 4.1/-3.9/1.0/0.0
7.1/1.1/-3.7/3.7/0.8
13.5/ 21.6/-3.0/ 2.9/4.0
-0.6/10.8/0.1/1.7/0.0
30.7/ 46.7/8.7/ 3.8/0.0
-3.8/8.5/-0.8/0.0/0.0
-4.5/9.3/2.5/1.7/0.0
0.3/ 14.3/ -3.4/ 2.8/ 0.0
4.2/ 20.8/ -0.8/ 1.8/ 1.0
10.6/5.6/-0.3/0.1/-1.0
36.6/ 30.8/ -0.2/ 1.8/ 0.0
1.3/26.2/-1.3/1.7/0.0
13.8/11.8/-0.7/0.1/0.0
50 changes

Appendix: List of Heteromyinae and outgroup taxa included in this study with locality number, collecting location (Country: Province: locality), and specimen identification numbers. Geographic abbreviations are as follows: BE = Belize; CR = Costa Rica; EC = Ecuador; ES = El Salvador; GU = Guatemala; MX = Mexico; NI = Nicaragua; PN = Panama; VZ = Venezuela. Locality numbers 1-58 are congruent with those of González and Rogers (manuscript in preparation—their locality #51 is not represented in this study), and localities 59-97 are new to this study. Museum abbreviations are as follows: AMNH = American Museum of Natural History; ASNHC = Angelo State Natural History Collections; BYU = Brigham Young University; CM = Carnegie Museum of Natural History; CMC = Collecion de Mamiferos CEAMISH (Centro de Educación Ambiental e Investigación Sierra de Huautla), Universidad Autónoma del Estado de Morelos; EBRG = Estación Biológica Rancho Grande; KU = Museum of Natural History, University of Kansas; LACM = Natural History Museum of Los Angeles County; LSUMZ = Louisiana State University Museum of Zoology; MVZ = Museum of Vertebrate Zoology; ROM = Royal Ontario Museum; TCWC = Texas Cooperative Wildlife Collection, Texas A&M University; USNM = National Museum of Natural History.

Locality No.	Current Name	Sampling Locality	Collector No.	Museum Voucher No.	Karyotype, Field, or Tissue No.
1	*H. anomalus*	VZ: Sucre: 40 km NW Caripito, 250 m, Andres Eloy Blanco	MDE 1999	CM 78166	AK 3411
	"	"	MDE 2033	CM 78167	AK 3436
	"	"	MDE 2034	CM 78168	AK 3437
	"	"	MDE 2062	CM 78169	AK 3449
2a	*H. anomalus*	VZ: Miranda: 25 km N Altagracia de Oricuto, 500 m, Acevedo	MDE 2087	CM 78170	AK 3468
	"	"	MDE 2091	TCWC 37494	AK 3472
	"	"	MDE 2130	CM 78172	AK 3483
2b	"	VZ: Miranda: 40 km N Altagracia de Oricuto, 500 m, Acevedo	MDE 2129	TCWC 39720	AK 3482
3	*H. australis*	PN: Darién: Cerro Pirre, Parque Nacional Darien		ROM 104356	F 38215
	"	"		ROM 104357	F 38216

4	*H. australis*	PN: Darién: abt. 6 km NW Cana, E slope Cerro Pirre, 1200 m	MSH 1187	LSUMZ 25452	TK 22565
5	Candidate species B	MX: Oaxaca: 23 mi. SSW (by road) Tuxtepec, 250 ft	DSR 936	AMNH 254697	AK 3110
6a	Candidate species B	MX: Veracruz: Ojo de Agua, 1400 ft	DSR 921	AMNH 254693	AK 3098
6b	Candidate species B	MX: Veracruz: Ojo de Agua, 600 m	EA 823	BYU 16042	
	"	"	EA 836	BYU 16043	
6c	Candidate species B	MX: Veracruz: Ojo de Agua	MDE 1010	AMNH 254694	
7	Candidate species B	MX: Veracruz: 1 mi. NW Motzorongo, 700 ft	DSR 922	CM 79532	AK 3099
	"	"	DSR 923	CM 79533	AK 3100
8	*H. desmarestianus*	MX: Veracruz: near Los Tuxtlas	HD1	-99	
9a	*H. desmarestianus*	MX: Oaxaca: Vista Hermosa, 1000 m	DSR 934	CM 79530	AK 3108
9b	*"*	MX: Oaxaca: Vista Hermosa, Distrito Ixtlán, 1000 m	DSR 1685	MVZ 161229	
10a	*H. desmarestianus*	MX: Chiapas: 12 km N (by road) Berriozábal	ASK 660	ASNHC 1424	
	"	"	ASK 689	ASNHC 1425	
	"	"	MDE 5003	ASNHC 3515	LAF 1689
10b	"	MX: Chiapas, Pozo de Petroleo, 7 mi. N (by road) Berriozábal	DSR 1686	MVZ 161230	
11a	*H. desmarestianus*	MX: Chiapas: 12.5 km S Palenque		ROM 96096	FN 29887
	"	"		ROM 96105	FN 29896
11b	*H. desmarestianus*	MX: Chiapas: 1.2 km E Ruinas de Palenque	ASK 29	ASNHC 1440	
	"	"	ASK 31	ASNHC 1441	
11c	*H. desmarestianus*	MX: Chiapas: 9 km S Palenque	ASK 49	ASNHC 5826	
11d	*H. desmarestianus*	MX: Chiapas: 6.6 km S Palenque	ASK 51	ASNHC 1426	
12a	*H. desmarestianus*	MX: Chiapas: 6 km E Rayon		ROM 97542	FN 33018
12b	*H. desmarestianus*	MX: Chiapas: 9 km SE Rayon	ASK 589	ASNHC 1431	
	"	"	ASK 591	ASNHC 1432	
13	*H. desmarestianus*	MX: Campeche: 25 km N Xpujil		ROM 96089	FN 29880

14	*H. desmarestianus*	MX: Campeche: 10 km N El Refugio		ROM 97050	FN 30853
	"	"		ROM 97051	FN 30854
	"	"		ROM 97052	FN 30855
	"	"		ROM 97053	FN 30856
15	*H. desmarestianus*	MX: Quintana Roo: 1 km N Noh-Bec		ROM 97520	FN 30995
	"	"		ROM 97521	FN 30996
	"	"		ASNHC 7051	FN 32561
	"	"		ASNHC 7052	FN 32562
16a	*H. desmarestianus*	BE: Stann Creek Dist: 7.7 km WNW Quam Bank, Cockscomb Basin		CM 91960	AK 7664
	"	"		CM 91951	AK 7665
16b	*H. desmarestianus*	BE: Stann Creek Dist: 6.8 km WNW Quam Bank, Cockscomb Basin		CM 91980	AK 7688
16c	*H. desmarestianus*	BE: Stann Creek Dist: 3.4 km WNW Quam Bank, Cockscomb Basin		CM 91988	AK 7663
17a	*H. desmarestianus*	BE: Toledo Dist: 1 km NNE Salamanca, Forestry Camp, Columbio Forest Reserve		CM 91991	AK 7540
17b	*H. desmarestianus*	BE: Toledo Dist: 2.4 km NNW Salamanca, Forestry Camp, Columbio Forest Reserve		CM 91989	AK 7555
17c	*H. desmarestianus*	BE: Toledo Dist: 2.1 km NNE Salamanca, Forestry Camp, Columbio Forest Reserve		CM 91994	AK 7586
	"	"		CM 91993	AK 7588
	"	"		CM 91995	AK 7589
18	*H. desmarestianus*	GU: Baja Verapaz: 5 km E Puruhla		ROM 98405	FN 31394
	"	"		ROM 98406	FN 31395
	"	"		ROM 98407	FN 31396
	"	"		ROM 98408	FN 31397
	"	"		-99	FN 31402
19	*H. desmarestianus*	GU: El Peten: Tikal		ROM 99292	FN 31842

	"	"		ROM 99293	FN 31843
	"	"		ROM 99294	FN 31844
20	*H. desmarestianus*	GU: El Peten: Biotope Cerro Cahui, El Remate		ROM 99639	FN 32211
	"	"		ROM 99603	FN 32272
	"	"		ROM 99604	FN 32273
	"	"		ROM 99605	FN 32274
21	*H. desmarestianus*	GU: El Peten: Campo los Guacamayos, 40 km N Biotopo Laguna del Tigre		ROM 99469	FN 32318
	"	"		ROM 99504	FN 32353
22	*H. desmarestianus*	GU: Sacatepequez: 5 km W San Miguel Duenas		ROM 98265	FN 31254
	"	"		ROM 98266	FN 31255
	"	"		ROM 98267	FN 31256
	"	"		ROM 98269	FN 31258
23	*H. desmarestianus*	ES: Santa Ana: Parque Nacional Montecristo, Bosque Nebuloso, 2,200 m		ROM 101369	F 35547
	"	"		ROM 101389	F 35567
	"	"		ROM 101390	F 35568
24	*H. desmarestianus*	CR: Alajuela: 10 km E Sucre, Parque Nacional, Juan Castro Blanco		ROM 113310	F 48617
	"	"		ROM 113311	F 48618
25	*H. desmarestianus*	CR: Cartago: Iztaru: Cerros de la Carpintera		ROM 113130	F 48436
	"	"		ROM 113131	F 48437
	"	"		ROM 113132	F 48438
26	*H. desmarestianus*	CR: Cartago: Catie: 4 km SE (by road) Turrialba, 600 m	FAR 111	ROM 97324	
	"	"	FAR 112	ROM 97325	
	"	"	FAR 113	ROM 97326	

	"	"	FAR 114	ROM 97327	
27	*H. desmarestianus*	CR: Cartago: Río Reventazón, 5.6 km SE (by road) Turrialba, 450 m	DSR 2153	MVZ 164823	
	"	"	DSR 2154	MVZ 164824	
	"	"	DSR 2166	MVZ 164825	
	"	"	DSR 2167	MVZ 164826	
	"	"	DSR 2246	MVZ 164827	
28	*H. desmarestianus*	CR: Guanacaste: Volcán Santa Maria		ROM 113245	F 48552
29a	*H. desmarestianus*	CR: Guanacaste: 5.0 km NE (by road) Tilarán, 650-675 m	DSR 2121	MVZ 164839	
	"	"	DSR 2122	MVZ 164840	
	"	"	DSR 2145	MVZ 164842	
	"	"	DSR 2235	MVZ 164843	
29b	*H. desmarestianus*	CR: Guanacaste: 4.1 km NE (by road) Tilarán, 650 m	DSR 2123	MVZ 164828	
	"	"	DSR 2124	MVZ 164829	
	"	"	DSR 2125	MVZ 164830	
	"	"	DSR 2134	MVZ 164831	
	"	"	DSR 2138	MVZ 164832	
30	*H. desmarestianus*	CR: Puntarenas: 1 km N, 5 km W Palmar Norte	MSH 1260	LSUMZ 28354	M-1833
31	*H. desmarestianus*	CR: San José: Bajo de Iglesia, SW Volcán Irazu, Cascajal de Coronado	EA 21	BYU 15197	
	"	"	EA 22	BYU 15198	
32	*H. desmarestianus*	CR: San José: Parque Nacional Braulio Carillo, Moravia Cerro Honduras	EA 78	BYU 15195	
	"	"	EA 79	BYU 15196	

33	*H. desmarestianus*	CR: Guanacaste, Area de Conservación Guanacaste, ca. 20 km NNE Liberia, Pailas, Sendro Palas near Rio Colorado, 800 m	MK 00-112	KU 158615	
34	*H. desmarestianus*	NI: Esteli		ROM 112284	F 48170
35	*H. goldmani*	MX: Chiapas: 15.5 mi SE (by road) Mapastepec, 150 ft	MDE 1224	CM 79529	AK 3150
36	*H. desmarestianus*	MX: Chiapas: El Triunfo, 10 km SSE Finca Prusia	LJB 3108	LACM 74200	LAF 1773
	H. goldmani	"	LJB 3109	LACM 74201	LAF 1774
	"	"	MDE 5049	ASNHC 3523	LAF 1790
37	*H. oresterus*	CR: Cartago: Catie: 4 km (by road; Pan American Hwy) Villa Mills		ROM 102753	
38	*H. oresterus*	CR: San José: 2.2 km E (by road) La Trínidad de Dota, 2600 m	DSR 2092	MVZ 164861	
	"	"	DSR 2107	MVZ 164863	
	"	"	DSR 2244	MVZ 165786	
39	*H. oresterus*	CR: San José: Cerro la Muerte, San Gerardo de Dota		ROM 113208	F 48514
	"	"		ROM 113229	F 48535
40	*H. nubicolens*	CR: Guanacaste: Monteverde, Campbell's Woods	DSR 1744	MVZ 161224	
	"	"	DSR 1745	MVZ 161225	
41	*H. nubicolens*	CR: Puntarenas, Monte Verde Biological Station, elevation 1,655 m		ROM 113257	F 48564
42	Candidate species A	CR: Limón: 4.6 km W (by road) Limón, 25 m	DSR 2150	MVZ 164844	
	"	"	DSR 2151	MVZ 164845	
	"	"	DSR 2155	MVZ 164846	
	"	"	DSR 2163	MVZ 164847	
	"	"	DSR 2165	MVZ 164849	

	"	"	DSR 2245	MVZ 164851	
43	Candidate species A	CR: Alajuela: 7 km NE (by road) Quesada, 2297 m	DJH 2469	LSUMZ 26357	M-607
44	Candidate species C	CR: Puntarenas: 1.1 km SE (by road) Ciudad Nielly, 25 m	DSR 2193	MVZ 164852	
	"	"	DSR 2195	MVZ 164854	
	"	"	DSR 2222	MVZ 164865	
	"	"	DSR 2242	MVZ 164856	
45	Candidate species C	PN: Chiriqui: Ojo de Agua, 2 km N Santa Clara		ROM 104296	F 38147
	"	"		ROM 104297	F 38148
	"	"		ROM 104307	F 38158
	"	"		ROM 104308	F 38159
	"	"		ROM 104324	F 38175
	"	"		ROM 104325	F 38176
	"	"		-99	F 38177
	"	"		ROM 104326	F 38178
46	Candidate species D	PN: Darién: abt. 6 km NW Cana, E slope Cerro Pirre, 1400 m	DJH 2427	LSUMZ 25451	
47	*H. gaumeri*	MX: Quintana Roo: 7 km NE Xul-Ha		ASNHC 7127	FN 32575
	"			ASNHC 7128	FN 32576
48	*H. gaumeri*	MX: Campeche: 7 km N Escarcega		ASNHC 7118	FN 32736
49	*H. gaumeri*	MX: Quintana Roo: Puerto Morelos		ASNHC 7127	AJ 389536
50	*H. nelsoni*	MX: Chiapas: Cerro Mozotal, 2930 m	DSR 7181	CMC 391	
	"	"	DSR 7187	BYU 20643	
	"	"	DSR 7189	BYU 20644	
	"	"	DSR 7191	CMC 396	
	"	"	DSR 7212	CMC 398	

52	*L. irroratus*	MX: Puebla: 4 mi. SW Xicotepec de Juarez	MDE 986	CM 79450	AK 3083
53	*L. irroratus*	MX: Tamaulipas: 2.2 mi. N Soto la Marina	MDE 3280	TCWC 42044	AK 4335
	"	"	MDE 3284	TCWC 42048	AK 4339
54	*L. irroratus*	MX: San Luis Potosi: Rancho La Laja, 6 km W Xilitla, 785 m, Mpio. Xilitla	EA 223	BYU 15266	
55	*L. irroratus*	MX: Jalisco: Ameca	EA 816	BYU 16047	
56	*L. irroratus*	MX: Michocán: 10 km S (by road) Pátzcuro, 2200 m	DSR 5215	BYU 16052	
57	*L. salvini*	CR: Guanacaste: 3.9 km SE (by road) Playas del Coco	DSR 2128	MVZ 164809	
58	*L. salvini*	CR: Puntarenas: Finca Mamos, Chomes, 60 m	EA 62	BYU 15203	
	"	"	EA 63	BYU 15204	
	"	"	EA 64	BYU 15205	
59a	*H. anomalus*	VZ: Falcón: Serranía de San Luis; Parque Nacional J.C. Falcón, Sector Cerro Galicia, ca. 10 km W 4 km N Cabure	JOG 4522	AMNH 276507 / EBRG 25308	
	"	"	RPA 253	EBRG 25386	
	"	"	RPA 261	EBRG 25311	
	"	"	RPA 265	AMNH 276557 / EBRG 25391	
59b	*H. anomalus*	VZ: Falcón: Serranía de San Luis; Parque Nacional J. C. Falcón, Sector El Haitón, ca. 8 km W 1 km N Cabure	JOG 4535	EBRG 25377	
	"	"	RPA 248	EBRG 25384	
	"	"	RPA 257	AMNH 276555 / EBRG 25388	
	"	"	RPA 264	AMNH 276556 / EBRG 25390	

59c	*H. anomalus*	VZ: Falcón: Serranía de San Luis; Parque Nacional J. C. Falcón, Sector El Chorro, ca. 9 km N Cabure	JOG 4560	EBRG 25309
	"	"	JOG 4573	EBRG 25399
	"	"	JOG 4574	AMNH 276521 / EBRG 25400
	"	"	JOG 4575	EBRG 25401
	"	"	JOG 4576	EBRG 25402
	"	"	JOG 4583	AMNH 276524 / EBRG 25408
59d	*H. anomalus*	VZ: Falcón: Serranía de San Luis; Parque Nacional J. C. Falcón, Sector Cumbres de Uria, ca. 9 km N Cabure	JOG 4570	AMNH 276519 / EBRG 25310
	"	"	JOG 4571	EBRG 25397
	"	"	JOG 4572	AMNH 276520 / EBRG 25398
	"	"	JOG 4578	EBRG 25404
	"	"	RPA 300	AMNH 276574 / EBRG 25419
	"	"	RPA 301	EBRG 25312
	"	"	RPA 302	AMNH 276575 / EBRG 25313
	"	"	RPA 303	no catalog #
	"	"	RPA 316	AMNH 276583 / EBRG 25428
	"	"	RPA 317	EBRG 25314
	"	"	RPA 318	EBRG 25315
	"	"	RPA 319	EBRG 25429
	"	"	RPA 325	EBRG 25434
	"	"	RPA 326	AMNH 276587 / EBRG 25316
	"	"	RPA 327	EBRG 25317

	"	"	RPA 328	AMNH 276588 / EBRG 25318	
60	*H. australis*	EC: Esmeraldas: 2 km S Alto Tambo		ROM 105784	F 40077
61	*H. australis*	PN: Darién: Cana		ROM 116253	F 48794
	"	"		ROM 116302	F 48843
62	*H. desmarestianus*	ES: Santa Ana: Parque Nacional Montecristo, Los Planes		ROM 101505	F 35683
	"	"		ROM 101510	F 35688
63	*H. desmarestianus*	CR: Guanacaste: Volcán Santa Maria		ROM 113246	F 48553
64	*H. desmarestianus*	CR: Alajuela: 12.7 km NE Zarcero		ROM 113293	F 48600
65	*H. nubicolens*	CR: Puntarenas: Sainta Elena, Monte Verde Station		ROM 114272	F 48710
66a	Candidate species D	PN: Darién: Mount Pirre		ROM 116257	F 48798
	"	"		ROM 116258	F 48799
	"	"		ROM 116259	F 48800
	"	"		ROM 116260	F 48801
	"	"		ROM 116261	F 48802
	"	"		ROM 116262	F 48803
	"	"		ROM 116263	F 48804
	"	"		ROM 116264	F 48805
	"	"		ROM 116265	F 48806
	"	"		ROM 116266	F 48807
	"	"		ROM 116267	F 48808
	"	"		ROM 116268	F 48809
	"	"		ROM 116269	F 48810
	"	"		ROM 116270	F 48811
	"	"		ROM 116271	F 48812
66b	*H. desmarestianus*	PN: Darién: Cerro Pirre		ROM 116273	F 48814

67a	*H. desmarestianus*	BE: Orange Walk: 4 km S Las Milpas Camp, 12 m mark, Rio Bravo area		-99	FN 29952
67b	*H. desmarestianus*	BE: Orange Walk: 8 km S Las Milpas, Rio Bravo		-99	FN 29971
68	*H. desmarestianus*	GU: El Peten: 1.5 km S, 1 km W Poptun		ROM 99230	FN 31780
69	*H. desmarestianus*	GU: El Peten: 10 km N of Tikal		ROM 99409	FN 31859
	"	"		ROM 99410	FN 31960
70	*H. desmarestianus*	GU: El Peten: Campo los Guacamayos, Biotopo Laguna del Tigre, 40 km N El Naranjo		ROM 99529	FN 32378
	"	"		ROM 99538	FN 32387
71	*H. desmarestianus*	MX: Quintana Roo: 6 km S, 1.5 km W Tres Garantias		ASNHC 7053	FN 32683
	"	"		ASNHC 7059	FN 32686
72	*H. desmarestianus*	CR: Guanacaste: Liberia, ~39 km N Pitilla, Sendero Orosilito	KM 99-091	KU 158510	
	"	"	KM 99-092	KU 158511	
	"	"	KM 99-093	KU 158512	
	"	"	KM 99-094	KU 158513	
	"	"	KM 99-102	KU 158514	
	"	"	KM 99-095	KU 158711	
73	Candidate species E	PN: Bocas Del Toro: Isla Popa, 1 km SE Deer Island Channel	J-501	USNM 464382	
	"	"	COH 14867	USNM 464383	
	"	"	COH 14887	USNM 464384	
	"	"	COH 14890	USNM 464385	
74	*H. desmarestianus*	GU: Quetzaltenango: 4 km SE Zunil, Finca la Chingada	WB 8425	USNM 569675	

75	*H. desmarestianus*	GU: Alta Verapaz: Chelemha, Yalijux Mountain		USNM 569852	TK 151027
	"	"		USNM 569866	TK 151041
	"	"		USNM 569945	TK 151134
	"	"		USNM 569949	TK 151139
	"	"		USNM 569956	TK 151150
	"	"		USNM 569981	TK 151178
	"	"		USNM 569984	TK 151183
	"	"		USNM 569985	TK 151184
	"	"		USNM 569991	TK 151190
	"	"		USNM 570003	TK 151126
	"	"		USNM 570007	TK 151140
76	*H. desmarestianus*	GU: Zacapa: Gualan Municipality: 9.5 km NW Gualan, El Limo, Sierra de las Minas	WB 8477	USNM 570034	
	"	"	WB 8478	USNM 570035	
	"	"	WB 8479	USNM 570036	
	"	"	WB 8517	USNM 570073	
	"	"	WB 8518	USNM 570074	
	"	"	WB 8546	USNM 570097	
	"	"	WB 8549	USNM 570131	
77	*H. desmarestianus*	GU: Baja Verapaz: 9 km S of Pasmola, btwn km 166 & 167 on CA-14, Hotel Country Delights	NW 1293	USNM 570134	
78	Candidate species E	PN: Bocas Del Toro: Nuri	FMG 2793	USNM 575655	
79	Candidate species E	PN: Bocas Del Toro: Peninsula Valiente, Quebrada Hido	FMG 2623	USNM 578383	
80a	Candidate species B	MX: Veracruz: 13.0 km NW (by road) Sontecomapan, Estacion Los Tuxtlas, IBUNAM, 40 m	DSR 8546	CMC 2004	

	"	"	DSR 8547	CMC 2005	
	"	"	DSR 8548	CMC 2006	
	"	"	DSR 8549	CMC 2007	
	"	"	DSR 8550	CMC 2008	
	"	"	DSR 8551	CMC 2009	
	"	"	DSR 8552	CMC 2010	
	"	"	DSR 8553	CMC 2011	
80b	Candidate species B	MX: Veracruz: 12.1 km NW (by road) Sontecomapán, 150 m	DSR 8561	CMC 2002	
	"	"	DSR 8562	CMC 2003	
81	*H. goldmani*	MX: Chiapas: 18.5 km S Frontera Comalapa		ROM 97673	FN 33154
	"	"		ROM 97674	FN 33155
82a	*H. nubicolens*	CR: Puntarenas: Monteverde Biological Station		ROM 113258	F 48565
	"	"		ROM 113259	F 48566
	"	"		ROM 113260	F 48567
	"	"		ROM 113261	F 48568
	"	"		ROM 113262	F 48569
	"	"		ROM 113263	F 48570
	"	"		ROM 113264	F 48571
	"	"		ROM 113265	F 48572
	"	"		ROM 113282	F 48589
82b	*H. nubicolens*	CR: Puntarenas: Monteverde, Cerro Amigos	TRM 3746	KU 142057	
82c	*H. nubicolens*	CR: Puntarenas: Monteverde, Cerro Amigos, Puntarenas-Guanacaste border	TRM 3869	KU 143455	
82d	*H. nubicolens*	CR: Puntarenas: Monteverde, Monteverde Cloud Forest Reserve, investigator trail	RMT 4461	KU 159022	

		"	RMT 4462	KU 159023	
		"	RMT 4467	KU 159024	
		"	RMT 4468	KU 159025	
		"	RMT 4469	KU 159026	
		"	RMT 4471	KU 159027	
83a	*H. nubicolens*	CR: Alejuela: Monteverde, Monteverde Cloud Forest Reserve, Cerro Amigos	CMM 222	KU 159101	
83b	*H. nubicolens*	CR: Alejuela: Monteverde, Monteverde Cloud Forest Reserve, Camino a Penas Blancas	CMM 245	KU 159102	
	"	"	CMM 258	KU 159103	
84	*H. oasicus*	VZ: Falcón: Península de Paraguaná; Cerro Santa Ana, ca. 4 km N Santa Ana	JOG 4460	EBRG 25450	
	"	"	JOG 4505	AMNH 276500 / EBRG 25485	
	"	"	JOG 4550	EBRG 25532	
	"	"	JOG 4554	EBRG 25533	
	"	"	RPA 209	AMNH 276534 / EBRG 25339	
85	*H. teleus*	EC: Los Rios: Rio Palenque Biological Station	ATS 183	KU 149134	
86	*H. desmarestianus*	CR: Alajuela: Parque Nacional Volcán Poas		ROM 113332	F 48640
87	*H. anomalus*	VZ: Zulia	RSV 1124	USNM 448559	
88	*L. adspersus*	PN: Province Panama: 1.8 km N (by road) Fort Clayton	DSR 2302	MVZ 165784	
89	*L. pictus*	MX: Chiapas: 7.5 km SW of Ixtapa	MDE 2420	TCWC 37059	AK 4200
90	*L. pictus*	MX: Nayarit: 4.6 km NE Jalcocotán	ASK 1701	ASNHC 3260	
91	*L. pictus*	MX: Colima: 5 km S Alzada	ASK 2034	ASNHC 3072	
92	*L. salvini*	MX: Chiapas: 1.1 mi. SE Cabeza de Torro	MDE 1105	CM 79513	AK 3137
	"	"	MDE 1107	CM 79514	AK 3139

	"	"	MDE 1108	CM 79515	AK 3140
	"	"	MDE 1109	CM 70516	AK 3141
93	*L. spectabilis*	MX: Jalisco: 3 mi NE of Contla	MDE 3012	TCWC 42412	AK 5884
	"	"	MDE 3014	TCWC 42413	AK 5885
	"	"		TCWC 42405	AK 5894
94	*Chaetodipus penicillatus*	MX: Sonora: 28 km W Hermosillo (highway to Bahia Kino), 50 m, Mpio. Hermosillo	EAA 482	BYU 15685	
	"	"	EAA 485	BYU 15661	
	"	"	EAA 487	BYU 15663	
	"	"	EAA 488	BYU 15664	
95	*Dipodomys ordii*	USA: Utah; Kane County, Devil's Garden, 37º35.0064' N, 111º24.5047'W, 1,475 m,	QRS 1	BYU 23376	
	"	"	QRS 2	BYU 23377	
96	*Perognathus apache*	USA: Utah: Kane County, Fourmile Bench, 37º23.3993'N, 111º41.3311'W, 1,770 m	QRS 181	BYU 23307	
	"	"	QRS 209	BYU 23308	